Appendix D

Numerical Simulation of Groundwater Flow in the LBNL Old Town System

Numerical Simulation of Groundwater Flow at the LBNL Old Town Site in Support of Remediation Strategies

Quanlin Zhou, Jens T. Birkholzer, Iraj Javandel, and Preston D. Jordan

Earth Sciences Division

Lawrence Berkeley National Laboratory

May 2004

ABSTRACT

A calibrated groundwater flow model for a contaminated site can provide substantial information for assessing and improving hydraulic measures implemented for remediation. We developed a three-dimensional transient groundwater flow model for a contaminated mountainous site at which interim corrective measures were initiated to limit further spreading of contaminants. This flow model accounts for complex geologic units that vary considerably in thickness, slope, and hydrogeologic properties, as well as large seasonal fluctuations of the groundwater table and flow rates. Other significant factors are local recharge from leaking underground storm drains and recharge from steep uphill areas. The zonation method was employed to account for the clustering of high and low hydraulic conductivities measured in a geologic unit. A composite model was used to represent the bulk effect of thin layers of relatively high hydraulic conductivity found within bedrock of otherwise low conductivity. The inverse simulator ITOUGH2 was used to calibrate the model for the distribution of rock properties. The model was initially calibrated using data collected between 1994 and 1996. To check the validity of the model, it was subsequently applied to predicting groundwater level fluctuation and groundwater flux between 1996 and 1998. Comparison of simulated and measured data demonstrated that the model is capable of predicting the complex flow reasonably well. Advective transport was approximated using pathways of particles originating from source areas of the plumes. The advective transport approximation was in good agreement with the trend of contaminant plumes observed over the years. The validated model was then refined to focus on a subsection of the large system. The refined model showed that most of the hydraulic measures implemented for remediation are effective.

TABLE OF CONTENT

LIST OF FIGURES

LIST OF TABLES

1. Introduction

The LBNL Environmental Restoration Program started in the late 1980s. The program deals with the identification and remediation of a variety of so-called Solid Waste Management Units (SWMU) and Areas of Concern (AOC) within Lawrence Berkeley National Laboratory (LBNL), some of which have caused significant groundwater contamination. Detailed investigation and monitoring, regarding the location and origin of hazardous wastes, groundwater plumes, vapor phases in soil, surface water and air, etc., have been conducted since the 1990s. During the last decade, Javandel and his coworkers (Javandel, 1990; LBNL, 2000, 2003) have accumulated a vast amount of data, including geologic profiles, hydrogeologic properties, groundwater levels, contaminant concentrations, and potential degradation. At the same time, interim corrective measures have been initiated toward removing the sources of contamination, excavating contaminated soils, limiting further spreading of contaminants, and cleaning up contaminated groundwater using suitable methods. As a result, most SWMU's and AOC's are of no further concern to regulators, with the exception of some groundwater plumes that are still being monitored, hydraulically contained, or treated (LBNL, 2000, 2003).

Of these plumes, the three plumes at the so-called Old Town site, the earliest developed part of the LBNL, are the most significant ones (see Figure 1). Originating from several sources, these groundwater plumes have a maximum concentration of more than 50,000 μg/L as of 2002. Presently, the contaminant sources have been removed, and several cleanup and containment measures have been initiated. Four groundwater collection trenches have been installed downstream from the plumes. One of them, the Building 7 trench, was installed in August 1996 as a source control measure. Contaminated groundwater has been pumped, treated, and re-injected into upstream wells to flush contaminated soils. Monitored contaminant concentrations in downstream wells are relatively stable, if not declining, because further movement of contaminants is limited by pumping contaminated groundwater from the trenches. However, pumping and treatment is expensive. Prediction of future concentration levels would help control this expense by indicating how long the cleanup and hydraulic containment activities will have to last. To that end, a numerical model was developed for simulating transient groundwater flow at the Old Town site, as a first step toward development of a transport model.

This report describes the development and validation of a transient groundwater flow model for the Old Town site. The groundwater flow model is based on a conceptual model which Javandel and his team developed from the large amount of gathered data (LBNL, 2000). The conceptual model included estimated locations and boundaries of hydrogeologic units, groundwater flow directions, and interpretation of piezometric measurements. In this study, we updated the conceptual model to incorporate new information.

This report consists of five sections: (1) the development of a hydrogeologic model to represent five hydrogeologic units; (2) the development of a transient groundwater flow model, including determination of model domain and boundary conditions, interpolation of initial conditions, and

estimation of net areal recharge and local recharge resulting from storm drain leakage; (3) the calibration of heterogeneous rock properties within the Moraga Formation, the Mixed unit, and the Orinda Formation, using the measured water levels at a number of monitoring wells and the measured flow rates at two trenches between July 1, 1994, and June 30, 1996; (4) model validation using a "blind" prediction for the groundwater flow during the period between July 1, 1996, and June 30, 1998; and (5) the assessment of hydraulic measures implemented for remediation using a refined smaller-scale model.

The modeling challenges involved in this study include complex geological conditions, steep hydraulic gradients, strong heterogeneity, complex boundary conditions at the mountainous site, and recharge through the unpaved ground surface and leaking underground storm drains. This report focuses on the development and validation of the groundwater flow model and the understanding of groundwater flow at the Old Town site. A smaller-scale transport model in the focused area of contaminant plumes around Building 7 will be developed in the future.

2. Development of Hydrogeologic Model

The morphological, geologic, and hydrological situations at the Old Town site are complex. Morphology is accentuated by steep hills, deep ravines, and large gradients. The Old Town geologic setting is complicated, consisting of several units with vastly different hydrological properties. The near-surface has been modified by landslides and man-made cuts and fills (see Figure 2).

To capture this complexity, we developed a hydrogeologic model for the Old Town site. The geological data used for model development include geologic profiles of 711 boreholes and wells, cross-sections, and outcrop maps. The uppermost five hydrogeologic units contributing to groundwater flow were considered in this hydrogeologic model. These five hydrogeologic units, in descending order from the ground surface, are the Artificial Fill unit, the Colluvium unit, the Moraga Formation, the Mixed unit, and the Orinda Formation. The Orinda Formation is deep and less conductive of groundwater; only the top portion of the entire unit was considered in numerical simulations. Full descriptions of these units may be found in LBNL (2000).

The hydrogeologic model was developed in three steps: first, all borehole data stored in different formats were assembled; second, a consistency analysis was conducted using borehole-bottom elevations and zero-thickness data points obtained from outcrop maps; and finally, Kriging interpolation was used to generate unavailable information on thickness of hydrogeologic units and elevations of top and bottom of each unit. The data analysis of the three steps aimed to construct the top elevations of the five hydrogeologic units and the thickness of the top four units in a uniform fine grid. Note that some units are not continuous at the site. In cases where a unit is absent, its top elevation is indicated by the bottom elevation of the overlying unit.

2.1. Available Data

Two borehole datasets for the elevation and thickness of different hydrogeologic units were used as the basis for geostatistical interpolation. The first dataset, which was used in the previous hydrogeologic conceptual model, consists of boreholes and wells drilled before 1997. The second dataset consists of 82 boreholes drilled after 1997. In addition, the geologic data on cross-section and outcrop maps are combined with the borehole data to refine the current hydrogeologic model.

The first dataset (pre-1997) consists of geologic depth-sections for 537 boreholes/wells, 15 excavations, 47 outcrops, and 30 roadcuts (for brevity, we referred to each type as a "borehole"). The data record of a borehole consists of UC coordinates, elevation of the ground surface (top of the Artificial Fill unit), depth from the ground surface to the top of each hydrogeologic unit (or the thickness of units), and the elevation of borehole bottom. Of the 629 boreholes, 458 are "full" boreholes, at which the measured top elevation of each hydrogeologic unit is available. There are 171 "partial" boreholes with unavailable thickness/elevations of at least one or more units (usually because boreholes were not drilled deep enough to penetrate into the Orinda Formation).

The second dataset (post-1997) consists of geologic profiles in 82 additional boreholes/wells. The data are in the format of the depth from the ground surface to the bottom of a measured core interval and the corresponding hydrogeologic unit. A unit may consist of a number of intervals. The thickness of each unit is extracted from this dataset and transformed into the data format of the pre-1997 dataset. For a "partial" borehole, in which drilling ended within a hydrogeologic unit, the full thickness of the unit is unknown; in this case, the bottom elevation of the borehole was used in the following consistency analysis.

The pre-1997 and post-1997 data sets were combined to yield a full dataset of 711 vertical geologic boreholes. Of these boreholes, 508 are "full" boreholes and 203 are "partial" boreholes. Each borehole may consist of the geological data for nine parameters: the top elevations of the Artificial Fill unit, Colluvium unit, Moraga Formation, Mixed unit, and Orinda Formation, and the thickness of the Artificial Fill unit, Colluvium unit, Moraga Formation, and Mixed unit. For each of the nine parameters, the total number of data points available is different; the number of available data points for the above nine parameters (in the order) is 708, 691, 671, 576, 511, 691, 671, 576, and 510, respectively. The top elevation of the Orinda Formation is more uncertain than that of the ground surface because fewer measurements are available. The hydrogeologic model requires interpolation of the nine parameters when they are not available at boreholes.

In addition to the 711-borehole dataset, seven cross-sectional maps and one outcrop map are available to better constrain the hydrogeologic model. Each of the cross sections provides detailed information about the elevation/thickness of hydrogeologic units and the location and bottom of monitoring wells and boreholes. The outcrop map provides zero-thickness points for the Moraga Formation and the Mixed unit. These were used to better constraint the thickness of the two hydrogeologic units. A total of 596 data points with zero thickness are available along the edge of the Moraga Formation bowls (see Figure 9), and 483 points are available for the Mixed unit (see Figure 10).

2.2. Consistency Analysis

As the second step of developing the hydrogeologic model, we conducted a consistency analysis to check and improve the hydrogeologic model using all available data. The unavailable data (elevation/thickness) at each of the "partial" boreholes were first interpolated using all other borehole data available. The interpolated data were then modified using the borehole-bottom elevations and information obtained in the geologic cross-sectional maps. Then, the zero-thickness data points for the Moraga Formation and Mixed unit obtained from the outcrop map were finally used to adjust the thickness of these two units.

In the first step, the unavailable data at each of the "partial" boreholes were interpolated using all available borehole data. The unavailable data points for each of the nine parameters were interpolated. For example, we simultaneously interpolated the top elevation of the Orinda Formation at the remaining 200 boreholes using the data in the 511 boreholes with this parameter available. Tecplot 8.0 (AmTec Inc., 1998) was used for this interpolation, based on the kriging algorithm. The same parameters of the interpolation were used for interpolating the elevation and thickness of each hydrogeologic unit.

For each borehole, the first five parameters (i.e., top elevation of each unit) can be used to determine the last four parameters (i.e., thickness of each unit), or the first elevation and the last four thickness parameters can be used to determine the hydrogeologic model. In other words, there is a redundancy in the measured borehole data that can be used for consistency analysis. Ideally, if all nine parameters have been measured at one borehole location, the two methods must give identical stratigraphy. However, if some of the parameters have to be interpolated because certain parameters were not measured, there may be an inconsistency between the thickness directly interpolated and the thickness obtained by the difference between the interpolated top and bottom elevations of a unit. For example, the interpolated thickness of the Moraga Formation may be different from the value obtained using the interpolated top elevations of the Moraga Formation and Mixed units. In general, interpolated thickness is considered less uncertain than interpolated elevations. Therefore, in this study, we used interpolated thickness to develop the hydrogeologic model. These values were compared with the thickness calculated from interpolated elevations (i.e., top elevation minus bottom elevation). If the thickness at a "partial" borehole obtained by the two different interpolation methods was significantly different, geological judgement was applied to make the dataset consistent. Because the Moraga Formation is the most important unit for conducting groundwater, and the top elevation of the Moraga Formation is slightly less certain than the elevation of the ground surface, we used the top of the Moraga Formation as the reference surface. The top elevations of the other four units were determined using this reference surface and the thickness of the top four units.

In the second step, the uncertainty of interpolated thickness values was reduced using the geological information on the cross-sectional maps and our knowledge about the drilling depth of "partial" boreholes. The bottom of a hydrogeologic unit that was only partially penetrated by a borehole must be lower than the borehole bottom. Therefore, in case the interpolated thickness is more

than the value obtained using the borehole bottom, the former was assigned to the thickness. Otherwise, the interpolated thickness was corrected and the thickness from the top of this unit to the borehole bottom was assigned. For example, at Borehole HLA:1.169, the boring bottom is 50 ft below the ground surface within the Mixed unit; the top of the Mixed unit is at a depth of 29 ft, indicating that the thickness of the Mixed unit is at least 21 ft; the interpolated thickness was only 0.3 ft because a steep gradient of geologic surface exists in this region. The interpolated thickness was also modified using the cross-sectional maps with information about wells/boreholes.

In the third step, a large number of data points with zero thickness for the Moraga Formation and Mixed unit (available in the outcrop map) were used to better constrain the lateral extent of the two units. For example, the 596 zero-thickness data points of the Moraga Formation were combined with the 711 borehole data points with measured or interpolated thickness, to interpolate the thickness at all locations in a uniform fine grid. This grid area ranges from 2,100 ft to 3,600 ft in the UC easting direction and –400 ft to 900 ft in the UC northing direction; and the discretization in the UC coordinates is 3.75 ft by 3.25 ft. Tecplot, with the kriging algorithm and its parameter values given above, was used for such an interpolation. For the Mixed unit, both zero-thickness data points and the borehole data points were used for the interpolation of its thickness. Only borehole data points were used in interpolating the thickness of the Artificial Fill and Colluvium units and the top elevation of the Moraga Formation, because no additional information about these parameters is available.

From the consistency analysis, we obtained all five parameters (one elevation value and four thickness values) for the 711 boreholes, either available from measurements or from interpolation. The top elevations of the other four units were calculated directly because all unavailable data in “partial” boreholes have been generated. The completed hydrogeologic model at the Old Town site thus consists of the nine parameters in each of the grid nodes in a uniform grid of [2,100, 3,600] by [-400, 900] ft.

2.3. Results and Discussion

Figures 3 through 6 show the top elevations of the Artificial Fill unit, Moraga Formation, Mixed unit, and Orinda Formation, respectively. “Full” boreholes are indicated by red squares; “partial” boreholes are indicated by black squares. Figures 7 through 10 show the thickness of the Artificial Fill unit, Colluvium unit, Moraga Formation, and Mixed unit, respectively. The purple squares in Figure 9 indicate the zero-thickness data points for the Moraga Formation obtained from the outcrop map, and those in Figure 10 indicate the zero-thickness data points in the Mixed unit. Note that the interpolation outside of the model boundary (to be discussed in Section 3) is not reliable, because few boreholes are available.

Figure 3 shows that the center of the Old Town area is located in a relatively flat part of the sloping LBNL site. The ground surface slopes steeply east of the Old Town area as well as downward to the west and south. The gradient of the ground surface in the north portion of the Old Town area is in the east-west direction; in the central portion, the gradient is from northeast to the southwest; in the south portion, from the north to the south. Two platforms of the ground surface can be defined: the first

is the one located around Building 25 and along Buildings 6, 7, and 27; the second is the lower one located in the area of Buildings 46, 47, and 58, with a large gradient connected to the first platform. Figure 4 indicates that with a few exceptions, the top surface of the Moraga Formation follows the ground surface. However, this is not the case for the top surface of the Mixed unit (or the bottom surface of the Moraga Formation) shown in Figure 5. One can see three areas (within the boundary of this study) where the bottom of the Moraga Formation forms deep bowls. Moreover, steep gradients can be seen along the edge of the three Moraga bowls, in particular along the south edge of Large Bowl in the north area. These steep gradients on geologic contact surfaces make it difficult to numerically capture the strong spatial variability in the groundwater flow (in terms of water table and velocity). Figure 6 shows the elevation contour of the bottom of the Mixed unit or the top surface of the Orinda Formation.

Figure 7 demonstrates that certain parts of the Old Town area have been artificially filled to create a flat ground surface. The maximum thickness (about 37 ft) of the Artificial Fill unit is located north of Building 6 and west of Building 7. This fill zone was established for the construction of Building 6. This fill zone is hydraulically important because the water table is located within this Artificial Fill unit. The other fill zones are not hydraulically important because the groundwater table is below this unit.

Figure 8 shows a thin layer of the Colluvium unit of less than 10 ft in most of the Old Town area. This soil layer does not conduct saturated groundwater in most of the area, where the water table fluctuates within underlying units. However, the Colluvium unit underlying Building 58 and west of Building 58 (with thickness of about 10 ft) does contribute to saturated groundwater flow under conditions of a stable water table.

Figure 9 clearly identifies the three major Moraga bowls at the Old Town site. The first one (Large Bowl) is located in the area of Buildings 52, 53, and 27; the maximum thickness is approximately 85 ft, and the saturated groundwater flows within the highly permeable zone from the upstream boundary downward to Building 46. The second Moraga bowl (Small Bowl) underlies Building 6, with a maximum thickness of 35 ft; this bowl is smaller, but may be important for transport because contaminants may spread within this bowl. In the south, the third Moraga bowl (South Bowl) underlies Building 25; groundwater flows mainly within the Orinda Formation underlying the Moraga bowl. These discontinuous bowls are important parts of the hydrogeologic model in that they may fill during the wet winter months, resulting in outflow if the water levels reach a critical level.

Figure 10 shows that the maximum thickness of the Mixed unit exists at the north edge of Building 7. Permeability in this area is very small; this low permeability helps maintain high water levels monitored in a cluster of monitoring wells in the area of Building 7. The major contaminant plume originated from this area. Note that no thickness plot was available for the Orinda unit because this unit is very deep.

As indicated in Figures 2 and 5, a geologic divide exists between Large Bowl and the area downstream of Building 58. This divide is formed by the low-permeability Mixed unit and Orinda Formation. To the east of the divide is the thick, water-bearing Moraga Formation. To the west there is a steep downhill slope to the ground surface. This divide prevents groundwater flow in the east-west direction and forms the constrained channel for groundwater flow within Large Bowl. It may explain the co-existence of two separate trends of the contaminant plume originating along the north edge of Building 7. As shown in Figure 1, the main plume forms within the Mixed unit toward Building 58, while a smaller plume exists in Large Bowl towards Building 46. Note also that a saddle at the lower top elevation of the Mixed or Orinda Formation exists within this divide east of Building 47. This saddle is overlain by a thin layer of the Moraga Formation. It may provide a pathway for groundwater flow from Large Bowl to the west when the groundwater level is high enough (e.g., in winter seasons).

3. Development of the Groundwater Flow Model

Based on the developed hydrogeologic model, we developed a numerical model to simulate the variably saturated groundwater flow at the Old Town site. The saturated flow below the water table and the unsaturated flow above the water table were simulated simultaneously, because the time-dependent water table level was unknown until the solution was obtained. Flow model development includes determination of model domain and boundary conditions, initial conditions, net recharge, storm drain leakage, and mesh generation. Model calibration and validation are presented in Sections 4 and 5, respectively.

3.1. Software Used

The TOUGH2 code with module EOS9 is used for the forward simulation of saturated-unsaturated groundwater flow (Pruess et. al., 1999). The module EOS9 accounts for pressure distributions in the saturated zone and saturation distributions in the unsaturated zone. While TOUGH2-EOS9 is designed specifically to simulate unsaturated and saturated flow, the main focus of this report is on saturated flow. A preprocessor and postprocessor are developed in C++ to construct the input files for TOUGH2 forward runs and to analyze simulation results for the complicated groundwater system.

Within the Old Town, an unsaturated zone of relatively small thickness exists in the top portion of the groundwater system. Since the detailed flow processes in the unsaturated zone are not the main focus of this report, a simple (linear) constitutive model is used for the relative permeability and capillary pressure functions. The residual saturation used is 0.1, and the saturation value for the relative permeability of 1.0 and the capillary pressure of 0.0 is 0.8 (Pruess et. al., 1999). The maximum capillary pressure used at the residual saturation is 980 Pa. Initially, all mesh elements above the water table are considered dry, and their saturation is at the residual value. Residual saturation is also assigned to all boundary elements above the water table specified in boundary conditions. This specification of residual saturation ensures that there is little or no boundary flux through the

unsaturated zone along the model boundary, a valid assumption because the flow in the unsaturated zone is mainly vertical.

The elevation of the water table was directly obtained from the pressure and saturation distributions obtained in TOUGH2 simulations. An element is considered saturated when its calculated pressure is larger than the reference air pressure and when saturation is close to or equals 1.0. The elevation of the water table is calculated using the elevation and simulated pressure of the first (top) saturated element in a vertical column, as follows

$$Z_{wt} = Z + \frac{P - P_{air}}{\rho_w g},$$

where Z_{wt} is the water table elevation (in meters), Z and P is the elevation and simulated pressure of the top saturated element, P_{air} is the reference pressure in Pa, ρ_w is the density of water, and g is the gravitational acceleration.

3.2. Model Domain

Several factors were taken into account in determining the extent of the model domain. First of all, the groundwater model was intended to provide a basis for understanding the contaminant transport at the Old Town site and was designed as a first step in the development of a full transport model. Therefore, the three major contaminant plumes at the site were included within the flow model system: the Building 7 plume (B7 lobe), the Building 52 plume (B52 lobe), and the Building 25A plume (B25A lobe). Second, the groundwater flow in the main water-bearing unit, the Moraga Formation, needs to be adequately described. Consequently, all three Moraga bowls defined in Section 2 need to be included. Finally, it is difficult to define appropriate boundary conditions for the system because the water table varies significantly in time and space. Therefore, the model boundaries were placed along monitoring wells so that the measured water levels could be used as boundary conditions. At some locations where monitoring wells are not available, flow paths were used to define no-flow boundaries.

Figure 11 shows the model domain in a plan view. The model boundary consists of four boundary-segment groups, with the water table prescribed and four no-flow boundary segments connecting these groups. The four groups are the upstream McMillan Road group, the Building 46 (B46) group, the Building 58 (B58) group, and the Building 6-Lawrence Road (B6) group. A boundary segment group may consist of one or more boundary segments, which in turn contain a number of boundary points (or columns in three dimensions). All boundary points share the same boundary conditions or the same interpolation scheme for boundary conditions. Figure 12 shows the hydrogeologic units in a vertical cross section along the model boundary. The cross section starts at the northwestern corner (Point A) at the UC coordinate (2530, 790) ft, and follows the boundary in a counterclockwise direction. The figure also shows the minimum and maximum water levels measured from 1994 to 1996.

The upstream boundary on the east is along McMillan Road from Point J at the UC northing of 800 ft down to Point G around Building 76 (see Figure 11). On the eastern side of the boundary group, few boreholes are available and the geology is unknown. Groundwater flowing from the uphill region into the model domain is a major water source for the Old Town groundwater system. On the upstream boundary, four monitoring wells were used to determine first-type boundary conditions. The water table changes from about 830 ft in the north up to 920 ft in the southeast. Of the several upstream segments, the segment between Points H and I in Figure 11 is the most important to the groundwater system. This is because most of the system inflow through the model boundary is through this segment, with groundwater flowing within the permeable Moraga Formation into Large Bowl (see Figure 12). This segment was referred to as "B52 influx" segment.

The downstream boundary consists of three boundary segment groups: the B46 group between Points A and B, the B58 group between Points C and D, and the B6 group between Points E and F. The B46 group is located at the east edge of Building 46. A groundwater collection trench extends along this boundary, where contaminated water has been collected for remediation. The water table is maintained at 800 ft in the trench, as observed in well MW46-93-12, and the uniform-constant-head condition can be specified along this boundary. As shown in Figure 12, a small cross-sectional area of the Moraga Formation below the water table accounts for almost all outflow through this boundary segment, through which most of the system outflow moves.

The B58 group (between C and D) was determined based on the groundwater collection trench and the measured water table contours. Contaminated groundwater has been collected in the trench since 1998. The measured flow rate in the trench was used for calibrating the groundwater model. Monitoring wells MW46-92-10 and MW58-95-14 were used to determine the first-type condition on the three boundary segments. Note that these wells have small seasonal fluctuations. Groundwater flows out of the system through the small cross-sectional area of the Artificial Fill unit, Colluvium unit, and Moraga Formation under the water table (see Figure 12).

In the B6 group, four boundary segments exist with first-type conditions. For the first segment along Building 6, few monitoring wells are available to determine the boundary conditions. Because the boundary segment is comprised mainly of the low permeable Orinda Formation, the flow rate crossing this boundary segment is small. The water table contour was drawn using the measured water levels at all monitoring wells, and was corrected by means of the measured water levels at MW37-92-18 and the additional information from the developed hydrogeologic model. The boundary was determined based on the estimated iso-water-level contour line through MW37-92-18. The remaining boundary segments were determined using MW37-92-18, MWP-8, and MW25-95-27. East of MW25-95-27, the boundary stretches along the measured-water table contour line through MW25-95-27.

No-flow boundary segments connect the above four boundary-segment groups. These segments were defined using water table contours measured in about 70 monitoring wells at the Old Town site. No-flow boundary segments are appropriate where (1) contours of the water table are approximately

parallel to contours of the ground surface and main hydrogeologic units, and (2) where this behavior is independent of seasonal fluctuations. The definition of these no-flow boundaries was confirmed below by the simulation results in Sections 4 and 5. Note that there are significant head drops along these model boundaries. For example, along the no-flow boundary between the B58 and B6 groups, the head drops from 830 to 780 ft. In such a mountainous system, steep gradients and significant head drops along and across model boundaries provide formidable modeling challenges.

The ground surface shown in Figure 3 defined the top boundary. The bottom boundary was set approximately 60 ft below the top surface of the Orinda Formation. The exact location of the bottom boundary is not important, as long as there is a sufficient vertical distance from the bottom boundary to the water table. Figure 13 shows the elevation of the bottom boundary, which give a domain thickness that varies from 60 ft to 110 ft.

3.3. Mesh Generation

WinGridder 2.0 (Pan, 2001) was used to generate a three-dimensional mesh for the TOUGH2 simulations. The hydrogeologic model and the model-domain boundary were used as input to WinGridder. Figure 14 shows the centroids of vertical columns in the three-dimensional TOUGH2 mesh. Four regions with different mesh resolutions were defined. The first region (Region 1) was defined so as to capture the flow in Large Bowl where groundwater flows toward Building 46. Here the discretization was 18 ft by 18 ft. In the second region (Region 2), the mesh was refined to capture the flow and contaminant plume starting from Building 7 and extending toward Building 58; the cell dimensions were 22 ft by 22 ft. In the northern region (Region 3), groundwater flows primarily from east to west; the discretization was 35 ft by 35 ft. In the southern section (Region 4), groundwater flow occurs mostly within the Orinda Formation, which has low hydraulic conductivity; the discretization was 35 ft by 35 ft. In addition, the mesh was oriented based on flow directions obtained from the measured and simulated water table data. For example, in Large Bowl, the mesh was generated in the direction of 140° with respect to the UC east-west direction and along the main flow direction toward Building 46.

With respect to the vertical direction, the maximum discretization for the Artificial Fill unit, Colluvium unit, Moraga Formation, Mixed unit, and Orinda Formation were 6, 6, 6, 7, and 10 ft, respectively. The minimum discretization for each hydrogeologic unit was 0.1 ft. If the thickness of a unit is less than the minimum discretization, then this unit does not appear in the generated mesh, and the thickness was added to the upper or lower unit.

For the mesh we have 931 vertical columns, including 107 boundary ones, 12,994 elements, and 41,319 connections. This relatively coarse mesh was generated because a large number of forward runs were needed in the calibration to be discussed in Section 4. A refined mesh was used for later model validation, in which only a forward run was needed.

3.4. Boundary Conditions

Boundary conditions for the numerical model were determined using the measured water levels at a number of monitoring wells located on or close to the model boundary. These boundary wells include MW46-93-12, MW46-92-9, SB58-98-17, MW58-95-18, MW37-92-18, MWP-8, MW25-95-27, MW26-92-11, and MW52-94-10 (see Figure 11). In addition, MW91-9 and MW52-95-2B, located within the model domain away from the boundary, were used to project the measured water levels to the upstream boundary. There are three kinds of conditions for boundary segments: no-flow condition, spatially uniform head condition, and spatially varying head condition. All boundary conditions with specified heads are time dependent, because of the strong seasonal changes in the groundwater system.

There are six no-flow boundary segments, marked in black in Figure 11. Of the six no-flow boundary segments, two segments are located in the upstream boundary group. These two segments are located next to the "B52 influx" boundary segment. The determination of the two segments was based on the observation that the water table remains time independent at the interface between the upper, permeable Moraga Formation and the lower, much-less-permeable Mixed unit and/or the Orinda Formation. Because flow through these less permeable units is negligible, a no-flow boundary was used. Groundwater flow in all other four no-flow segments is along the boundary, which is perpendicular to water table contour lines.

There are six boundary segments marked in red in Figure 11. On each of these boundary segments the water levels are spatially uniform, but vary in time to represent seasonal fluctuations. Uniform head condition was specified using the measured water level at a representative well. For example, the measured water level at MW46-93-12 was used to specify hydraulic head on the segment for the B46 group.

There are six boundary segments with spatially varying head conditions, so specified, because the water level varies significantly along their boundary segments. The condition in each boundary column located within a boundary segment was determined by linearly interpolating the measured water levels at two representative wells. For example, the water levels in the boundary segment between MW37-92-18 and MWP-8 were determined by spatial interpolation of the measured water levels in the two wells.

In some cases, boundary wells started to measure after the onset of simulation. When the starting time of measurements of the water level is later than the initial time of simulation (July 1, 1994), an extrapolation of water level was calculated using a representative well, close to the boundary well. For example, there are two representative wells for the "B52 influx" boundary segment: MW52-94-10 and MW52-95-2B. The water level at MW52-95-2B was interpolated for the first simulation time period using the measured water level at MW53-93-9. Extrapolation was conducted using the minimum water level and the ratio of seasonal changes between the two wells. The measured water level at MW46-92-9 is not reliable; the water level at this well was interpolated using the levels at MW46-93-12 and MW51-94-15. At SB58-98-7, which is located in the Building 58 collection trench,

the water level fluctuates between 778 ft in the summer and 780 ft in the winter. Linear interpolation in a year at the well was used, and the same pattern was used for each year.

Note that seasonal water level changes in the upstream boundary group are significantly larger than those in the downstream boundary groups. For example, the measured water-level fluctuates between 913.9 ft in the summer to 926.5 ft in the winter at MW26-92-11; the measured water level at MW52-95-2B ranges from 837.1 ft to 859.2 ft. In the B58 boundary group, the seasonal change in water level is less than 4.0 ft (see Figures 22 and 23).

Figure 12 shows the maximum and minimum water levels specified along the model boundary with hydrogeologic information. Along the downstream boundary, there are two segments with significant groundwater flow resulting from large hydraulic conductivity. The first is along Building 46 (Section Segment A–B), where groundwater flow leaves the model domain through a small saturated cross-sectional area of the Moraga Formation. This area accounts for most of the outflow from the groundwater system. The second most significant outflow is located in the B58 group (Section Segment C–D), with a small cross-sectional area of the Artificial Fill and Colluvium units. This small area may account for 10-20% of the total outflow of the system. Most segments of the downstream boundary are located within the Orinda Formation of low hydraulic conductivity, so that these boundary segments account for a small fraction of the total outflow.

On the upstream boundary, the most important boundary segment is the so-called “B52 influx” segment (H–I). In the winter, when the water table is higher, a large influx occurs within the large saturated cross-sectional area of the Moraga Formation. In the summer, when the water table is lower, influx is much smaller, as can be inferred from Figure 12.

3.5. Initial Conditions

The initial condition for the transient simulation runs was interpolated based on the measured water levels at a number of monitoring wells. The starting time for the simulation was selected at June 30, 1994, which is in the dry, summer season. The groundwater system can adjust to the specified initial conditions for a few months prior to the first rainfall in September 1994.

The measured water levels at 47 monitoring wells and the interpolated water level along the boundary were used to interpolate the water table for the 931 columns (in the numerical mesh for model calibration). For the monitoring wells completed after June 1994, we used the measured water levels at June 30, 1995 or 1996 to approximate the initial water levels at June 30, 1994.

Figure 15 shows the interpolated initial water table at June 30, 1994 and the wells used for interpolation. Because the interpolation does not reflect the effect of rock-property heterogeneity, the effect of South Bowl on the water table was not represented. In addition, the sharp change in the water table at the southern edge of Large Bowl was also not accounted for. A better representation of the buildup of the water table was achieved at the northern edge of Building 7, where a cluster of monitoring wells were available.

3.6. Recharge and Storm Drain Leakage

Groundwater flow at the site is strongly affected by direct infiltration from rainfall, as well as from leakage from storm drains and other underground utilities, such as domestic water lines and drains. Careful estimate of the infiltration from these water recharge sources is essential for the model, because the seasonal fluctuations of the groundwater table are strong in most of the system, indicating that recharge is an important contribution to water balance.

The areal net recharge through the unpaved areas of the model domain was calculated from the rainfall intensity, the size of the unpaved areas, and a recharge factor (fraction of rainfall infiltrating into groundwater). Appropriate recharge factors were estimated from the slope of the topography and the properties of the surficial soil. Some buildings also contribute to direct infiltration because the rainfall on their roofs directly drains into neighboring unpaved areas. For all paved areas, like parking lots or streets, we used a small recharge factor of 0.02 to represent unaccounted infiltration through small flower beds and pavement joints and cracks, which are too small to be included individually. Figure 16 shows the four types of infiltration areas defined on the basis of the types of land surface coverage and topographic slopes. In each type of infiltration area, further classification was conducted based on the properties of the surface geology.

Table 1. Recharge factor for different kinds of topography

	Paved		Unpaved	
	Building roofs	Others	Steep Slope	Gentle Slope
Soil/Fill	0.07	0.02	0.01	0.07
Moraga	0.40		0.01	0.40
Orinda	0.07		0.01	0.07

Evidence of corroded metal pipes and ruptured concrete pipes has been observed in the field (Zhou et al., 2004). While leakage through such storm drains is critical to the local groundwater system, estimating the amount of leaking water is difficult because it depends on many parameters, such as catchment area, type of damage, and soil type. In the model, storm-drain leakage was calibrated in a systematic manner. First, subsurface utility maps were employed to locate zones of potential leakage from corroded storm drains. Second, for each of the corroded storm drains, the number of pipe segments contributing to leakage and their corresponding discharge catchments were determined. Third, a simple pipe model was developed, based on water balance, without considering changes in mass storage inside a pipe segment. Finally, the recharge factor for each segment was calibrated (with rock properties) using the measured groundwater level at monitoring wells.

In the Old Town area, three locations were confirmed to have a significant amount of water leaking out of storm drains or other underground utilities, as shown in Figure 17. The first one is in the north edge of Building 7. This storm drain consists of four pipe segments with different catchment

areas; the first segment at the upstream end receives discharge from the purple catchment of 5,991 sq ft; the catchment directly discharging to the second segment covers 49,745 sq ft; the catchment to the third segment covers 17,534 sq ft; no catchment exists for the fourth segment. The total flow rate into a segment depends on its catchment area, the flow rate coming from the upstream pipe, a recharge factor defining the relative amount of leakage into the underlying volume, and the rainfall rate. It was assumed that 98% rainfall in the catchment areas discharges into the inlet of the pipe, because most of the catchments are paved with a small recharge factor. The total flow rate effectively leaking into the groundwater system, R_i, in the *i*th segment was calculated as:

$$R_i = F_i\left(A_i I + Q_{i-1}\right) \text{ and } Q_i = \left(1 - F_i\right)\left(A_i I + Q_{i-1}\right)$$

where *F* is the recharge factor for the pipe segment, *A* is the area of catchment discharging directly into the pipeline, *I* is net rainfall rate, the Q_{i-1} is the discharge flow rate into the *i*th pipe segment from the upstream segment, and Q_i is the discharge flow rate away from the *i*th segment into the $i+1$ segment. As mentioned above, the catchment areas for the four segments in the B7 storm drain are 5,991, 49,745, 17,534, and 0 sq ft, respectively. The recharge factor for the four segments was 2, 4, 2, and 2%, respectively.

In the TOUGH2 model, each storm-drain segment was represented by a specific element that was added to the mesh. The connections between a storm-drain element and the underlying elements were included within the connection block. Since the lateral spread of the leaked water within the unsaturated zone cannot be appropriately modeled using the mesh selected, we elected to approximate the infiltration by assuming that water was introduced into an effective area around the drains that is three mesh-elements wide.

Storm-drain leakage was also believed to occur in the north edge of Building 14 and in a narrow strip between Buildings 6 and 7 as shown in Figure 17. The recharge from the two storm drains was estimated using a recharge factor. The recharge areas for the two storm drains were 1856 and 2420 sq ft, and the recharge factors were 0.4 and 0.6, respectively.

4. Calibration of Rock Properties

The hydraulic conductivity and “effective” porosity in the five hydrogeologic units were calibrated using the iTOUGH2 code (Finsterle, 1999). In the three-step process, we first defined rock zones of different rock properties for each hydrogeologic unit to capture the heterogeneity of rock properties; the zonation was based on measured hydraulic conductivity values obtained by slug and pumping tests. Second, we calculated the geometric mean and standard deviation of log hydraulic conductivity in each rock zone using the hydraulic conductivity measurements. Finally, we calibrated rock properties for each rock zone by matching the simulated and measured water levels in a number of monitoring wells and by matching the simulated and measured flow rates in the trenches at

Buildings 46 and 58. The time period for the transient calibration is from July 1, 1994, to June 30, 1996.

4.1. Hydraulic Conductivity Measurements

Three methods were used for measuring hydraulic conductivity at the LBNL site: slug tests, pumping tests, and tracer tests (LBNL, 2000). Slug tests were conducted in 105 wells. Test data were analyzed using a computer curve-matching program based on the method of Cooper and others (Cooper et al., 1967) and assuming radial flow away from a fully penetrating well in a confined aquifer. The calculated hydraulic conductivities range from approximately 10^{-10} to 10^{-4} m/s for the five hydrogeologic units. The slug-test calculations for a four-level well cluster indicated extremely low hydraulic conductivity, on the order of 10^{-12} to 10^{-13} m/s, in the Orinda Formation. Pumping tests were conducted in a limited number of wells, primarily in the area of the Old Town groundwater plumes where a sufficient drawdown could be generated. Hydraulic conductivity and storativity were computed using the computer program AQTESOLV, employing a modified Theis solution (Neuman, 1975).

In the entire Old Town area, there are 17, 9, 39, 6, and 37 measured hydraulic conductivity values available for the Artificial Fill unit, Colluvium unit, Moraga Formation, Mixed unit, and upper Orinda Formation, respectively. However, many of these measurements are located outside of the model domain. In the model domain, there are 1, 1, 30, 6, and 13 measured hydraulic conductivities assigned to the five units, respectively. We combined the measurements obtained from slug tests and pumping tests. When both tests were conducted at a well, the results from pumping tests were used. Figures 18–20 show the measured hydraulic conductivity values available for the Moraga Formation, Mixed unit, and Orinda Formation in the model domain, respectively.

In the Artificial Fill unit, the one measured hydraulic conductivity in the model domain is 1.58×10^{-8} m/s. This measurement is located in a large artificial fill zone in the north edge of Building 6. In the entire Old Town area, the measured hydraulic conductivity ranges from 2.24×10^{-9} to 4.00×10^{-6} m/s, with a geometric mean of 2.75×10^{-7} m/s. There is one measured hydraulic conductivity of 3.98×10^{-6} m/s available for the Colluvium unit in the model domain. The nine measurements in the entire Old Town area range from 5.01×10^{-10} to 3.98×10^{-6} m/s, with a geometric mean of 1.12×10^{-7} m/s.

For the Moraga Formation, the 39 measurements in the entire Old Town area have a geometric mean of 2.81×10^{-6} m/s. The 30 measured hydraulic conductivity values in the model domain indicates that the Moraga Formation is strongly heterogeneous (see Figure 18). Three major zones of hydraulic conductivity within the model domain can be defined. The most permeable zone is located in Large Bowl. Small Bowl along Building 6 and South Bowl have intermediate values of hydraulic conductivity. The least permeable zone is located in the north edge of Building 7 at the edge of Large

Bowl. The largest value of measured hydraulic conductivity occurs in the east edge of Building 46, with a value of 3.98×10^{-4} m/s; the smallest value is located in the north edge of Building 7, with a value of 1.26×10^{-9} m/s.

The six measured hydraulic conductivity values for the Mixed unit are available around Building 7 within the model domain (see Figure 19). Apparently, there are three zones of hydraulic conductivity. In the east edge of Building 6, the Mixed unit is most permeable, with a geometric mean value of 1.58×10^{-6} m/s. In the west of Building 7, the Mixed unit is the least permeable, with a geometric mean of 3.55×10^{-9} m/s. To the east of Building 7, the mean hydraulic conductivity is 1.58×10^{-7} m/s.

Figure 20 shows that the Orinda Formation is very permeable to the north of Buildings 5 and 25. The two permeable areas are connected through a narrow area to form a highly permeable zone, with a (geometric) mean hydraulic conductivity of 3.69×10^{-5} m/s. In the northwest portion of the model area, one measurement of hydraulic conductivity is available, with a value of 1.0×10^{-11} m/s. In the south of the model domain, the hydraulic conductivity in the Orinda Formation is on the order of 10^{-7} m/s with strong variability. In the Old Town area, the geometric mean of the 37 measured hydraulic conductivities of the Orinda Formation is 4.27×10^{-8} m/s.

4.2. Zonation of Rock Properties

It can be seen in Figures 18-20 that the Moraga Formation, Mixed unit, and Orinda Formation are strongly heterogeneous in the model domain. Therefore, it is necessary to define rock zones of different rock properties in each of the three units to accurately simulate groundwater flow for both global and local characteristics. Heterogeneity plays an important role in affecting the local groundwater features, particularly beneath the north edge of Building 7. In the Artificial Fill and Colluvium units, few measurements of hydraulic conductivity in the model domain are available to define the heterogeneity of rock properties. However, the major fraction of these units lies above the water table and therefore they do not contribute to the saturated groundwater flow. For this reason, we assumed uniform rock properties within each of the two units.

The zonation of the three major groundwater-bearing units (the Moraga Formation, the Mixed unit, and the Orinda Formation) was based on the analysis of the measured hydraulic conductivity values and the availability of monitoring wells in each of the zones. It was also based on our understanding of local features of the groundwater system. Rezonation was needed for some zones based on the match between measured and simulated water levels at a number of monitoring wells.

Figures 18–20 show the zonation of rock zones of different rock properties for the Moraga Formation, the Mixed unit, and the Orinda Formation, respectively. There are nine rock zones for the Moraga Formation, five zones for the Mixed unit, and four zones for the Orinda Formation. Within

some of the rock zones, the values of measured hydraulic conductivity are very close to each other, exhibiting the clustering feature of similar hydraulic conductivity.

Tables 2–4 list the definition of rock zones, available hydraulic conductivity measurements, the geometric mean and standard deviation, and available monitoring wells for the Moraga Formation, the Mixed unit, and the Orinda Formation, respectively. In each zone, the geometric mean of measured hydraulic conductivity values was calculated when one or more measurements are available; when there is no measurements for a particular zone, the geometric mean of all measurements in the model domain was used. The standard deviation was calculated directly using the measurements in a zone when three or more measurements are available; otherwise, the standard deviation calculated for the entire model domain was used. The geometric mean of hydraulic conductivity in a zone was used as prior information to the optimal rock properties to be calibrated; the standard deviation was used as the weighting factor in iTOUGH2.

The appropriate zonation of rock properties is particularly important in the area north of Building 7. In this area, the local groundwater system is very complicated because of the interaction between the different hydrogeologic units and the strong heterogeneity of rock properties. The water table builds up at the steep slope of the interface between the Moraga Formation and the Mixed or Orinda Formation. To improve the initial zonation, we found it necessary to make the following changes: (1) extend the Moraga zone 7 (mrg37) to the east to include MW16-94-13; (2) extend the Mixed zone 3 (mix43) east to the upstream boundary; and extend the Orinda zone 3 (ord53) south to be in contact with Orinda zone 2 (ord52). This rezonation increased the water table in the B7 area and improved the match between the measured and the simulated water table in this area. The other important zone is the Orinda zone 2 (ord52), located close to the upstream boundary in the north of Buildings 5 and 25. Unlike other zones of the Orinda Formation, this zone is highly permeable, conducting groundwater from the upstream boundary downstream to Small Bowl underlying Building 6. This zone supplies a stable discharge to the Building 58 boundary.

One rock zone was used for the Artificial Fill and Colluvium unit. The geometric mean and standard deviation of the measured hydraulic conductivity in the entire Old Town area for the two units was calculated and used to represent those in the model domain. The mean log conductivity is –6.6 for the Artificial Fill unit and –6.9 for the Colluvium unit. The standard deviation is 0.9 and 1.31 for the two units, respectively, as shown in Table 4.

Table 2. Rock zones of different rock properties for the Moraga Formation, with available hydraulic conductivity measurements and monitoring wells

Zone name	Log hydraulic conductivity			Monitoring wells
	Measurements (log m/s)	Mean	Standard deviation	
Zone 1 (mrg31) (base case)	-6.0	-6.0	1.15*	
Zone 2 (mrg32) (upstream boundary)	-5.7, -5.8, -5.9	-5.8	1.15*	B46 Boundary flux
Zone 3 (mrg33) (large Moraga bowl)	-4.8, -4.4, -4.2, -4.5, -4.7	-4.5	0.24	MW91-8, MW53-93-17, MW53-93-9, MW52-95-2B, MW91-7, MW53-93-16B
Zone 4 (mrg34) (B46 boundary)	-3.4, -4.9	-4.1	1.15	MW27-92-20, MW46-93-12
Zone 5 (mrg35) (B6 Moraga bowl)	-6.1, -6.3, -6.5, -6.4, -5.9, -5.7, -6.0, -5.6, -5.5	-6.0	0.32	MW6-92-17, MW16-95-3, MW6-95-14, MW7-92-16, MW58-95-11, MW58-93-3
Zone 6 (mrg36) (B25 Moraga bowl)	-5.2, -6.3	-5.8	1.15*	MW25-95-5, MW25-93-15, MW25-94-12
Zone 7 (mrg37) (B7 low K edge)	-6.6, -8.0, -8.9, -5.9	-7.4	1.35	MW7B-95-21, MW7-95-22, MW7-95-23, MW7B-95-24, MW7B-95-25, MW90-2, MW7-92-19, MW52B-95-13, MW16-94-13, MW7-94-3
Zone 8 (mrg38) (B58 bowl)	-7.8, -5.3	-6.6	1.15*	MW58A-94-14
Zone98 (mrg39) (B25 North)	-4.4, -6.0	-5.2	1.15*	

*Note: for a rock zone with less than four measurements, the standard deviation calculated using all the measurements in the Moraga Formation is used.

Table 3. Rock zones of different rock properties for the Mixed unit with available hydraulic conductivity measurements and monitoring wells

Zone name	Log hydraulic conductivity			Monitoring wells
	Measurements (log m/s)	Mean	Standard Deviation	
Zone 1 (mix41) (base case)		-7.0	1.25*	
Zone 2 (mix42) (B6)	-5.5, -6.1	-5.8	1.25*	MW6-92-17, MW16-95-3
Zone 3 (mix43) (B7 east)	-6.6, -7.0	-6.8	1.25*	MW52B-95-13, MW16-94-13, MW7-94-3, MW52-93-14
Zone 4 (mix44) (B7 west)	-8.0, -8.9	-8.5	1.25*	MW7B-95-21, MW7-95-22, MW7-95-23, MW7B-95-24, MW7B-95-25, MW7-92-19, MW90-2
Zone 5(mix45) (B25 mixed bowl)		-7.0	1.25*	MW25-95-5, MW25-93-15, MW25-94-12

*Note: for a rock zone with less than four measurements, the standard deviation calculated using all the measurements in the Mixed unit is used.

Table 4. Rock zones of different rock properties for the Orinda Formation, with available hydraulic conductivity measurements and monitoring wells, and rock zones of the Artificial Fill and Colluvium units

Zone name	Log hydraulic conductivity			Monitoring wells
	Measurements	Mean	Standard deviation	
Zone 1 (ord51) (base case)	-6.7, -6.7, -7.1, -8.1, -10.5	-7.8	1.42	MW25A-95-4, MW37-92-5, MW25A-95-15
Zone 2 (ord52) (B25 high K)	-4.0, -4.6, -4.7, -6.2	-4.9	0.38	MW91-9, MW5-93-10
Zone 3 (ord53) (North Low K)	-10.9	-10.9	2.07*	
Zone 4(ord54) (South Low K)	-6.1, -7.6, -7.9	-7.2	2.07	
Artificial Fill (fil11) (the Old Town area)	-7.3, -6.5, -6.4, -6.2, -6.1, -6.1, -5.7, -7.8, -7.5, -7.3, -7.0, -8.6, -6.3, -6.0, -5.6, -5.6, -5.4	-6.6	0.90	
Colluvium (quu21) (the Old Town area)	-9.3, -8.9, -6.5 -5.9, -7.0, -6.7 -6.5, -6.2, -5.4	-6.9	1.31	

*Note: for a rock zone with less than four measurements, the standard deviation calculated using all the measurements in the Orinda Formation is used.

4.3. Groundwater Subsystems

To better understand and describe the Old Town groundwater system, we divided the entire system into four subsystems, based on the heterogeneity of rock properties and local characteristics of groundwater flow and the water table (see Figure 26). The first subsystem (called the Large Bowl subsystem) is located in Large Bowl, where flow occurs in the highly permeable and thick Moraga Formation. The water table is flat with large seasonal fluctuations. This subsystem is recharged by the influx from the upstream boundary and by rainfall. Groundwater flows toward Building 46 within Large Bowl confined by the interface between the Moraga Formation and the underlying Mixed or Orinda Formation (see Figure 5).

The second subsystem (called the B7 subsystem) is located at the north edge of Building 7, between the first and the third (or the fourth) subsystem. There are several wells installed for monitoring the water table and the contaminant transport in the Building 7 area. The heterogeneous

rock properties and the steep slope of the bottom of the Moraga Formation make it difficult to accurately simulate the local features of water table and groundwater flow.

The third subsystem (called the Small Bowl subsystem) is in Small Bowl underlying Building 6. This subsystem is recharged by groundwater from the upstream Orinda Formation and two possible leaking storm drains located at the north of Building 14 and between Buildings 6 and 7. Groundwater in this subsystem supplies stable discharge to the Building 58 area, where groundwater has been collected in the B58 trench at a rate of about 10,000 gal/month.

The fourth subsystem (called the South Orinda subsystem) is located in the south of the Old Town area. The saturated groundwater flow occurs primarily within the Orinda Formation with low hydraulic conductivity. The water table changes from above 900 ft on the upstream boundary down to about 830 along the downstream boundary (the B6 boundary group).

4.4. Inverse Modeling

We applied the iTOUGH2 code (Finsterle, 1999) to the calibration of rock properties in the defined 20 rock zones within the five hydrogeologic units. The most important properties are the rock hydraulic conductivity and “effective” porosity. The “effective” porosity was defined for the modeling purposes as the mean continuum porosity of a rock zone, possibly representing the composition of the complicated rock porosity. For example, in the Mixed unit, thin layers of higher hydraulic conductivity have been found within the bedrock of very low conductivity, leading to a fast response in water table changes with seasonal fluctuations (Zhou et al., 2004). The “effective” porosity may be less than the actual physical porosity calculated using rock cores. “Effective” porosity and hydraulic conductivity in each zone were calibrated as model parameters. The measurement inputs to iTOUGH2 are the measured water-level series at 37 monitoring wells, and the flow-rate series collected in the Building 46 trench and Building 58 trench.

In addition, the geometric mean of measured hydraulic conductivity described in Section 4.2 was used as prior information for the parameters to be calibrated. For the three different kinds of measurements (measurements of hydraulic conductivities, water levels, and boundary flow rates), the weighting factors of each measurement in the objective function were selected based on its standard deviation. The standard deviation of 2,000 Pa (0.2 m) was used for the measured water level at each monitoring well. The values of 4,000 gallon/month were used for the standard deviation of flow rates measured in the B46 and B58 trenches. The standard deviations shown in Tables 2–4 were used for the measured hydraulic conductivities in different rock zones.

Because the four groundwater subsystems are separated yet interconnected. We conducted the calibration in two steps. In the first step, rock properties specific to a subsystem were calibrated independently, using the measurements within the subsystem. For example, the hydraulic conductivity of Moraga Zones 2, 3, and 4 (see Table 2 and Figure 18) was calibrated in the Large Bowl subsystem. The measurements used are the measured water levels at the monitoring wells: MW27-92-20, MW91-

8, MW53-93-17, MW53-93-9, and MW53-95-12, and the flow rates collected in the B46 trench. In the second step, the rock properties common to two or more subsystems were calibrated using all measurements in the entire groundwater system. This calibration method was used to avoid unphysical results obtained using the do-it-all-at-once method, which produces very small seasonal fluctuations around the mean water levels at some wells.

4.5. Calibration Results

Table 5 shows the calibrated values of hydraulic conductivity and "effective" porosity for the 20 rock zones in the five hydrogeologic units. Figure 21 shows the comparison between the calibrated hydraulic conductivity values and their prior ones.

The calibrated hydraulic conductivity for Moraga Zone 3 (mrg33) in Large Bowl is close to the geometric mean of the measured values in this zone. The measurements, obtained using pumping tests at five monitoring wells (MW91-7, MW91-8, MW27-92-20, MW53-93-9, and MW53-93-17) within the rock zone, are reliable, with a small standard deviation of 0.24.

The calibrated hydraulic conductivity for Moraga Zone 2 (mrg32) on the upstream boundary may not be the physical conductivity there. This is because on this boundary segment, where the most inflow occurs, uncertainties exist in determining the boundary conditions (water table) using linear interpolation between Well MW52-94-10 and MW52-95-2B, and in the development of the hydrogeologic model. This calibrated value represents the optimal value obtained under the given assumptions. The calibrated hydraulic conductivity in Moraga Zone 4 (mrg34) may be influenced by various uncertainties in the estimation of recharge and upstream inflow rates. The calibrated hydraulic conductivities for mrg32 and mrg34 are also close to their prior values, indicating that the measured hydraulic conductivities in the two rock zones are reliable.

For Moraga Zone 5 (mrg35) in the Small Bowl subsystem, the calibrated and the measured hydraulic conductivities are in close agreement, indicating that the measured hydraulic conductivities are reliable. Of the nine measurements listed in Table 2, four were obtained using pumping tests and the others were obtained using slug tests. All nine measured hydraulic conductivities are very close, with a small standard deviation of 0.32. It can be seen that Small Bowl is less permeable than Large Bowl.

The rock zone of mrg39 was used to control the flow rate from the north high-permeability zone of the Orinda Formation to the high-permeability zone of the Moraga Formation in South Bowl. As the flow rate largely depends on the calibrated hydraulic conductivity of mrg39, we see in Figure 21 that the small calibrated hydraulic conductivity results in a small flow rate recharging South Bowl from the upstream boundary. The calibration of mrdg39's hydraulic conductivity was based mainly on the match between the simulated and measured water-level series for three monitoring wells (MW25-94-12, MW25-93-15, and MW25-95-5) in South Bowl. In dry, summer seasons, the measured water levels are at the interface between the Moraga Formation and the underlying Mixed unit or Orinda

Formation, indicating that the flow rate is low. In wet, winter seasons, there is saturated groundwater flow within South Bowl, because the water level is within the Moraga Formation (see Figure 37).

The largest difference between prior and calibrated hydraulic conductivity occurs for the rock zone (ord53) in the north Orinda Formation. This difference may result from the lowest measured hydraulic conductivity, on the order of 3.5×10^{-11} m/s, which was used as the prior value for calibration. The significant difference may show that the single measured hydraulic conductivity is not reliable.

At the north edge of Building 7, the calibrated hydraulic conductivities for the Moraga Formation (Zone 7), Mixed unit (Zones 3 and 4), and Orinda Formation (Zone 3) units are smaller than in any other locations. This is consistent with what can be seen from measured hydraulic conductivities in Figures 18–20. The water table is located mainly within the Moraga Formation or the Mixed unit in the B7 subsystem. The Orinda Formation has very small hydraulic conductivity, and forces upstream groundwater to flow within the Moraga Formation or the Mixed unit. The low hydraulic conductivity of the Moraga Formation and Mixed units makes it possible to maintain the water table at a relatively high elevation.

Table 5. Calibrated hydraulic conductivities (m/s) and "effective" porosity for the 20 rock zones

Hydrogeologic unit	Zone name	Hydraulic conductivity		Effective porosity
		Prior	Calibrated	
Artificial Fill Unit	fil11	2.5e-7	4.0e-7	0.30
Colluvium Unit	quu21	1.3e-7	4.0e-7	0.30
Moraga Formation	Zone 1, mrg31	1.0e-6	9.7e-6	0.05
	Zone 2, mrg32	1.6e-6	7.0e-6	0.05
	Zone 3, mrg33	3.2e-5	1.9e-5	0.04
	Zone 4, mrg34	7.9e-5	3.7e-5	0.04
	Zone 5, mrg35	1.0e-6	6.3e-7	0.02
	Zone 6, mrg36	1.6e-6	9.7e-6	0.10
	Zone 7, mrg37	4.0e-8	5.0e-8	0.05
	Zone 8, mrg38	2.5e-7	2.5e-6	0.05
	Zone 9, mrg39	6.3e-6	4.0e-8	0.05
Mixed Unit	Zone 1, mix41	1.0e-7	4.3e-8	0.02
	Zone 2, mix42	1.6e-6	2.2e-8	0.07
	Zone 3, mix43	1.6e-7	5.0e-9	0.02
	Zone 4, mix44	3.2e-9	3.0e-8	0.02
	Zone 5, mix45	1.0e-7	4.3e-8	0.02
Orinda Formation	Zone 1, ord51	2.5e-8	1.5e-8	0.03
	Zone 2, ord52	1.3e-5	1.5e-6	0.05
	Zone 3, ord53	1.3e-11	7.0e-9	0.03
	Zone 4, ord54	1.3e-7	2.5e-8	0.03

The match between the calibrated and measured water levels at a number of monitoring wells and the match between the calibrated and measured flow rates at two groundwater trenches for the calibration period from July 1, 1994, to June 30, 1996, will be discussed in the next section, together with the model validation for the time period between July 1, 1996 and June 30, 1998.

5. Model Validation

The development of the conceptual and numerical models has been described in previous sections. The developed model was validated using the "blind" prediction of groundwater flow at the Old Town site for the period from July 1, 1996, to June 30, 1998. During this period, some facilities were established for the remediation of contaminated groundwater. Using these facilities, the contaminated groundwater was extracted by pumping, treated, and then reinjected into the groundwater system to help flush the contaminated groundwater. The effects of the remediation facilities on the local flow were neglected in the model validation, because the model validation was intended to investigate the general picture of groundwater flow. These effects were taken into account in a smaller-scale flow model focusing on the groundwater plume in the north of Building 7, as described in Section 6.

The coarse mesh used for model calibration, described in Section 4, was intended to reduce the computational burden of single forward run on model calibration. The coarse mesh was refined to reduce the inaccuracy of simulation results caused by low mesh resolution. The horizontal discretization in the refined mesh was 18 ft. To match the measured water table at a number of monitoring wells, TOUGH2 nodes were introduced at most of these wells, because the gradients of interfaces between different hydrogeologic units is very large at some locations. The refined mesh consists of 1,901 vertical columns, 39,211 elements, and 118,048 connections. To check the trend of the simulated water table in the entire groundwater system, we simulated the groundwater flow from July 1, 1994, to June 30, 1998, a four-year period that includes both the calibration and validation periods.

Figures 22 and 23 show the measured water-level series at boundary wells in the downstream and upstream boundary groups. The water level in most of the downstream boundary groups is within the Orinda Formation, except for a small cross-sectional area within the Moraga Formation and Artificial Fill/ Colluvium units, as shown in Figure 12. The seasonal fluctuations of the water level are less than 10 ft in the B6 group and less than 4 ft in the B58 group. There are no seasonal fluctuations along the B46 group, because the groundwater collection trench maintains a stable water level of 800 ft. Figure 23 shows the measured water levels at four boundary wells along the upstream boundary. MW26-92-11 and MW52-94-10 are located exactly at the boundary, whereas MW91-9 and MW52-95-2B, which are away from the boundary, were projected to the boundary to represent the water level on the boundary. At MW26-92-11, the seasonal fluctuation of the water level is about 12-14 ft, within the permeable Orinda Formation. At MW52-94-10, the water level is affected by the interface between the

permeable Moraga Formation and the underlying Mixed unit of low permeability. This means that the water level at this well is always above this interface (in the winter) or exactly at this interface (in the summer).

5.1. Groundwater Budget

Sources of the Old Town groundwater system are (1) recharge by rainfall on unpaved areas, (2) recharge from leaking storm drains and other underground facilities located in the areas of Buildings 6, 7, and 14, and (3) the inflow from the upstream boundary with a water table higher than the downstream boundary segments. The most important boundary inflow is from the saturated cross-sectional area of the Moraga Formation on the northeast side of Building 52 (Boundary Segment H–I). The outflow through the B46 and B58 groups is the most significant outflow from the system. The annual average values of the rainfall, net areal recharge, storm-drain recharge, boundary influx and outflux, and the change in the groundwater storage in the system, are listed in Table 6. Note that the annual water budget was calculated from July 1 of a given year to June 30 of the next year, because June and July are in dry, summer seasons. Figure 24 shows the monthly rainfall, net areal recharge through unpaved areas, recharge through storm drains at Buildings 14 and 6, and recharge through the storm drain at Building 7. Figure 25 shows the total inflow through upstream boundary segments, total outflow through downstream boundary segments, and water-storage change in comparison with initial water storage in the groundwater system.

As shown in Figure 25a, we obtained good matches between the predicted flow rate at the B46 boundary group and the measured flow rate at the B46 trench, both in terms of transient patterns and minimum/maximum fluxes. For all winter season high flow rates, the matches between predicted and measured processes are very good. However, the matches are not as good for the dry, summer seasons. The reason for the summer-time discrepancies is because the bottom-surface elevation of the Moraga Formation in the north area was possibly underestimated in the hydrogeologic model because of the limited number of boreholes that penetrate into the Orinda Formation in this area. Hence, the simulation overestimated the groundwater flow rates through this permeable unit in summer months. Accurate description of the hydrogeology in the channel near the B46 boundary is critical for an accurate prediction of the minimum flow rates.

As shown in Table 6, the most important boundary inflow is from the saturated cross-sectional area of the Moraga Formation on the northeast side of Building 52, although the net areal recharge through unpaved areas and the recharge through leaking underground facilities are also important. The outflow through the B46 boundary segment accounts for 81% of the total outflow of the system, while that through the B58 boundary-segment group accounts for 12%. We can see a large mass storage obtained at the end of the validation period (June 30, 1998) because a high water table was still maintained on the boundary and within the model domain. The mass-balance error is small for the system, because TOUGH2 is locally and globally mass conservative.

Table 6. Water budget of the Old Town groundwater system during the period of 1994-1998. Note that the unit for flow rates is gallon/year

		1994–1995	1995–1996	1996–1997	1997–1998
Rainfall (inch/year)		45.1	34.24	31.61	60.78
System Input	Net areal recharge	576,475	437,661	404,044	776,900
	B7 storm drain recharge	129,876	98,602	91,029	175,031
	B14 storm drain recharge	27,060	20,544	18,966	36,468
	B6 storm-drain recharge	45,151	34,279	31,646	60,849
	B52 boundary flux	1054,000	738,425	887,825	759,303
	B25 boundary flux	375,049	324,177	288,551	300,078
	Influx on other upstream boundary segments	40,808	39,689	38,904	39,470
System Output	Outflow through the B46 boundary segment group	1536,000	1354,660	1426,590	1455,600
	Outflow through the B58 boundary segment group	133,702	207,836	222,926	210,196
	Outflow through other downstream boundaries	100,641	114,296	110,442	122,328
Change in storage (gallons)		455,500	62,900	-11,400	414,800

5.2. Water Table and Velocity Fields

Figures 26–29 show the water table contours and the two-dimensional velocity-vector fields for different seasons and different years. In winter seasons, the water table rises to a higher level because of recharge and the higher water table on the upstream boundary. The two-dimensional velocity field was defined using the velocity field on the water table. The water table contours and velocity fields show distinct difference between four groundwater subsystems.

The velocity in Large Bowl subsystem is large in comparison to the velocities in the other three subsystems. In dry, summer seasons, the recharge to Large Bowl is from inflow through the upstream boundary and from the South Orinda subsystem because of the large hydraulic gradients. The flow goes via a narrow channel of the saturated Moraga Formation from the southeast to the northwest. The water table is lower, and the total flow-bearing area of the channel is small in comparison with wet winter seasons. This area varies from the southeast to the northwest. The smallest area occurs at the

Building 46 boundary (see Figure 9), resulting in the maximum velocity in the subsystem. In wet, winter seasons, the groundwater flow results primarily from the areal recharge caused by rainfall, the inflow from the upstream boundary, and from the South Orinda subsystem. The flow-bearing cross-sectional area of the saturated Moraga Formation on the upstream boundary is much larger than in summer seasons, and more inflow occurs through the boundary. As a result, the water table rises to a higher level, producing larger capacity of discharge of the channel resulting from its larger flow-bearing cross-sectional area. More water goes through the channel from the upstream boundary to the downstream boundary. The outflow rate through the B46 boundary group is also much larger.

A smaller amount of flow goes through Small Bowl in the Small Bowl subsystem. This system is recharged from (1) the upstream flow in the permeable Orinda area around MW91-9 and MW5-93-10, and (2) recharge on the unpaved areas and storm-drain leaks. The flow rate is relatively stable downstream from the subsystem. In addition, the effect of recharge resulting from the storm-drain leakage can be seen in wet winter seasons.

In the B7 subsystem, the water table remains at a high level, within the Moraga Formation or the Mixed unit. In this subsystem, all hydrogeologic units are much less permeable than elsewhere. As a result, the velocity or flux is small. This subsystem receives recharge (1) from the South Orinda subsystem, (2) from unpaved areas by rainfall, and (3) from the leaking storm drains. Groundwater flows into the Large Bowl subsystem because of large hydraulic gradients. In the winter, the leakage of the storm drains in the north edge of Building 7 results in significant flow into the Large Bowl subsystem. The groundwater flowing away from the Building 7 area extends to the northwest and then is divided by the geological divide of the Mixed and Orinda Formation (see Figure 5). This groundwater feature explains the two co-existing contamination plumes, one toward Building 46 along the west edge of Large Bowl, and the other toward Building 58. The latter contains much higher concentrations of contaminants than the former plume, because concentrations in the former plume have decreased, diluted by clean groundwater flow from the upstream boundary.

In most of the South Orinda subsystem, flow rate is very small because of the small hydraulic conductivity of the Orinda Formation. In the area of Orinda zone 2 (ord52) with higher hydraulic conductivity, we can see noticeable velocities from the boundary around MW26-92-11 down to the area around MW91-9 and MW5-93-10. It is this flow rate that recharges Small Bowl underlying Building 6. In South Bowl, the noticeable velocity results from the high hydraulic conductivity of the Moraga Formation in South Bowl.

In addition, local water mounds arise during the wet, winter seasons, as shown in Figures 27 and 29. All water mounts occur in unpaved areas, where the underlying rock has low hydraulic conductivity (the water table builds up locally as a result of infiltration). In the summer, the water table is smooth, and lower than in winter seasons.

Figures 30 and 31 show very good agreement between the simulated and the measured water table at eight monitoring wells (MW27-92-20, MW91-8, MW53-93-17, MW53-93-9, MW52-95-2B,

MW91-7, MW53-93-16B, and MW53-95-12) in the Large Bowl subsystem. The first seven wells are located within the core of Large Bowl, which has a thickness of more than 60 ft. The saturated groundwater flows within the Moraga Formation, with the (saturated Moraga) thickness of 15–30 ft in the summer, and 30–36 in the winter. The seasonal fluctuations in the water table range from 12 ft in the upstream side down to 10 ft in the downstream side. As seen in the water table patterns in these wells, as well as those in the boundary wells, the groundwater is recharged mainly from the upstream boundary and flows northwesterly towards Building 46 in the confined channel of the saturated Moraga Formation. MW53-95-12 is located on the west edge of Large Bowl, and on the geological divide of the Mixed unit and Orinda Formation; the simulated water table within the permeable Moraga Formation is higher than the measured one.

For the B7 subsystem, the simulation and calibration of groundwater flow is difficult, because of the strong heterogeneity of rock properties and the steep gradients at the bottom surface of the Moraga Formation. Figure 32 shows the reasonable match in four monitoring wells in the central area of Building 7: MW7B-95-21, MW7-95-22, MW7B-95-24, and MW7B-95-25. The most important feature for comparison is the average elevation of the water table. The water table in this area is within the Moraga Formation or Mixed unit of low hydraulic conductivity. Note that the water table at MW7B-95-21 was affected by the established facilities for remediation; the measured water table in the summer of 1997 is higher, and stays at a high level afterwards. Figure 33 shows the match at four wells away from the central area of Building 7. Good matches are also found in MW7-94-3 and MW16-94-13, where the water table is within either the Mixed unit or both the Moraga Formation and the Mixed unit. At MW52B-95-13, differences of only 2-4 ft are obtained between the simulated and measured water table. At MW7-92-19, the difference is more than 5 ft, because this well is a “partial” borehole with the boring bottom ending within the Moraga Formation, and the inaccurately interpolated bottom elevation was used in the hydrogeologic model. The interpolated bottom elevation of the Moraga Formation at this well is very similar to that in the four monitoring wells shown in Figure 32, resulting in a simulated water level very similar to that in the four wells. However, the measured water level at MW7-92-19 is 10 ft less than that in the four wells.

For the Small Bowl subsystem, good to excellent agreements were obtained between the simulated and measured water levels at eight monitoring wells (MW16-95-3, MW6-92-17, MW7-92-16, MW6-93-4, MW90-2, MW58-95-11, MW58-93-3, and MW58A-94-14) (Figures 34 and 35). Excellent agreements were found at the two upstream wells: MW16-95-3 and MW6-92-17. At MW6-93-4, the simulated water level is smaller than the measured one by 10 ft, indicating that there may be some local recharge of groundwater into this area. Downstream from Small Bowl, the water level in the Moraga Formation moves into the Artificial Fill and Colluvium units of high porosity, which produce a relatively stable water level with time. This stable water level in turn produces a stable boundary flow rate, as measured in the B58 trench.

Figure 36 shows a reasonable match between the simulated and the measured water level at four wells (MW91-9, MW5-93-10, MW25A-95-4, and MW25A-95-15) in the South Orinda

subsystem. MW91-9 and MW5-93-10 are located in the permeable Orinda Formation (Orinda Zone 2), which exhibits seasonal water level changes of more than 10 ft. The simulated water level at MW91-9 is higher than the measured one. At MW5-93-10, the match is very good; groundwater flows downstream within the permeable Moraga Formation. It can be seen from the water table patterns that MW25A-95-4 and MW25A-95-15 are hydraulically disconnected because of the embedded highly permeable Orinda Formation between them. Figure 37 shows the match in three wells (MW25-94-12, MW25-93-15 and MW25-95-5) located in South Bowl. The water level at MW25-94-12 is within the Moraga Formation and has the seasonal fluctuations of 5 ft (and above the top of the Orinda Formation). At MW25-93-15, the water level is exactly at the top of the Mixed unit for most of the years, with a small seasonal rise in the winter. At MW25-95-5, the water level is within the Moraga Formation about 15 ft above the bottom of the Moraga Formation, but its seasonal change is small (less than 5 ft).

In summary, the model prediction of the groundwater flow at the Old Town site using the calibrated rock properties with our conceptual model is reasonable, as shown in comparison with the extensive measured water levels in a number of monitoring wells and the groundwater flow rates measured at two trenches. The numerical model helps us understand groundwater flow in this strongly heterogeneous system. It can also be used to accurately predict groundwater flow in the future. Meanwhile, it can be used with a transport model (to be developed) to predict the transport processes of the contaminants in the two plumes in the Old Town area. The simulation of flow and transport can be used to determine how long the current remediation measures will have to last.

5.3. Advective Contaminant Transport

As a first step toward understanding contaminant transport, particle trajectories have been analyzed and calculated (Zhou et al., 2003) and are discussed in this section. A more comprehensive transport model, including advective and dispersive transport, as well as degradation processes, will be developed in the future. The particles move with the transient groundwater flow, featuring seasonal fluctuations in the water table and strong variations in groundwater velocity (as shown in Figures 26 to 29). For the purpose of demonstration, we show the trajectories of particles originating from the source area of contaminants in the B7 lobe, B52 lobe, and B25A lobe, using steady-state pore velocity fields at July 1997, October 1997, January 1998, and April 1998. Figures 38 to 41 show the steady-state trajectories of particles at these particular times, respectively.

Particles originating from the B7 lobe migrate in two different directions in any season: northwesterly to the B58 boundary, and northerly to the B46 boundary. However, some particles may change their directions in different seasons, depending on the local flow field. In July 1997, the particles originating in the southwest of the major plume move toward the B58 boundary, whereas the particles originating in the northeast side of the major plume move northward along the geological barrier to the B46 boundary. Particles originating from the center of the major plume move downgradient northwesterly until they reach an area where the velocity field is very complex. South of

B53, the flow stagnants, and the particles cannot go further toward the model boundary. Here, the regional flow in Large Bowl encounters the flow moving northward from the geological barrier. In July 1997, no flow occurs at the saddle of the geological barrier, and no particles are found to go through the barrier saddle toward the B58 boundary. In October 1997, recharge from the 9-inch rainfall event elevated the water table, and some water flowed through the barrier's saddle toward the B58 boundary. This flow results in some particles from the major plume migrating through the saddle toward the B58 boundary. There is no stagnant area around the major plume, and particles originating in the center of the plume migrate northward along the geological barrier. In January 1998, the rainfall was very heavy, 19 inches for that month. As a result, the water table in Large Bowl became very high, and the velocity became very large. On the other hand, the water table at the geological barrier was elevated because of the large recharge through the overlying unpaved areas. As a result, no flow occurs at the barrier's saddle, and no particles migrate westward to the B58 boundary through the saddle. By April 1998, the velocity in Large Bowl remained very large, but the water mound in the geological barrier area had disappeared. As a result, a large amount of water flowed through the saddle to the B58 boundary. Most particles originating from the center and the north edge of the major plume migrate northward and turn westward at the saddle to the B58 boundary.

Overall, the calculated pathways of particles originating from the B7 plume lobe are in good agreement with the measured contaminant plumes. The particles originating immediately south of the core plume and all particles from the core area in winter seasons move towards the B58 boundary. This is consistent with the trend of the main B7 plume because the plume is elongated primarily in the northwest direction. Particles originating north of the core plume move northward in summer seasons along the western edge of Large Bowl and the eastern edge of the geologic divide. This is consistent with the elongated plume of low concentrations in the north direction. Note that this part of the plume has smaller concentrations than the core plume. This is because clean groundwater flows into Large Bowl from the upstream boundary, thus diluting the contaminant plume. The other reason is that particles from the north portion of the core area of the B7 lobe move in northerly only in summer seasons with small travel velocity. As a consequence, more contaminants are expected to migrate in a northwesterly direction, primarily because of larger velocity in winter seasons. The consistency between the measured plumes and the particle pathways indicates that the groundwater flow model can reproduce the flow fields reasonably well.

In July 1997, all particles from the area east of Building 52 migrated along the Moraga Channel downstream to the B46 boundary. Some particles originating south of the B52 lobe moved northwesterly passing the plume of the B7 lobe contaminants. Once the water table rose, owing to recharge from rainfall and the higher water table at the upstream boundary, particles from the B52 lobe moved directly toward the B46 boundary, bypassing the B7 plume. Later, with an elevated water table in Large Bowl, the particles originating from the south end of the B52 lobe move westward, combining with those from the B7 lobe and moving further westward to the B58 boundary. The measured plume is elongated toward the B46 boundary, similar to the main particle flow direction. Therefore, the

pathways of the particles and the elongated plume are in good agreement. In addition, the mingling of particles originating from the B52 and B7 plume lobes in winter seasons is also consistent with the formation of a large contaminant plume for the low-concentration contour line.

For particles originating in the B25A lobe, the trajectories show less time dependent. All particles originating from the northeast area of Building 25A migrate northward to the B46 boundary. In the south area of the B25A lobe, particles move southward. Some particles may change directions from northwesterly in the summer to southerly in the winter.

6. Assessment of Hydraulic Measures for Remediation

The site-scale groundwater flow model developed was refined to assess the efficiency of existing hydraulic measures in restoring the contaminated site. The refinement was conducted with a focus on the main contaminant plume (the B7 lobe), therefore excluding the large area in the south of the site-scale model (see Figure 42). The refined model covers the northern area of the site-scale model, incorporating the B7 lobe and the B52 lobe. All perturbations to the groundwater system, including pumping and injection, were considered in the refined model. The efficiencies of two trenches located within the model area (for source control) and two trenches located on the model boundaries (for avoiding contamination of the surrounding environment) were assessed using this refined model. Conditions at the external boundary and initial conditions at June 1, 1996, were based on the simulated groundwater level of the site-scale model. The simulation time is from June 1, 1996 to June 30, 2000.

Perturbations to the global flow fields caused by the operation of two internal trenches were considered in the refined model. Groundwater was pumped at the B7 trench, treated, and continuously reinjected at the upstream sump, which is represented by six vertical columns in the model that are maintained at the measured water table of 975.40 ft (see Figure 42). The B7 trench is composed of two trench segments of filled gravel that are separated by a short segment of bedrock, each of which is represented by six vertical columns in the computational mesh. The boundary conditions in the two segments were specified using the measured groundwater level at two extraction wells within the trench. At the B53-58 trench, groundwater was also pumped, treated, and re-injected into the system. This trench is composed of eight gravel-filled columns, and the groundwater level at each column is specified at constant values, varying from 810 ft to 821.78 ft.

Figure 43 shows the simulated groundwater level contours and velocity vectors on the water table in October 1999, which represents a dry season. The elevated groundwater level upstream from the B7 trench is caused by the re-injection of treated groundwater at the former sump. Downstream from the B7 trench, the groundwater level decreases as a result of the pumping in the B7 trench. The groundwater from the sump to the trench flows mainly within the permeable Moraga Formation, resulting in large recirculation fluxes. The bottom of the trench is 57.4 ft below the groundwater surface, and in the Orinda Formation. Thus, in the vertical direction, the trench controls almost the

entire contaminated groundwater flow. A mass balance indicates that the trench is capable of capturing about 70% of the groundwater injected at the sump.

The B53-B58 trench was installed in May 1999, based on the observed concentration contour measured at that time. This trench was expected to control the B7 plume at the downstream end of the high concentration portion. It is about 36 ft below the ground surface, penetrating the Mixed unit (24.6 ft thick) and ending in the Orinda unit. The water level imposed at the B53-B58 trench is lower than that in the surrounding area, resulting in convergent groundwater flow toward the trench. However, since the trench is located at the geologic divide and within the Mixed or Orinda unit of low hydraulic conductivity, the amount of groundwater flowing toward the trench is less significant than that in the B7 trench. The simulated flow field and the concentration field recently observed indicate that this trench may not be as effective as hoped, because a major fraction of the contaminants migrate south of the trench (Figure 43c).

At the B58 trench, the large flow velocities indicate that the trench is effective in preventing contaminated groundwater from leaving the model area and contaminating the downgradient environment. The concentration field suggests that the trench can be used to collect most of the advective flux of contaminants flowing through the B58 boundary. The same conclusion can be drawn for the B46 trench, which collects large amounts of contaminated groundwater for further treatment. However, in light of the differences between dry summer and wet winter conditions observed in Figures 38 through 41, there is the possibility during wet seasons that contaminants may migrate through the saddle toward the B58 boundary instead of proceeding towards the B46 trench. Further investigation is needed to evaluate whether these contaminants are being captured in the B58 trench.

7. Conclusions

In the late 1980s groundwater contamination was detected at the LBNL Old Town site. Since then, a large amount of data was collected on stratigraphy, hydogeologic properties, groundwater levels, and contaminant concentrations. Interim corrective measures were initiated to prevent further spreading of contaminants. This report describes the development of and simulation results from a three-dimensional transient groundwater flow model designed to (1) improve our basic understanding of the flow and contaminant transport patterns and (2) support the decision-making process for remediation measures.

A detailed hydrogeologic model was developed to describe the complex hydrogeology at the mountainous site, featuring several geologic units with strongly varying thickness and steep slopes. Based on detailed information from several hundred boreholes, a unique geologic setting was identified, with three isolated bowl-shaped rock masses of the Moraga Formation embedded in heterogeneous bedrock of much lower permeability (i.e., the Mixed unit and the Orinda Formation). Another modeling challenge was the strong seasonal patterns of groundwater flow, mainly affected by significant water recharge from upstream steep hills. In such a setting, the definition of appropriate

model domain and boundary conditions is complicated, but essential to model development. In the model, the relevant model boundary passes through a number of groundwater monitoring wells, and the measured transient groundwater levels in these wells were used for boundary conditions.

The groundwater model was calibrated using groundwater levels and fluxes collected between 1994 and 1996. The rock zone method was used to deterministically define the spatial variability of rock properties within the same hydrogeologic unit, based on the observed clustering characteristics of measured hydraulic conductivities. A composite model was used to account for the internal heterogeneity of the rock, with thin permeable sand layers located within solid rock of low hydraulic conductivity. Transient inverse modeling was conducted to obtain the effective hydraulic conductivity and porosity for each of the 20 defined rock zones. Also calibrated were recharge factors for areal infiltration through rainfall and local infiltration through leaking underground utilities. It was found that modeling the local recharge from confirmed leaking storm drains is critical for accurate simulations because this recharge significantly affects the groundwater levels measured in low-permeability areas. Also note that the calibrated effective-porosity values are considerably smaller than the actual physical porosity of the rocks. Such small effective porosities demonstrate that only the thin sandstone layers embedded in the bedrock of low hydraulic conductivity are hydraulically important. These small porosities explain the rapid groundwater-level changes observed in response to precipitation events.

The calibrated groundwater flow model was validated using a blind model prediction conducted for the period between July 1996 and June 1998. The calibrated model produced good matches between the simulated and measured groundwater level in a large number of monitoring wells, and also captures the trend observed in the flow rates measured at two groundwater collection trenches. In addition, the simulated advective transport based on particle tracking is in good agreement with the measured extent of contaminant plumes. The validation results indicate that the developed model can accurately predict the complex groundwater flow at the LBNL site.

Finally, the calibrated and validated model was refined to focus on the main contaminant plume and on the effects of the perturbations caused by hydraulic measures for remediation. The assessment of hydraulic measures concluded that most of the hydraulic measures are effective in controlling the contaminant sources and in collecting contaminated groundwater to prevent further contamination from entering the surrounding environment. However, one trench may need to be relocated to control the high-concentration area of the main plume. In any case, the groundwater flow model provides a valuable tool for improving the decision-making process with respect to site remediation, and can be used as the basis for further development of a contaminant transport model.

Acknowledgements

This work is part of the Berkeley Lab’s Environmental Restoration Program that is supported by the Office of Environmental Management of the U.S. Department of Energy.

REFERENCES

Amtec Engineering, Inc, *Tecplot Version 8.0, User's Manual*, Amtec Engineering, Inc, Bellevue, 1999.

Cooper, H., Bredehoeft, J., and Papadapulos, I., Response of a finite-diameter well to an instantaneous charge of water, Water Resources Research, 3(1), 263–269, 1967.

Finsterle, S., *iTOUGH2 User's Guide*, Report LBNL-40040, Lawrence Berkeley National Laboratory, Berkeley, California, 1999.

Javandel, I., *Preliminary environmental investigation at the Lawrence Berkeley Laboratory*, Report LBNL-29898, Lawrence Berkeley National Laboratory, Berkeley, California, 1990.

LBNL, *Draft Final RCRA Facility Investigation Report, for the Lawrence Berkeley National Laboratory Environmental Restoration Program*, Lawrence Berkeley National Laboratory, Berkeley, California, 2000.

LBNL, *Site Environmental Report for 2002, Volume 1*, Lawrence Berkeley National Laboratory, Report LBL-27170, Berkeley, California, 2003.

Neuman, S., Analysis of pumping test data from anisotropic unconfined aquifers considering delayed yield, Water Resources Research, 11(2), 329–342, 1975.

Pan, L., Hinds, J., Haukwa, C., Wu, S., Bodvarsson, G., *WinGridder, an Interactive Grid Generator for TOUGH, User's Manual*, Report LBNL-42957, Lawrence Berkeley National Laboratory, Berkeley, California, 2001.

Pruess, K., Oldenburg, C., and Moridis, G., *TOUGH2 User's Guide, Version 2.0*, Report LBNL-43134, Lawrence Berkeley National Laboratory, Berkeley, California, 1999.

Zhou, Q., Birkholzer, J. T., Javandel, I., and Jordan, P. D., Simulation of Groundwater Flow at the LBNL site Using TOUGH2, Proceedings of TOUGH Symposium 2003, May 12–14, 2003, Berkeley, Calif., 2003.

Zhou, Q., Birkholzer, J. T., Javandel, I., and Jordan, P. D., Modeling three-dimensional groundwater flow and advective contaminant transport at a heterogeneous mountainous site in support of remediation strategy, *Vadose Zone Journal* (in press), 2004.

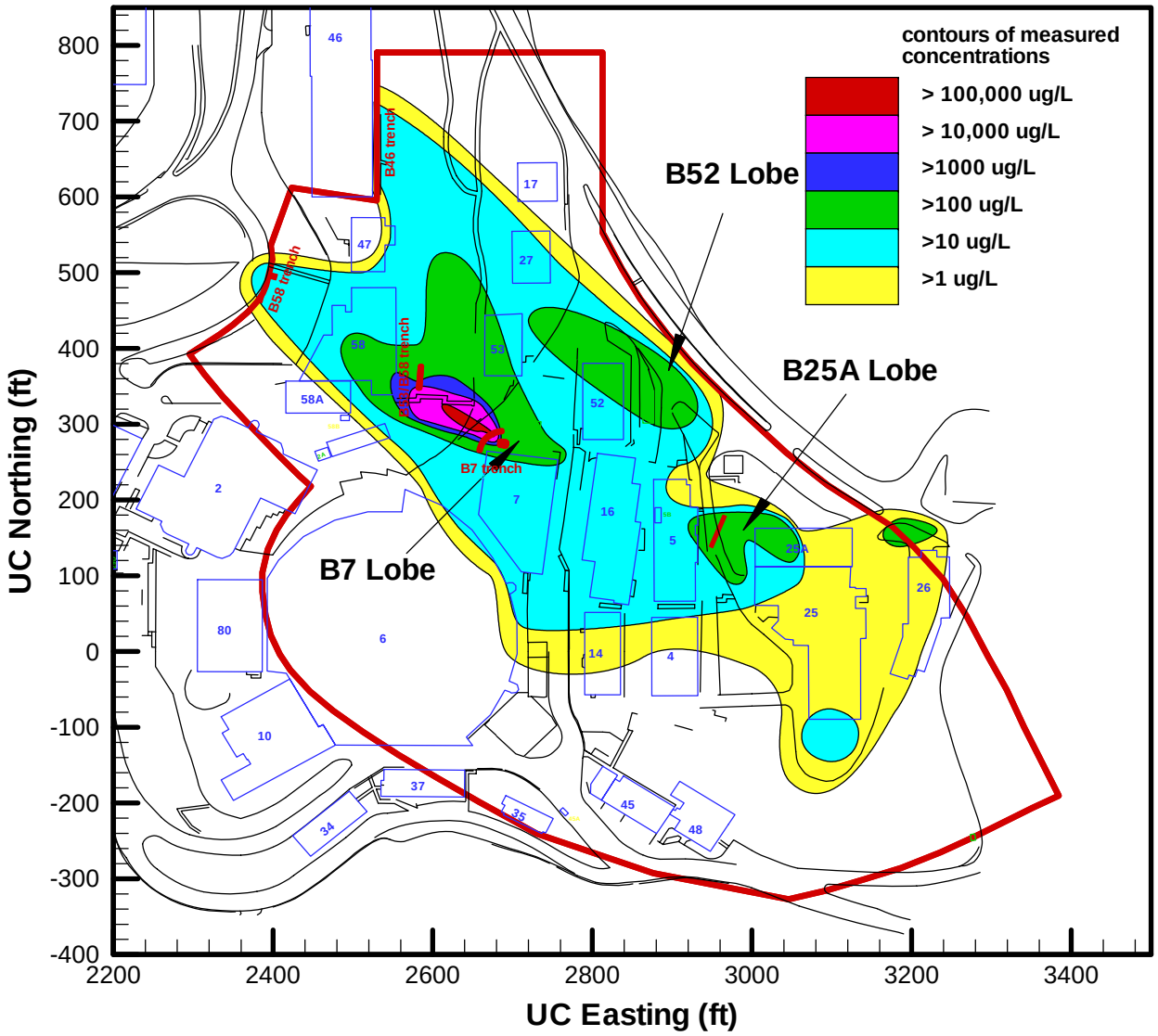

Figure 1. The Old Town map with buildings and their numbers in blue polygons and roads in black lines, and contaminant plumes measured in 1999 and groundwater collection trenches.

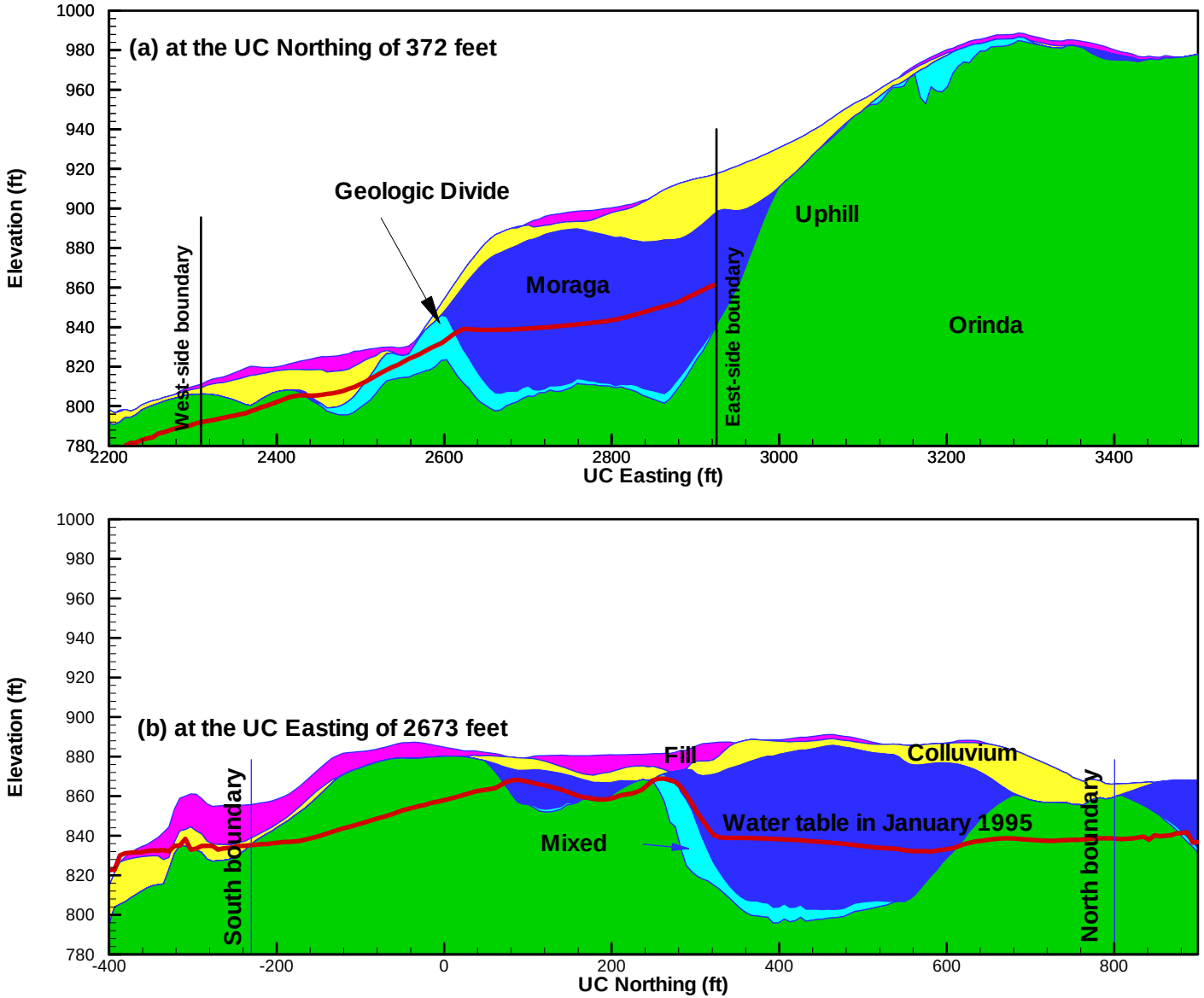

Figure 2. Geological profiles in vertical cross sections (a) in the UC Easting direction and (b) in the UC Northing direction, with representative water table.

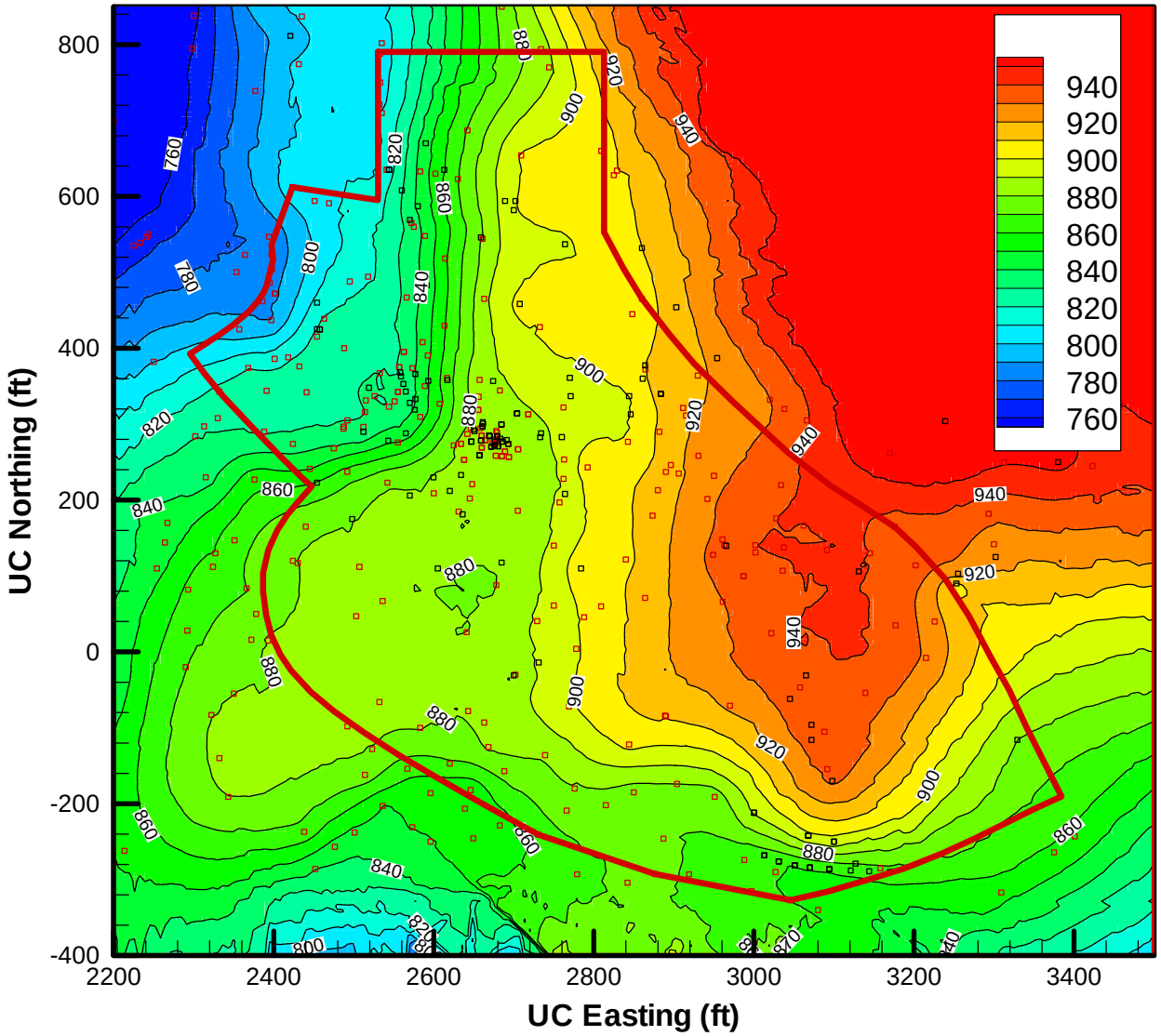

Figure 3. Surface elevation contours (ft) (the top of the Artificial Fill unit). Red squares indicate “full” boreholes and black squares indicate “partial” boreholes.

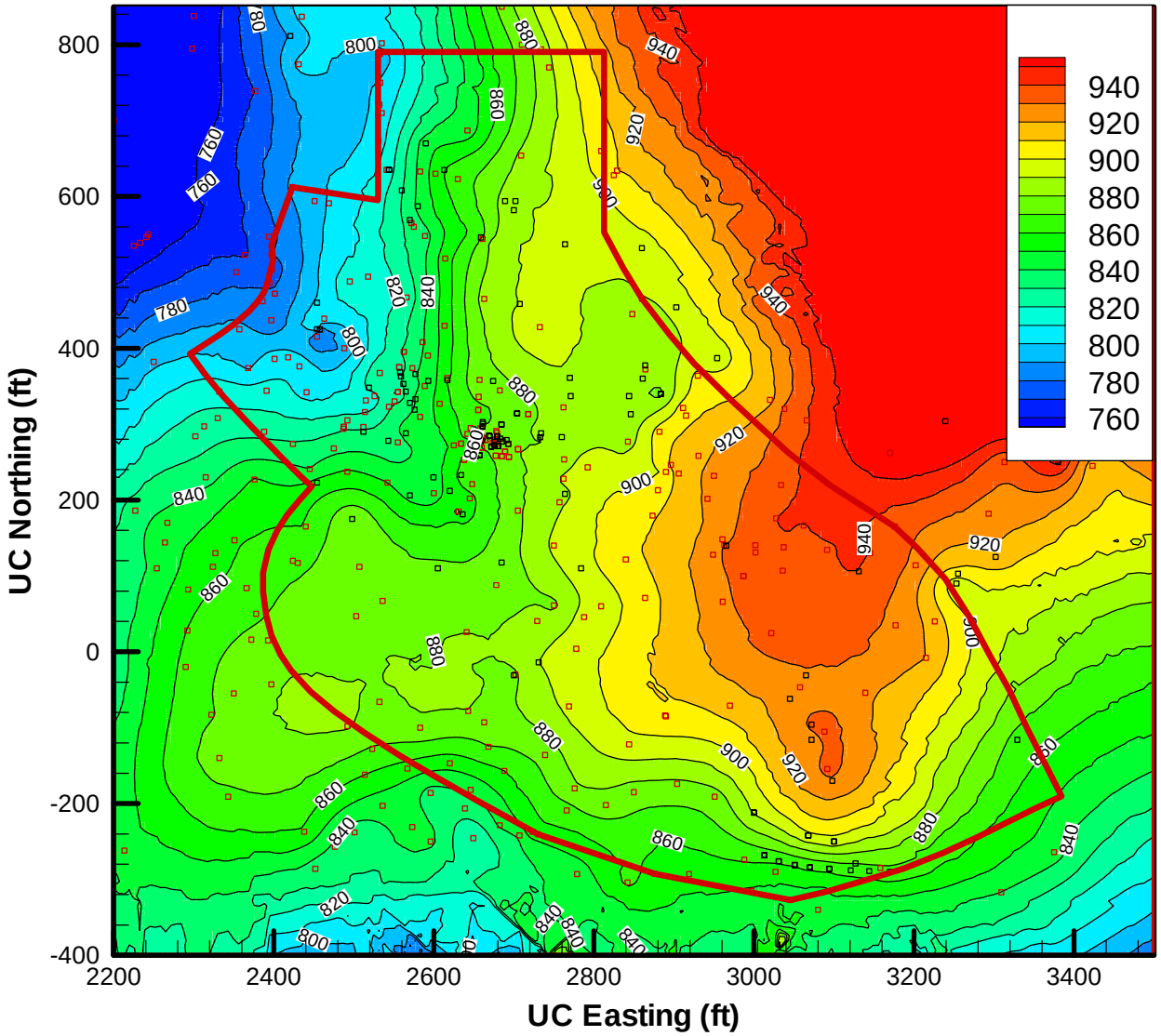

Figure 4. Structural contours of the top elevation (ft) of the Moraga Formation unit. Red squares indicate “full” boreholes and black squares indicate “partial” boreholes.

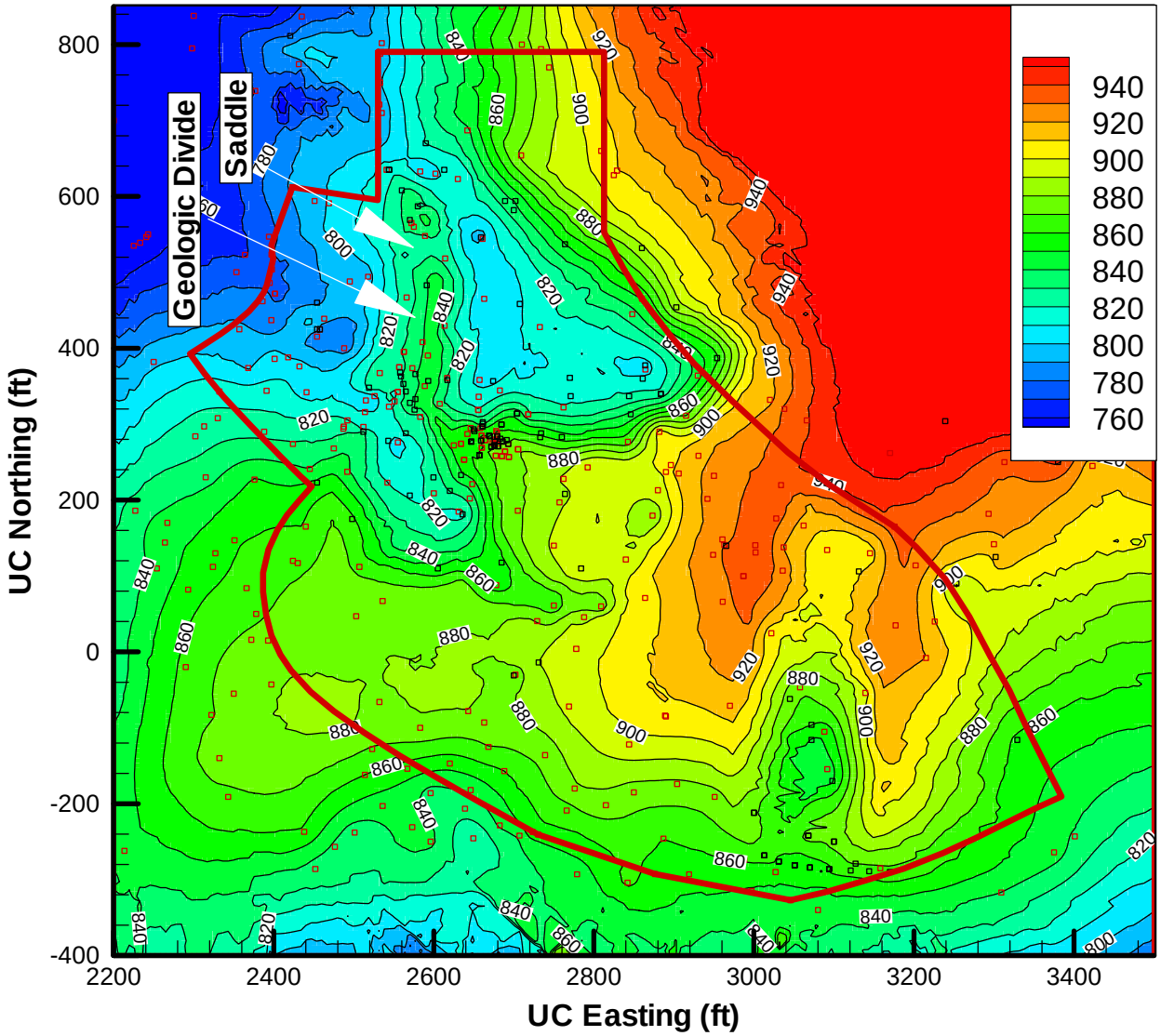

Figure 5. Structure contours of the top elevation (ft) of the Mixed unit. Red squares indicate “full” boreholes and black squares indicate “partial” boreholes.

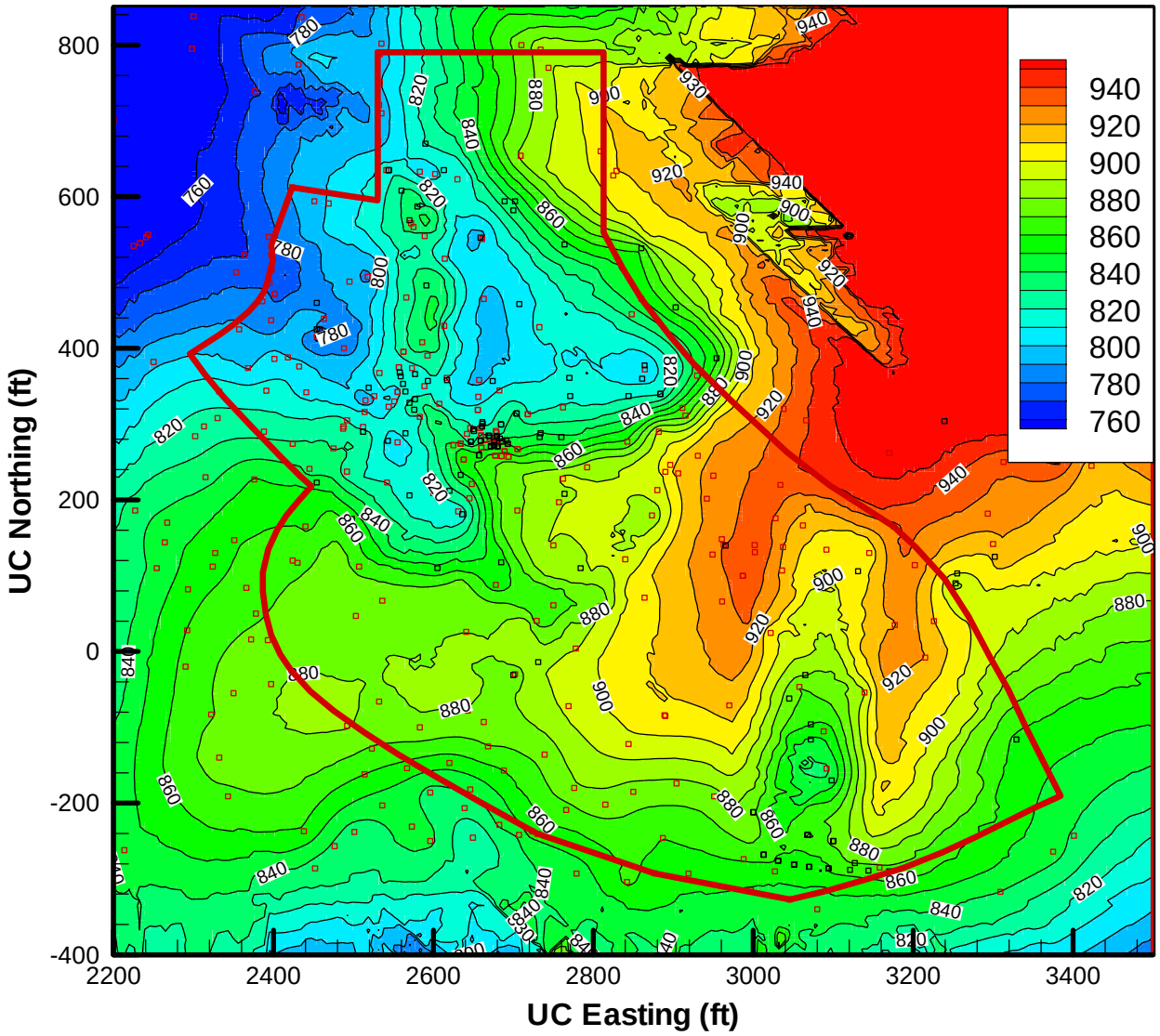

Figure 6. Structure contours of the top elevation (ft) of the Orinda Formation. Red squares indicate “full” boreholes and black squares indicate the interpolated top of the Orinda Formation for “partial” boreholes. Note that poor quality of interpolation can be seen in the east of the model domain.

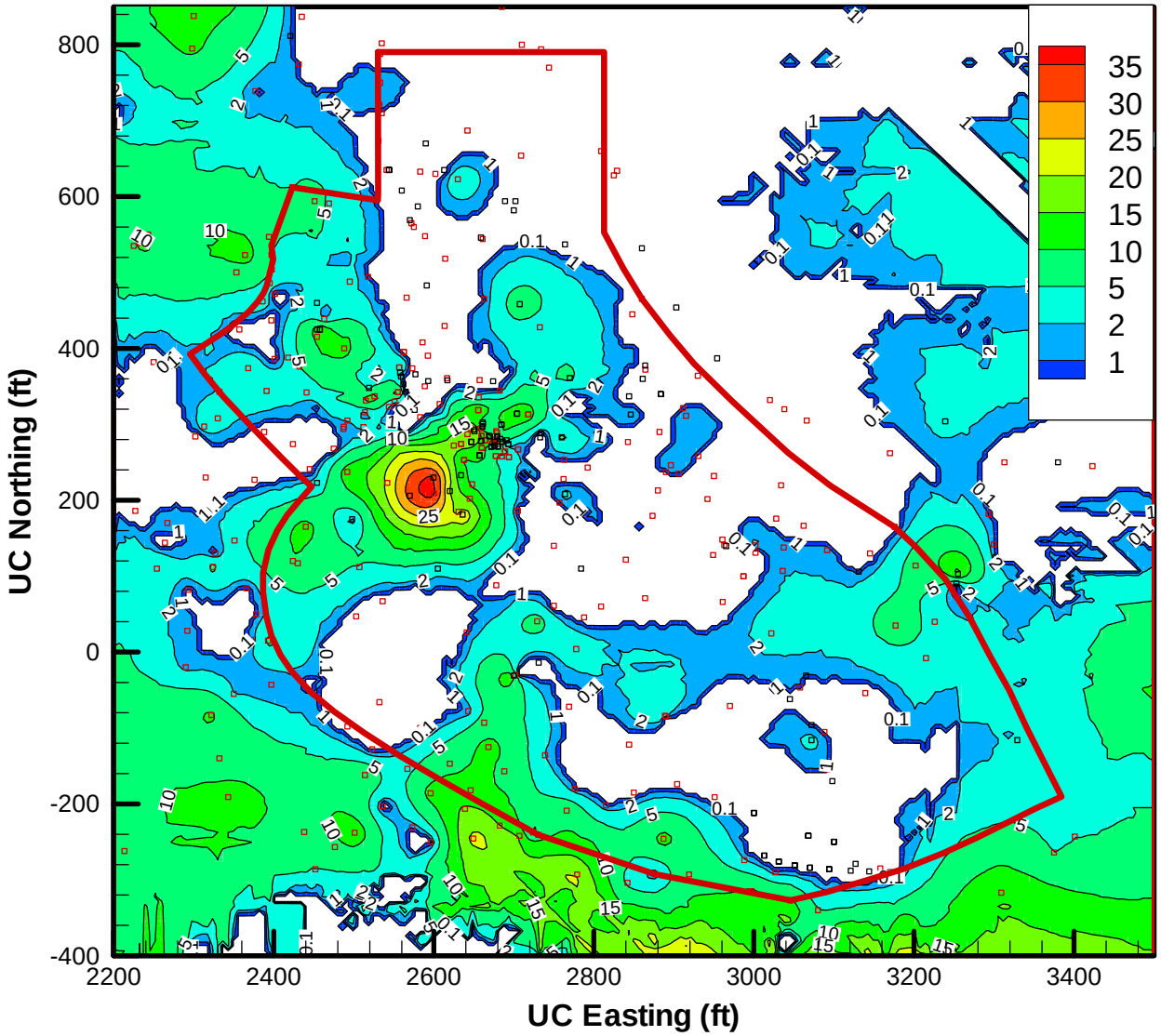

Figure 7. Thickness contours (ft) of the Artificial Fill unit. Red squares indicate “full” boreholes and black squares indicate “partial” boreholes.

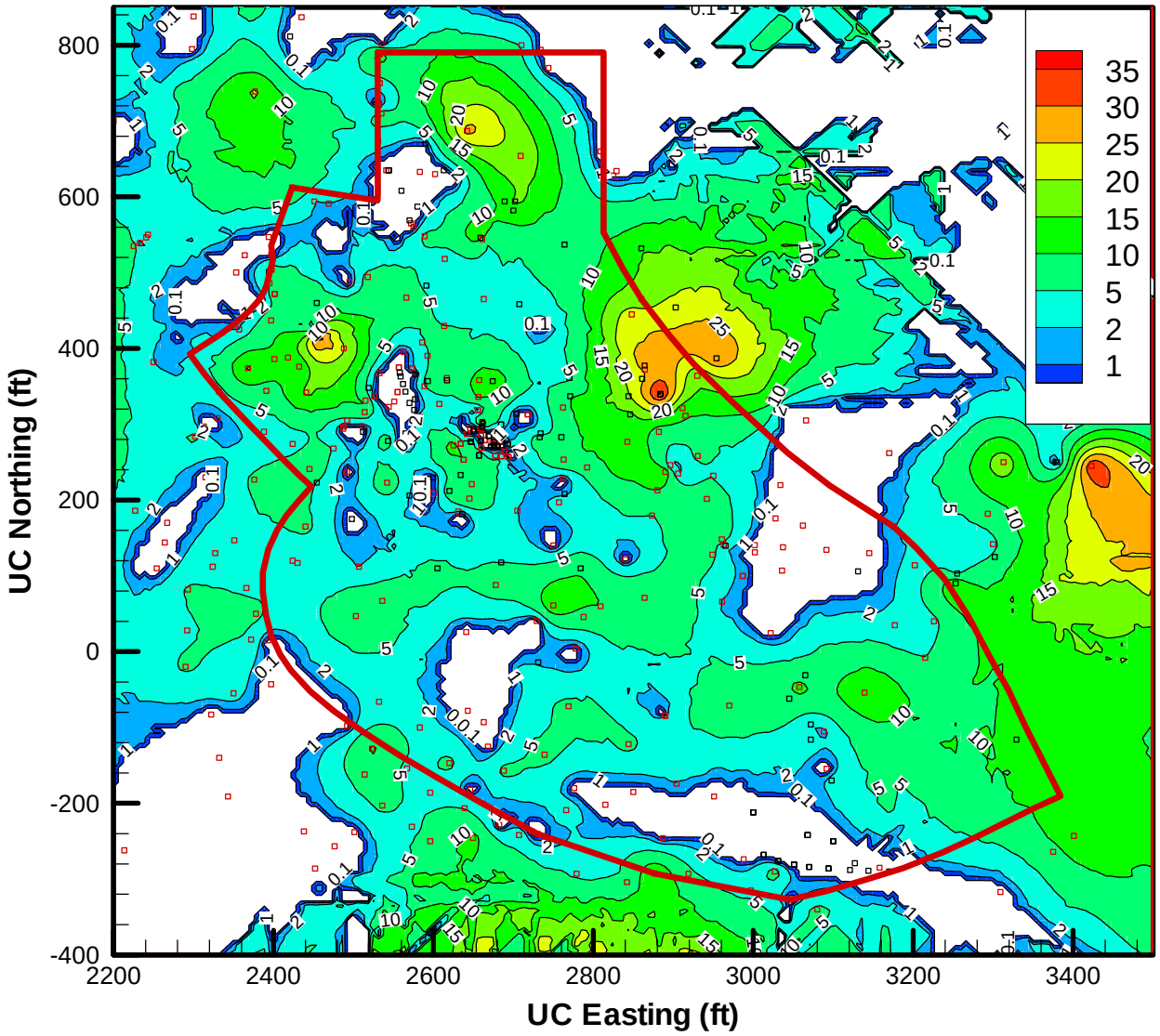

Figure 8. Thickness contours (ft) of the Colluvium unit. Red squares indicate “full” boreholes and black squares indicate “partial” boreholes.

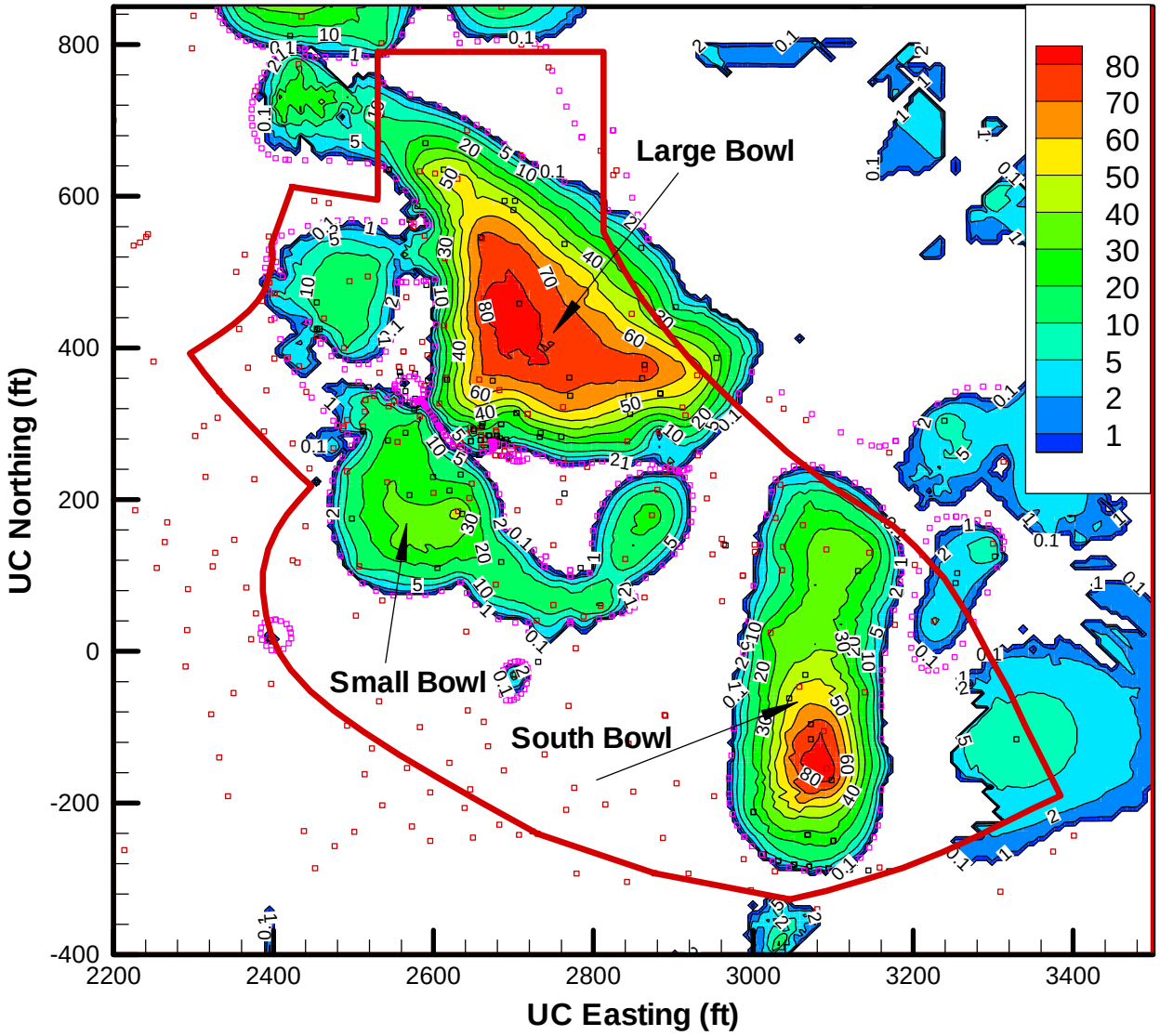

Figure 9. Thickness contours (ft) of the Moraga Formation unit. Red squares indicate “full” boreholes, black squares indicate “partial” boreholes, and purple squares indicate the zero-thickness data points obtained from the outcrop map.

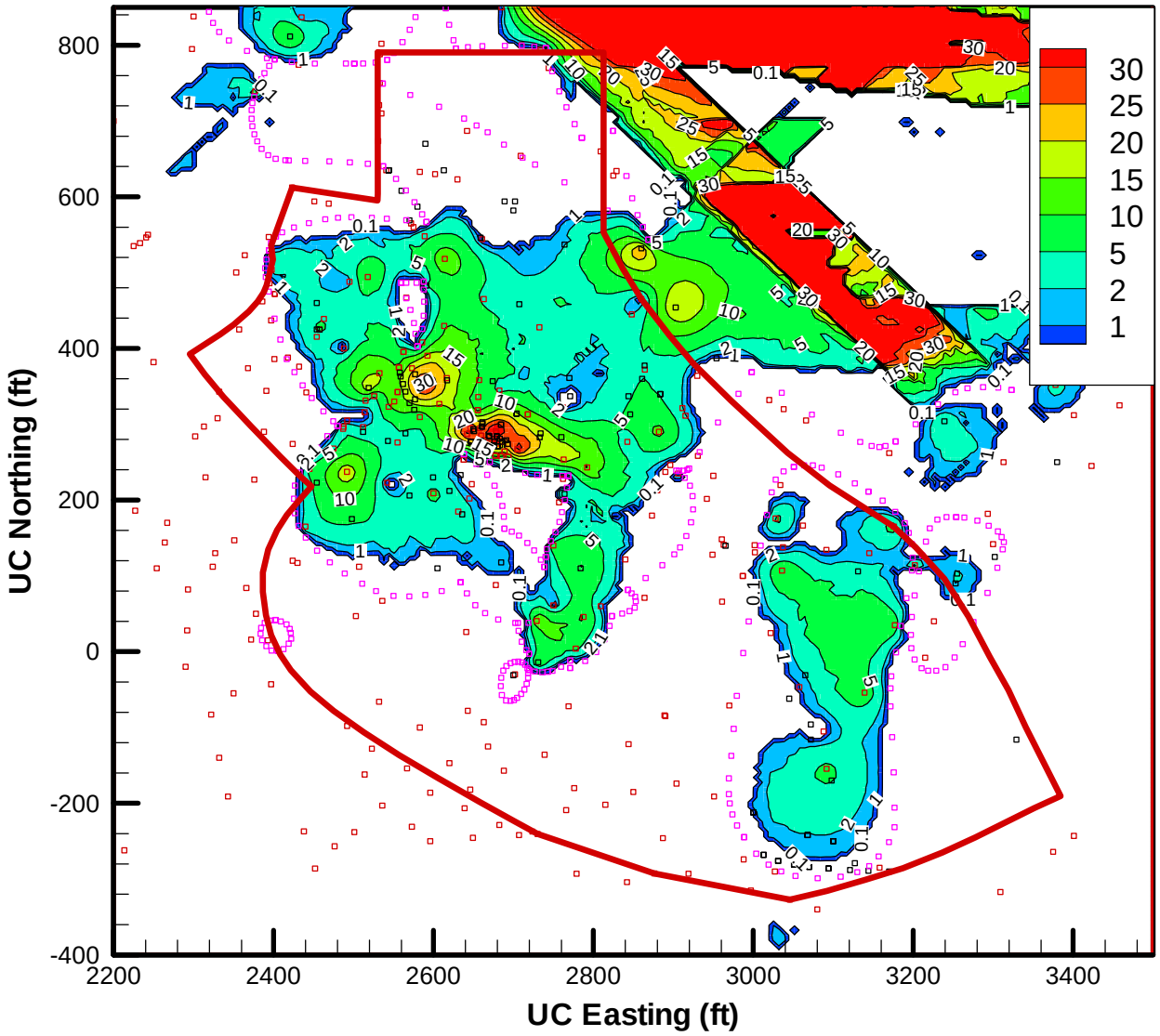

Figure 10. Thickness contours (ft) of the Mixed unit. Red squares indicate “full” boreholes, black squares indicate “partial” boreholes, and purple squares indicate the zero-thickness data points obtained from the outcrop map.

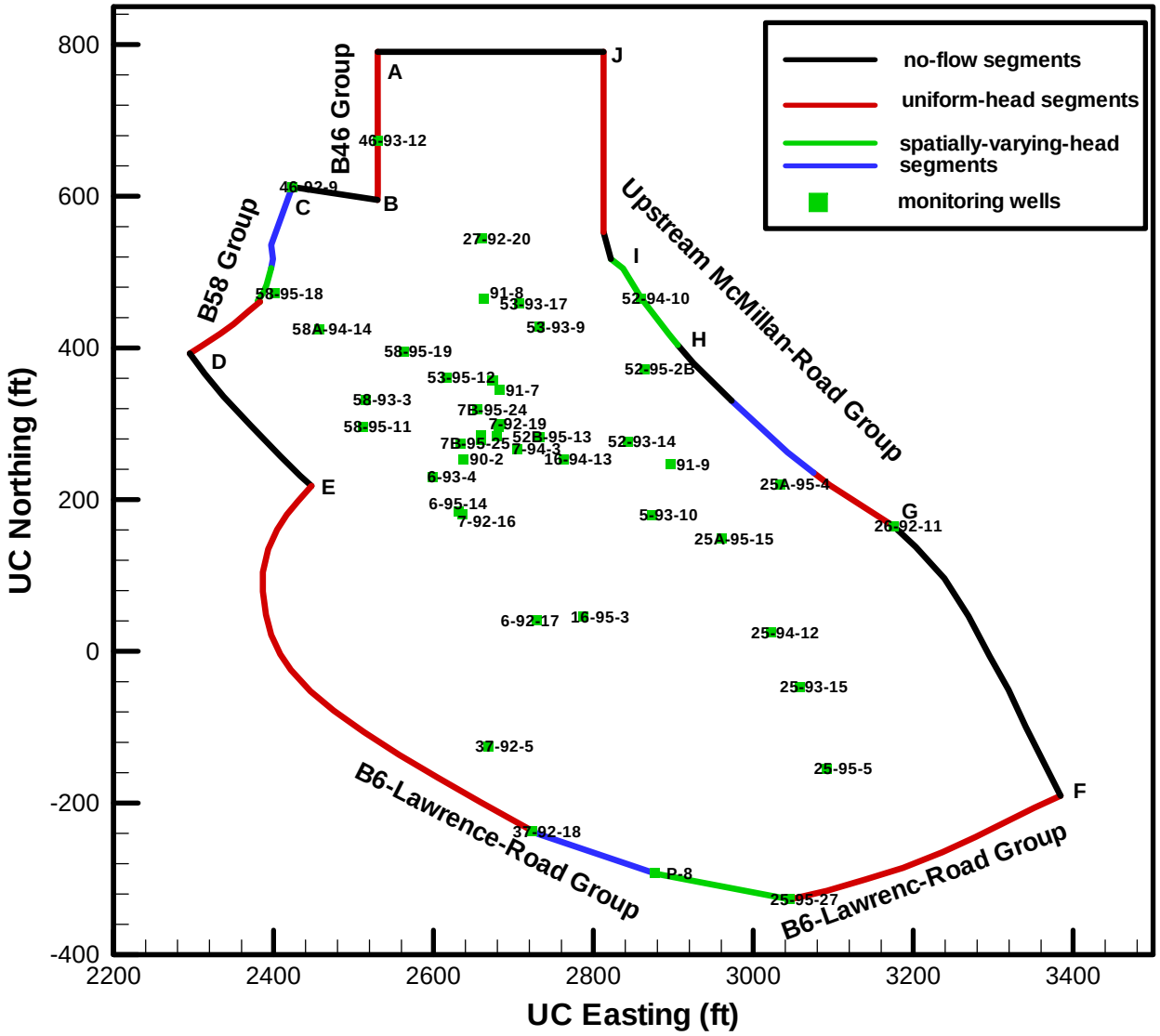

Figure 11. Model boundary, boundary condition types, boundary wells, and other monitoring wells used for determining initial conditions.

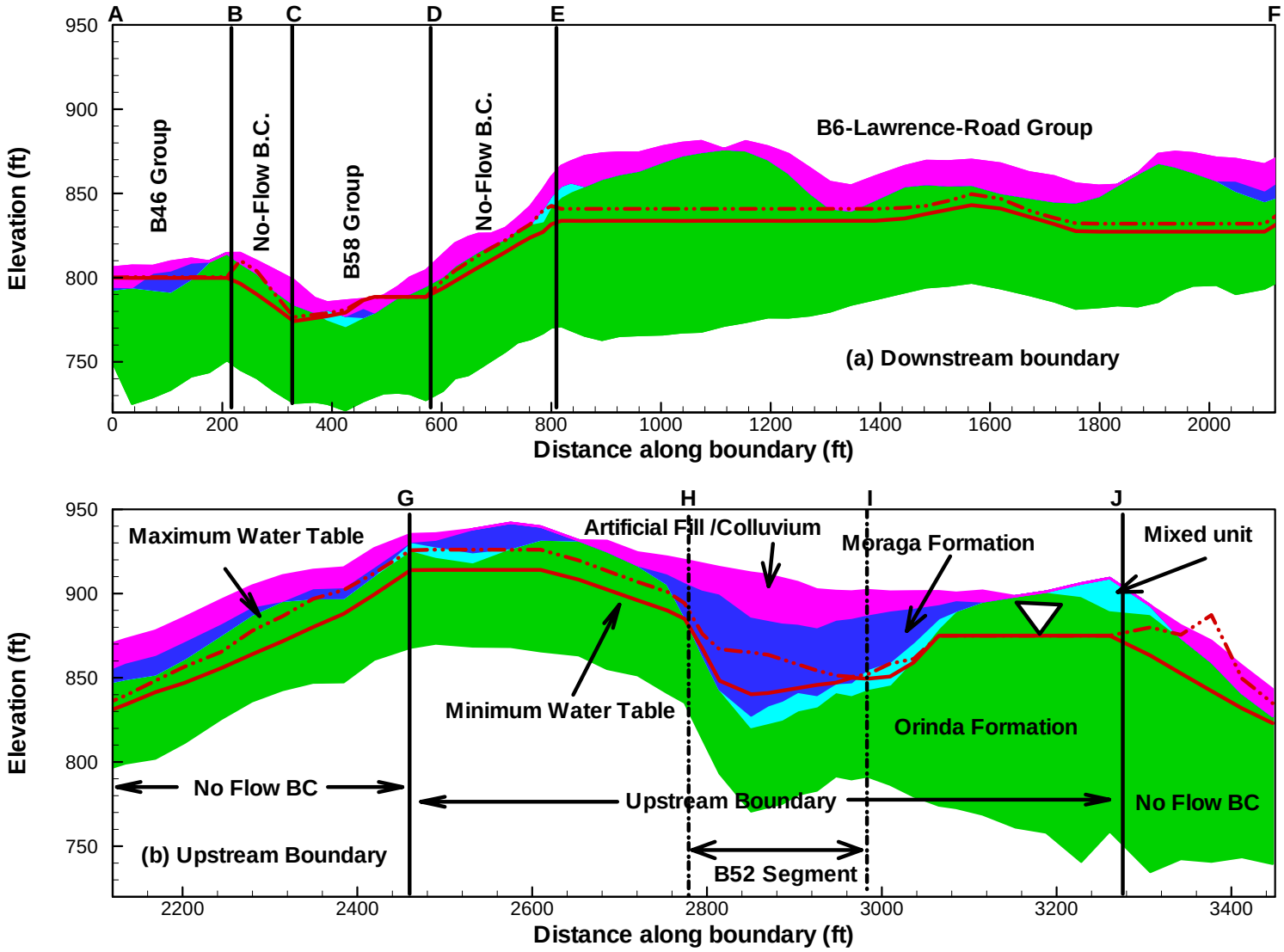

Figure 12. Geologic cross sections along the downstream and upstream boundaries of the model shown in Figure 11, with measured maximum and minimum water table specified on the boundary as boundary conditions.

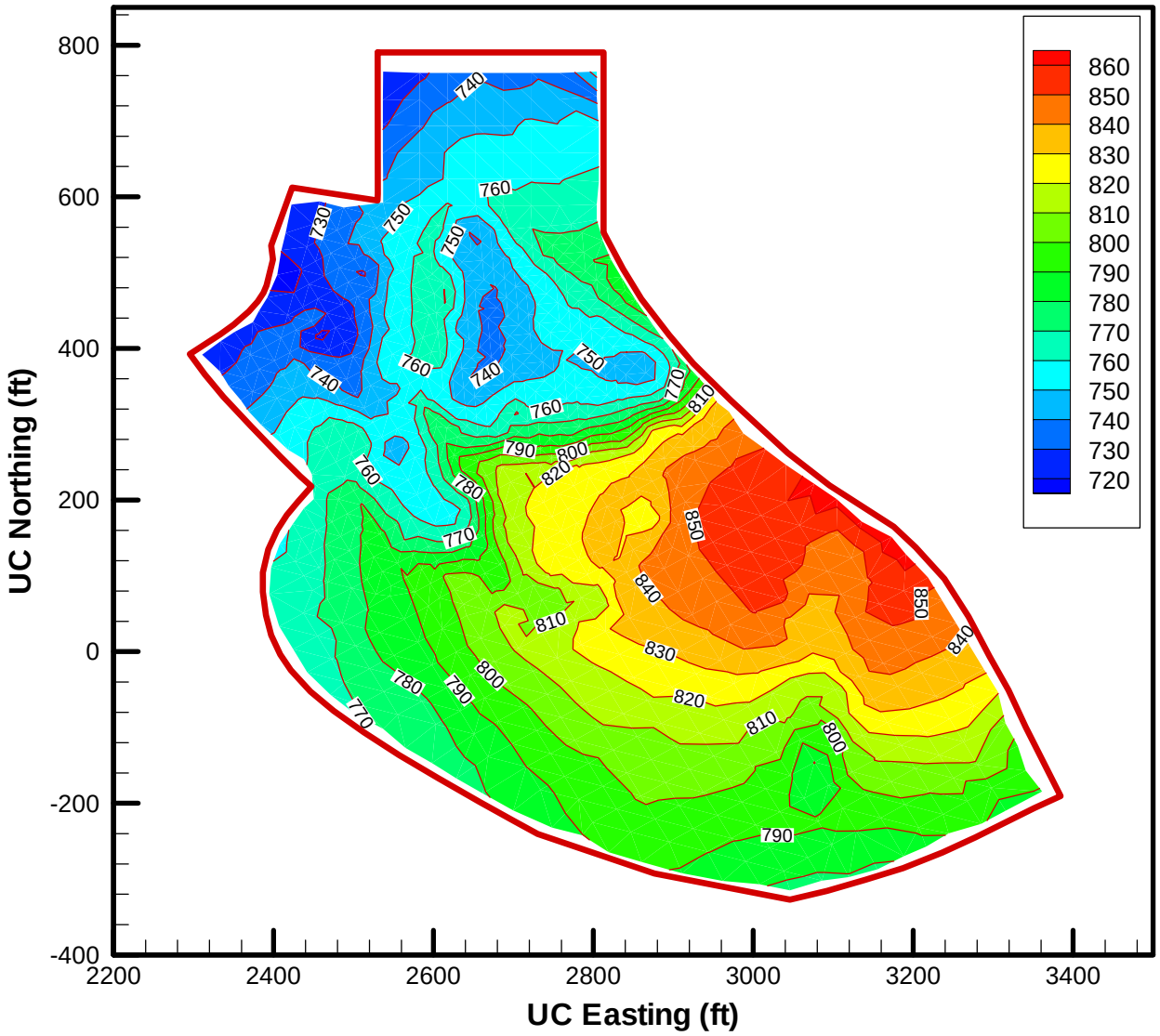

Figure 13. Elevation contours (ft) of model bottom boundary.

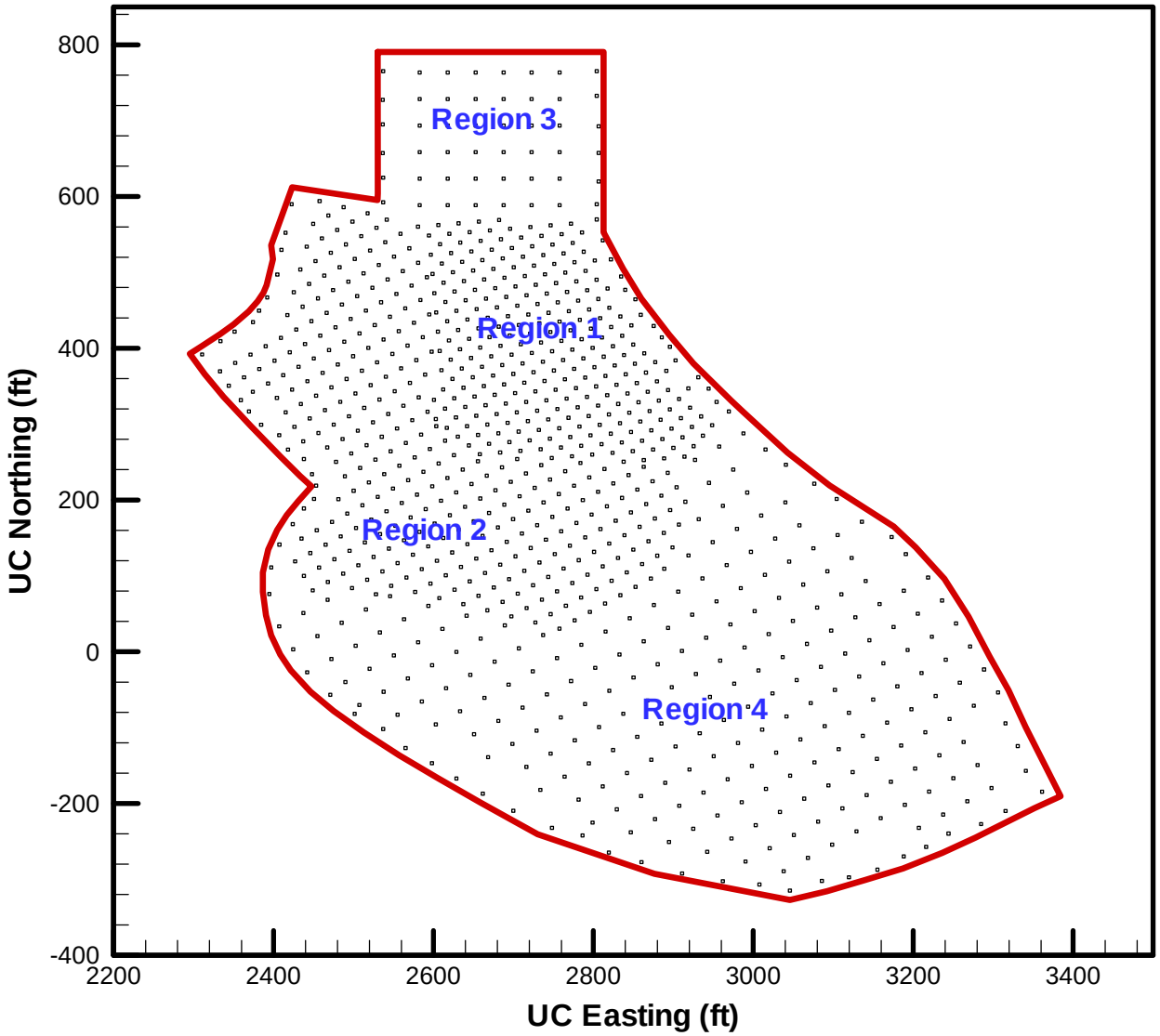

Figure 14. Plan view of the three-dimensional TOUGH2 grid for model calibration. Block dots are the centroids of vertical columns.

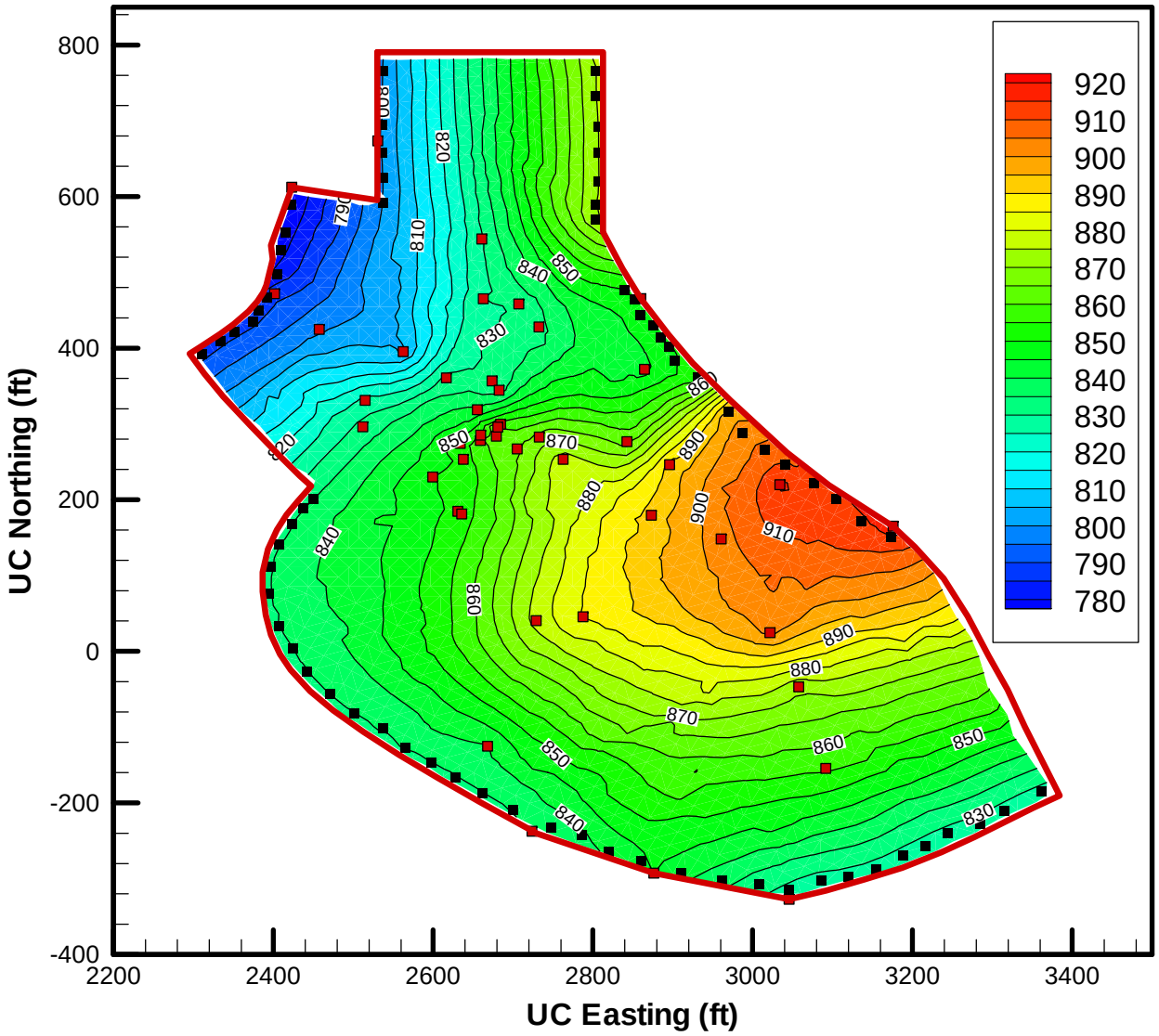

Figure 15. Elevation contours of the initial water table (ft) on June 30, 1994 obtained using the measured water levels at 47 monitoring wells (in red squares) and boundary conditions in boundary cells (in black squares).

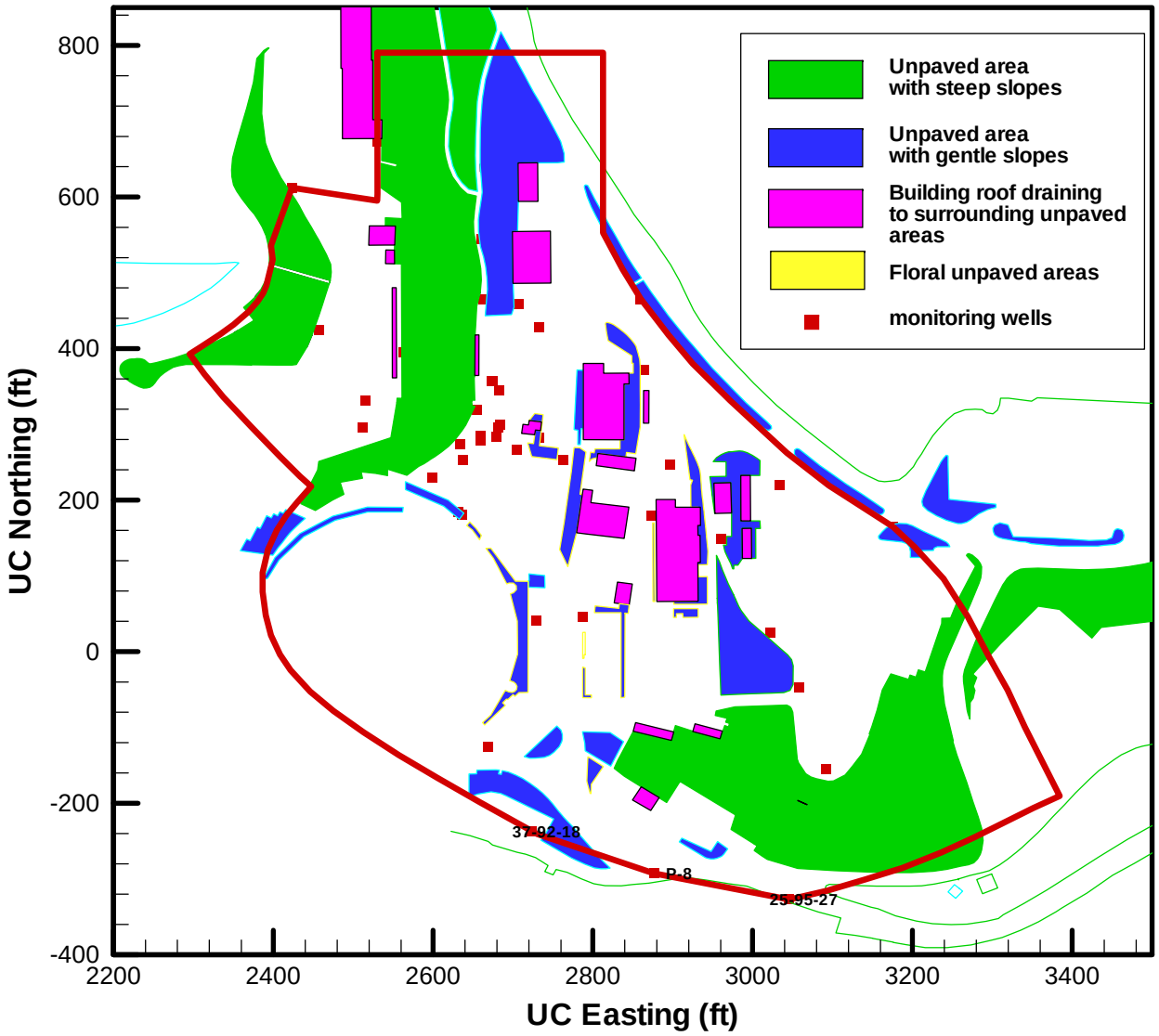

Figure 16. Map of the paved and unpaved areas for net recharge estimation. Green indicates the unpaved areas with steep slopes larger than 30°, whereas blue indicates those with gentle slopes. The purple areas are buildings with rainfall intercepted draining into neighboring unpaved areas.

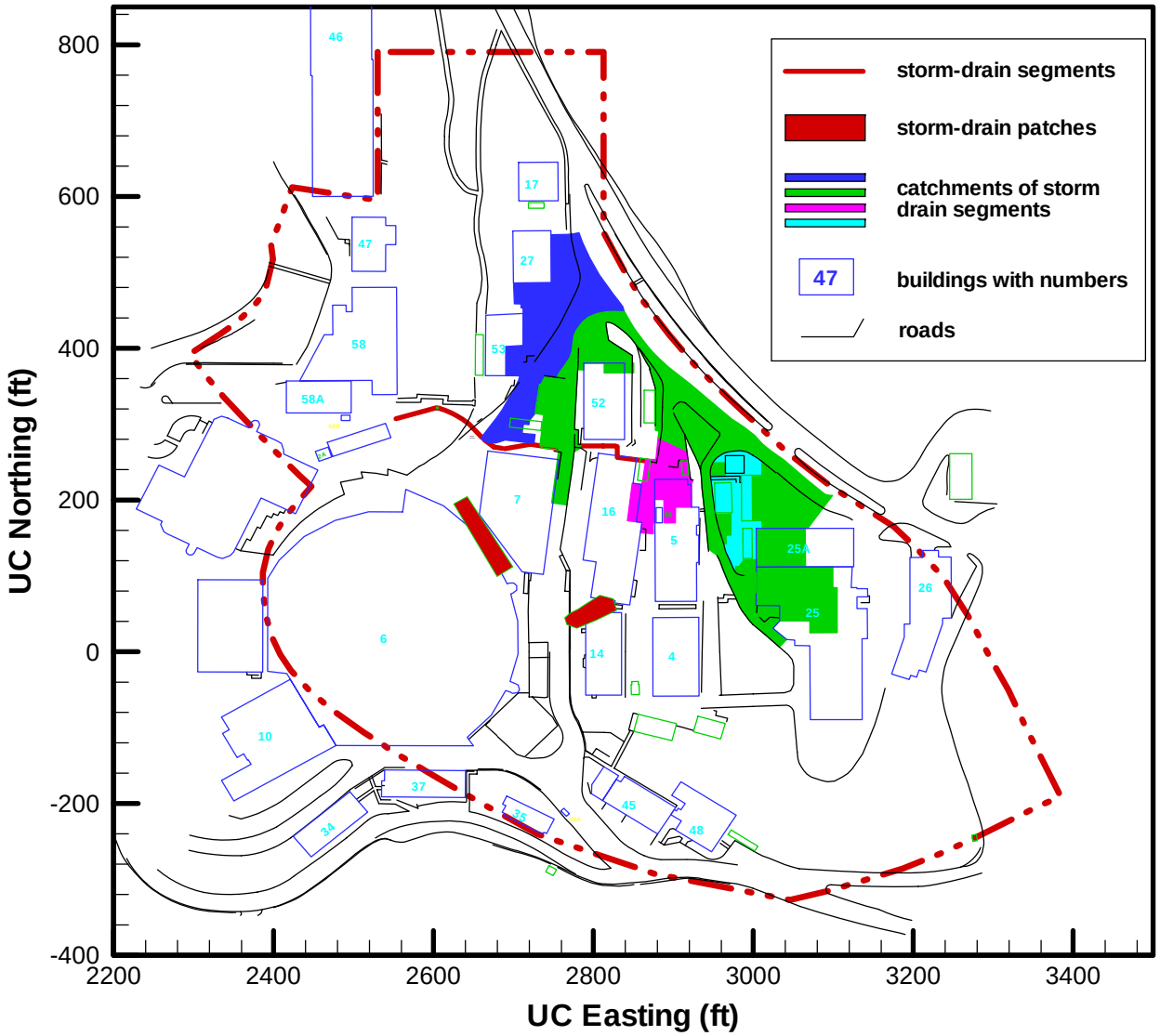

Figure 17. Confirmed leaking storm drains in red lines and patches and their discharge catchments. The main storm drain around Building 7 consists of four pipeline segments, each of which has a catchment for the discharging rainfall into pipeline. The storm drains in the north of Buildings 6 and 14 are in red patches.

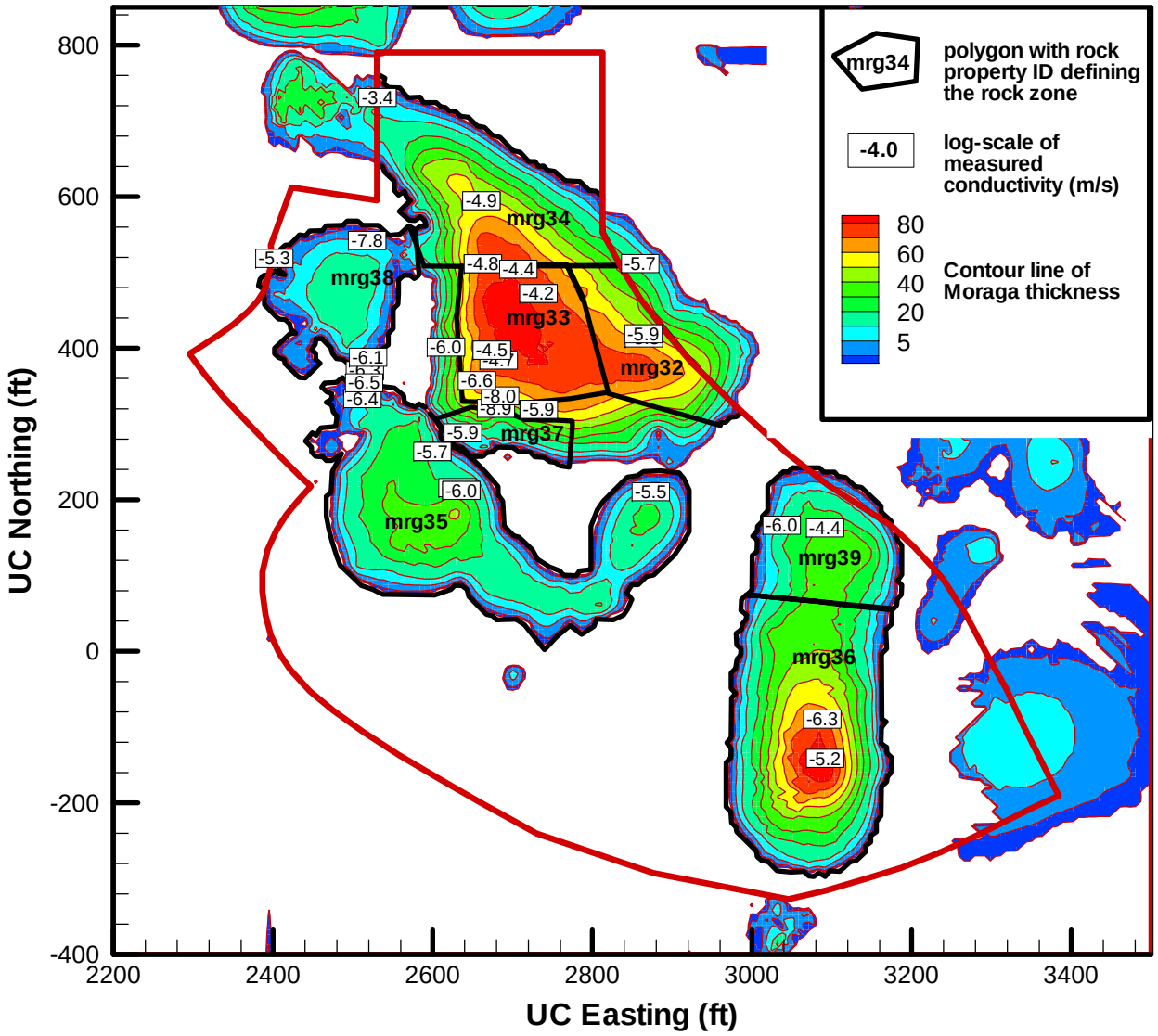

Figure 18. Definition of nine rock zones of different rock properties in the Moraga Formation unit, showing the measured hydraulic conductivities (m/s) in the log scale.

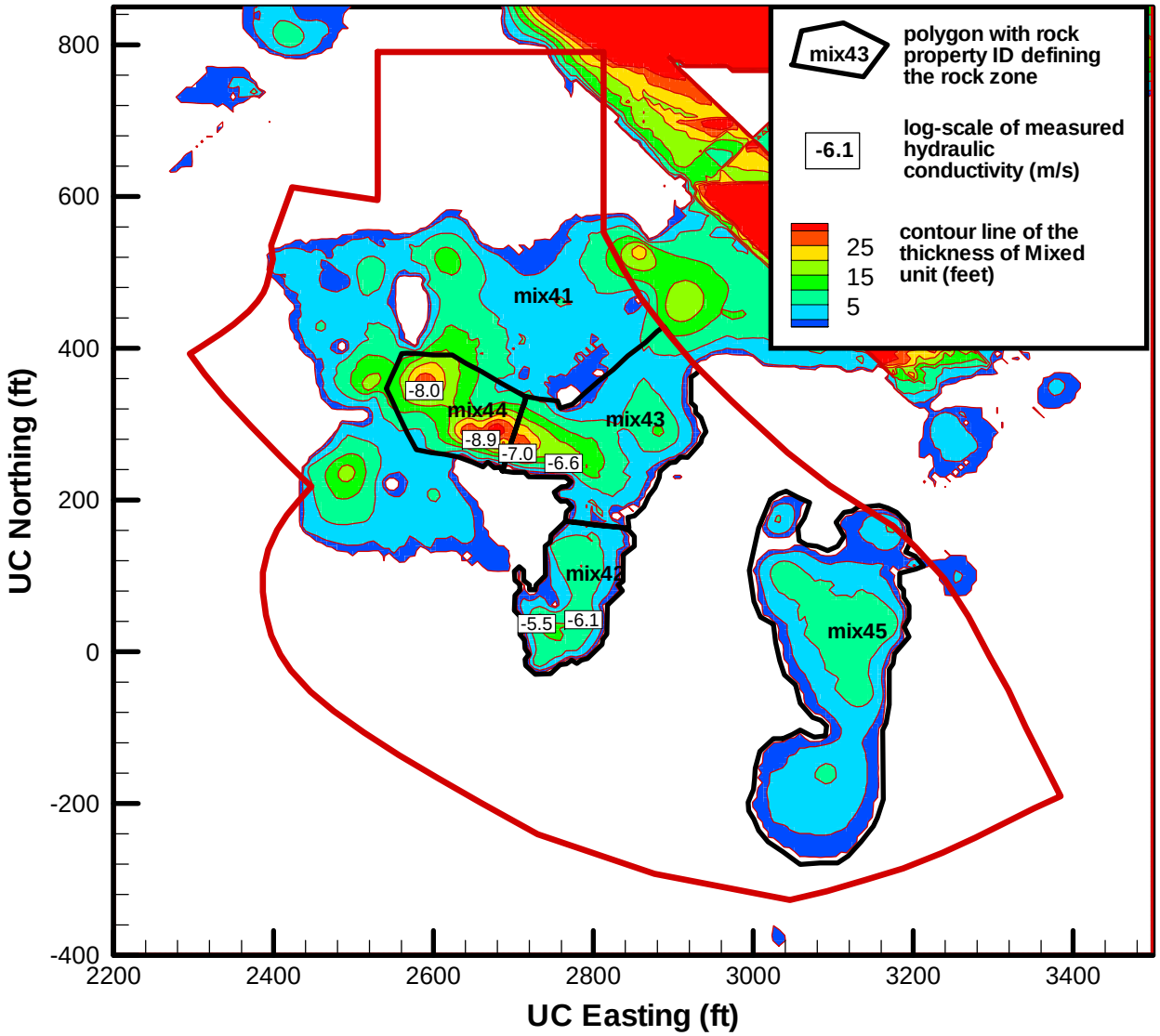

Figure 19. Definition of five rock zones of different rock properties in the Mixed unit, showing the measured hydraulic conductivities in the log scale.

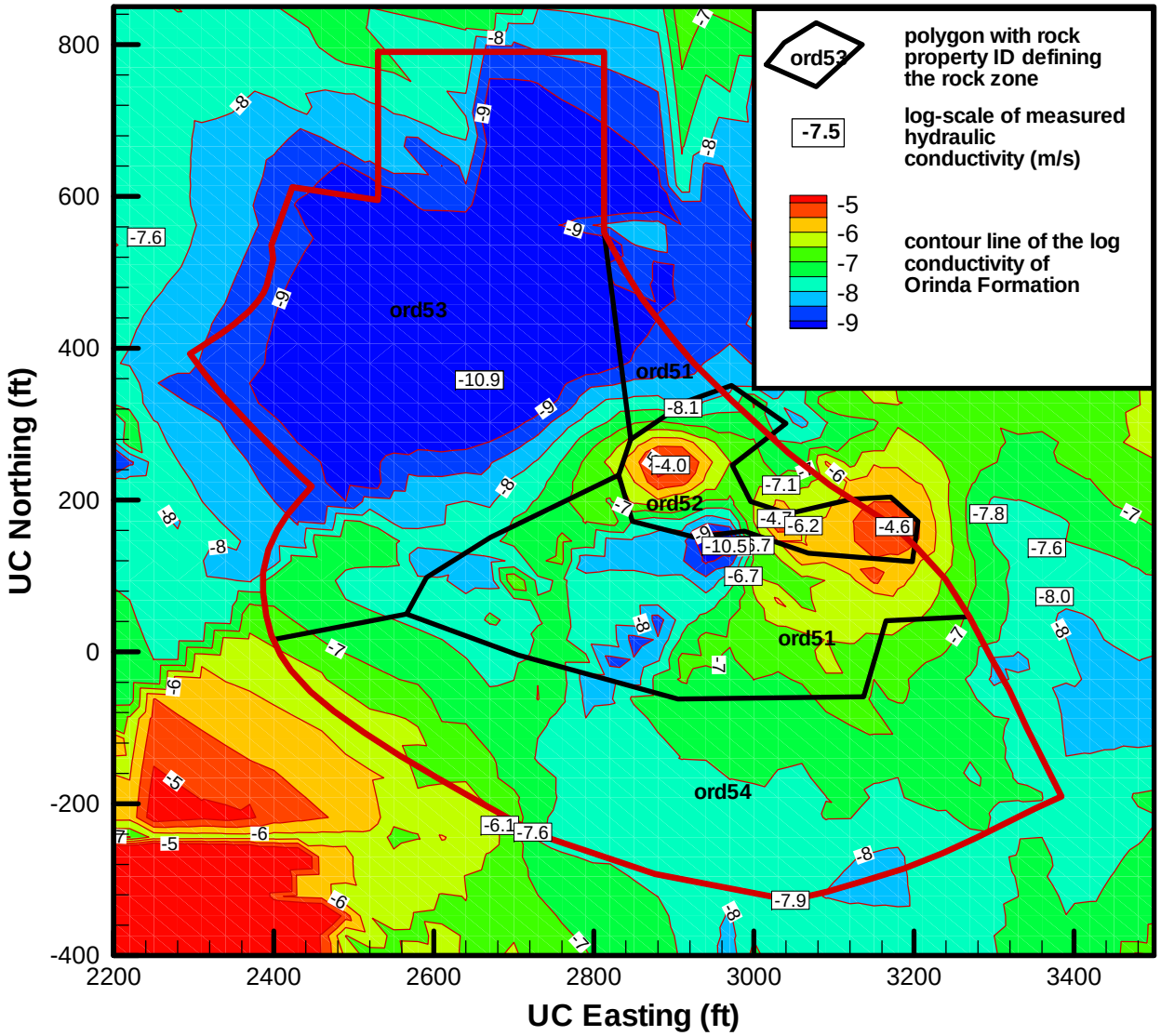

Figure 20. Definition of four rock zones of different rock properties in the Orinda Formation unit, showing the measured hydraulic conductivities in the log scale.

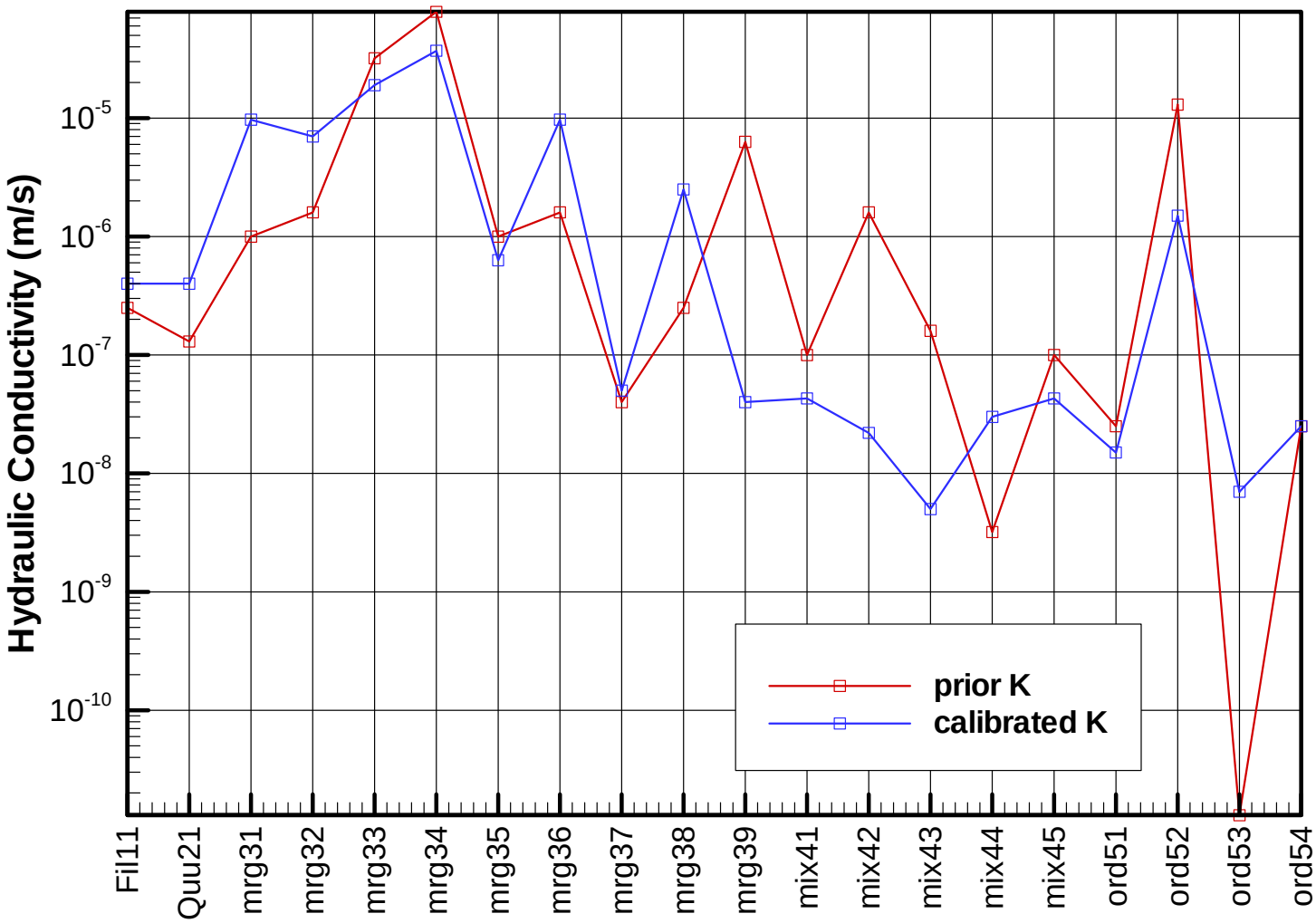

Figure 21. Comparison between the calibrated hydraulic conductivities and the prior ones obtained using hydraulic conductivity measurements for the 20 rock zones. See Figures 18-20 for the locations of the zones.

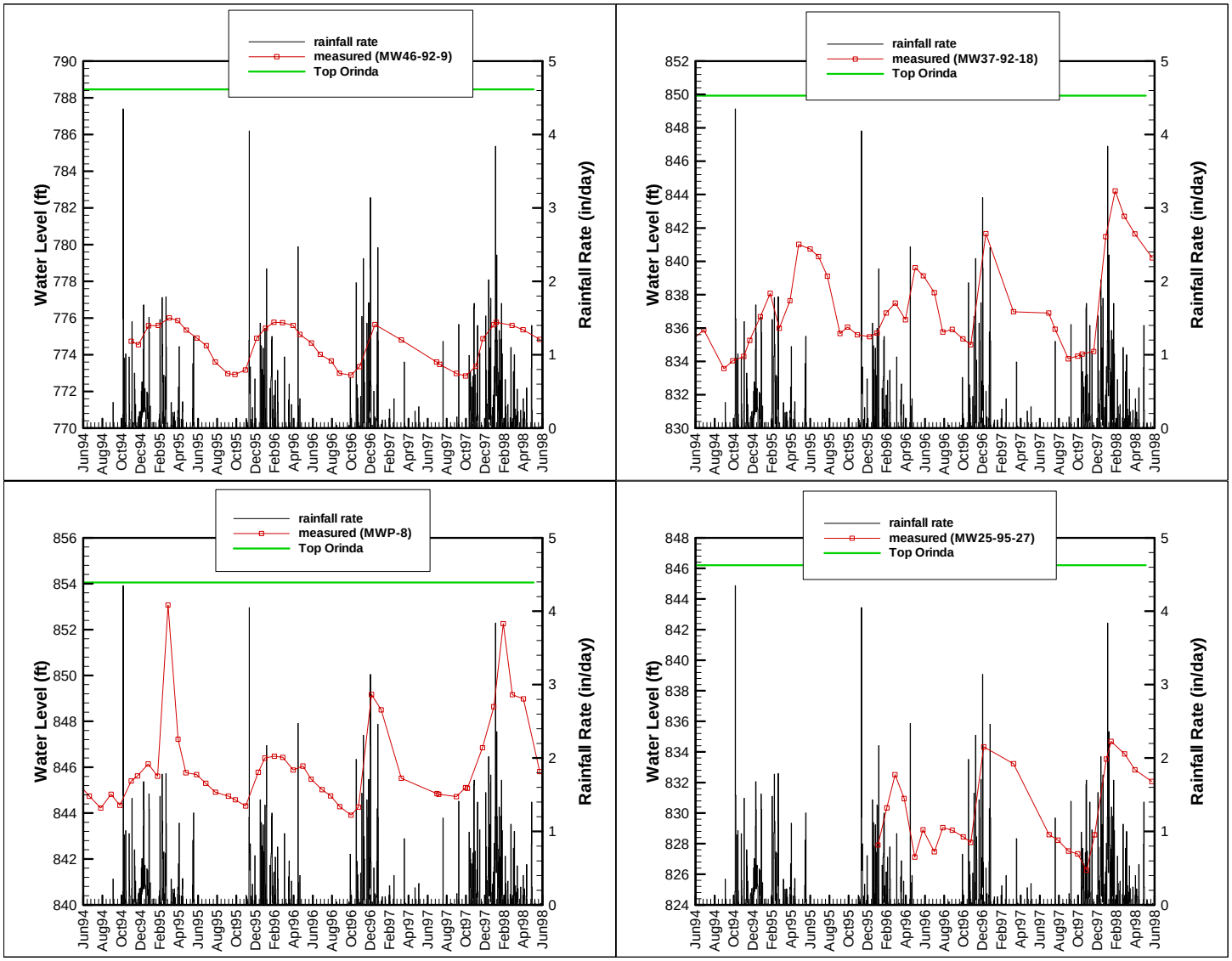

Figure 22. Measured water levels at four monitoring wells on the downstream boundary.

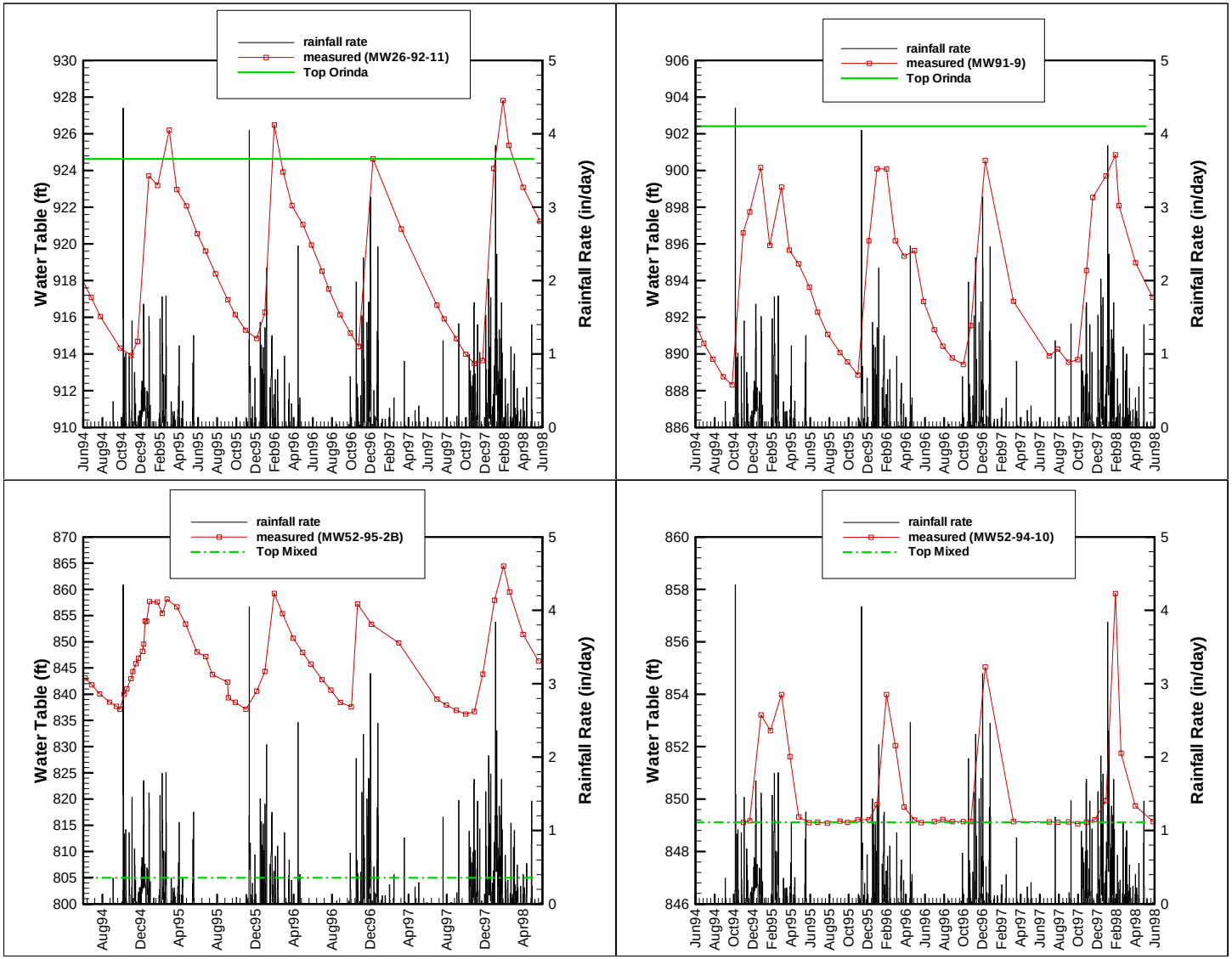

Figure 23. Measured water levels at four wells on the upstream boundary.

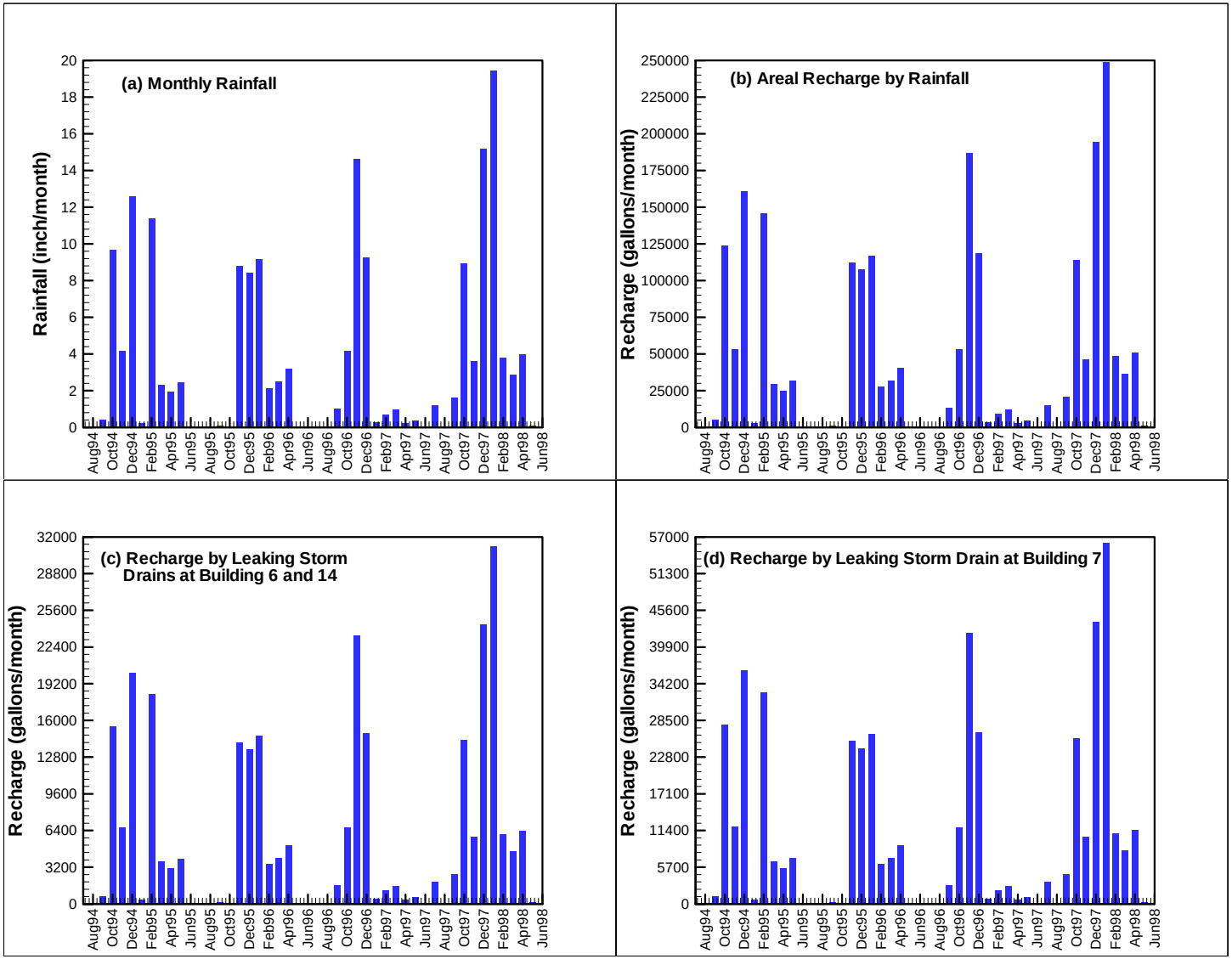

Figure 24. Transient processes of (a) monthly rainfall, (b) net areal recharge via unpaved areas, (c) recharge by storm drain at Building 6 and 14, and (d) recharge by storm drain in the north of Building 7 during the period from July 1994 to June 1998.

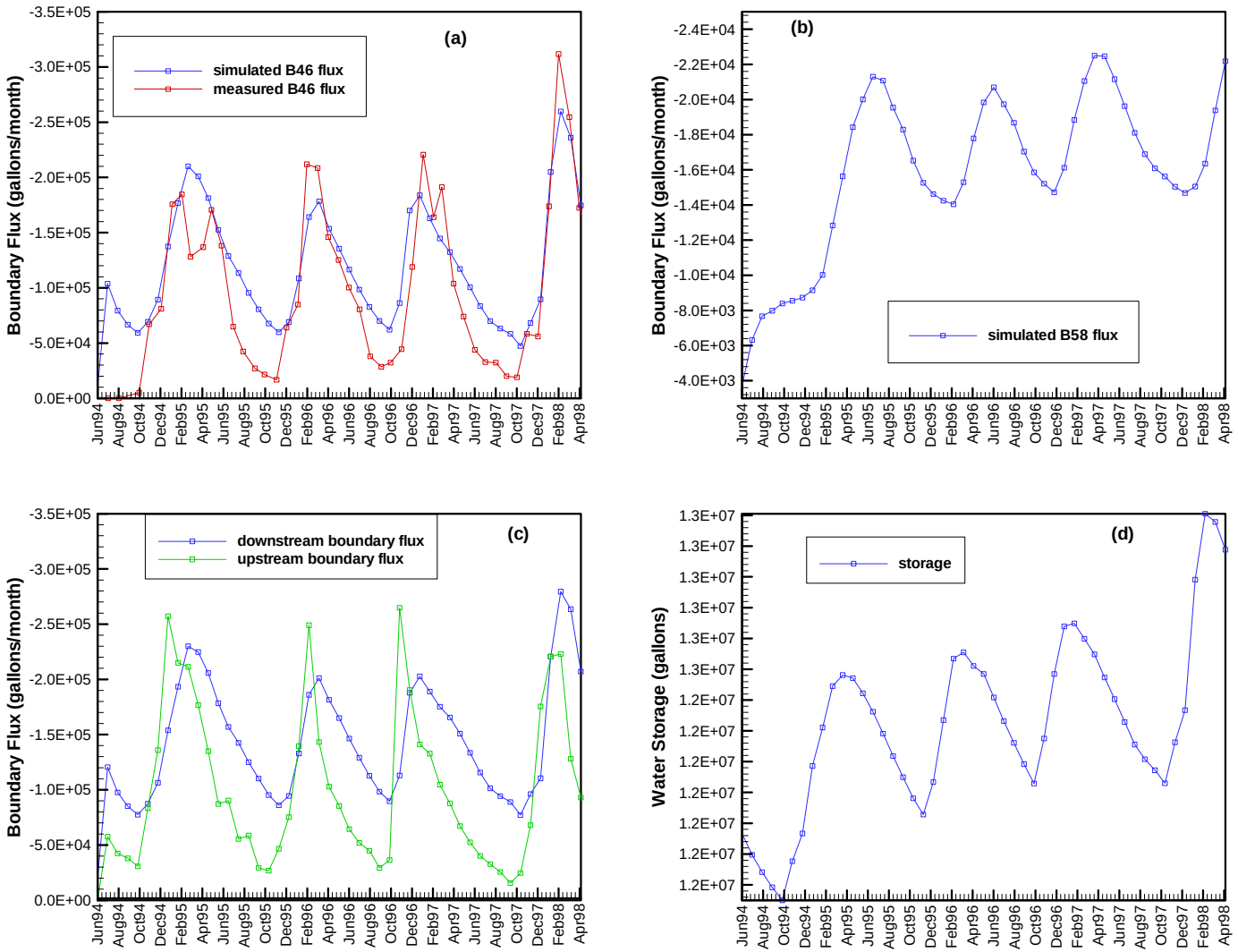

Figure 25. Transient processes of (a) the simulated and measured flow rate (gallons/month) through B46 boundary segment group, (b) the flow rate through B58 boundary segment group, (c) total inflow and outflow rates through the upstream boundary and downstream boundary, and (d) water-storage change (gallons) in the system during the period from July 1994 to June 1998.

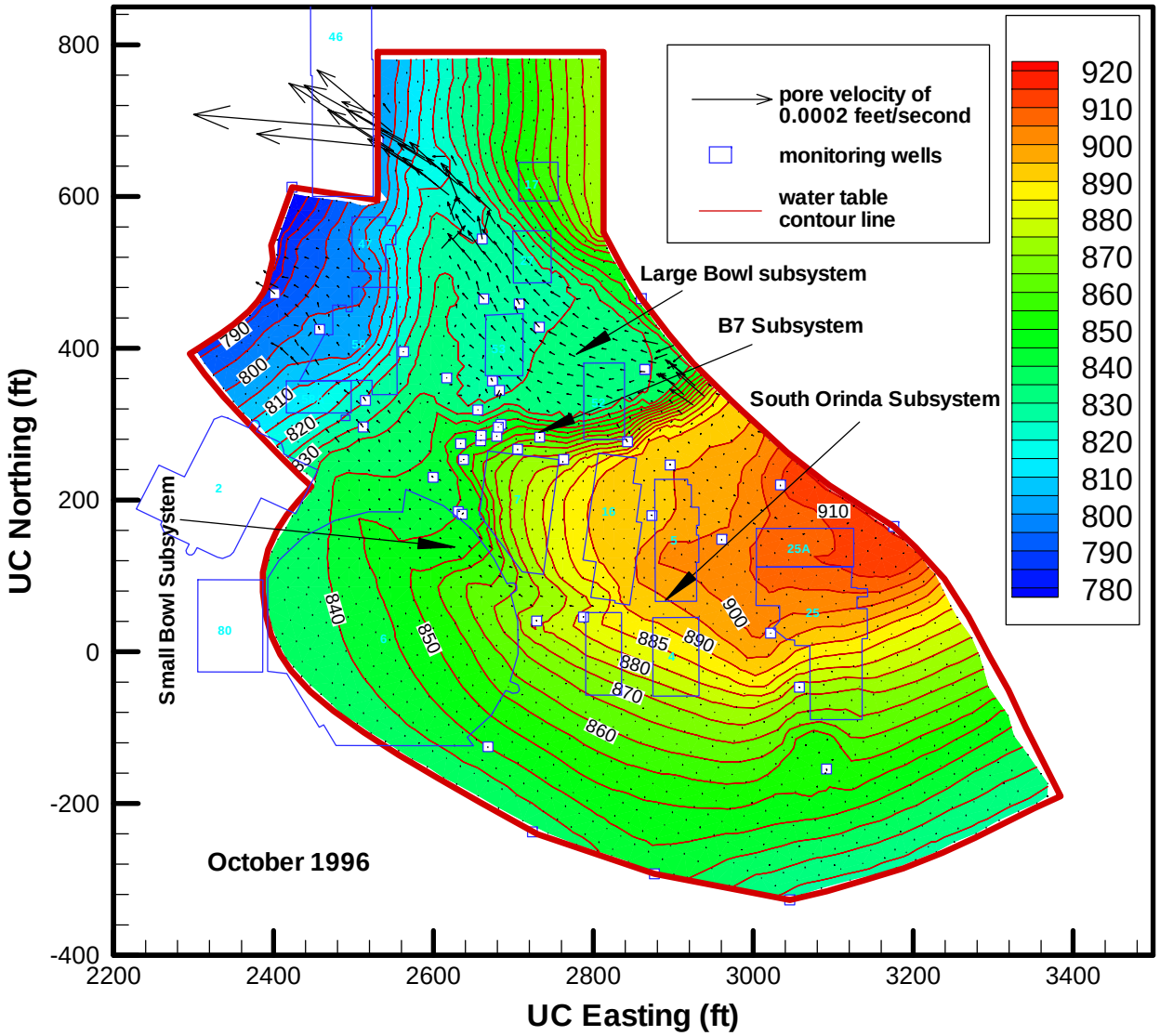

Figure 26. Contour of the simulated water table and vector field of simulated velocity on the water table at October 1996. The blue-white symbols indicate the location of monitoring wells.

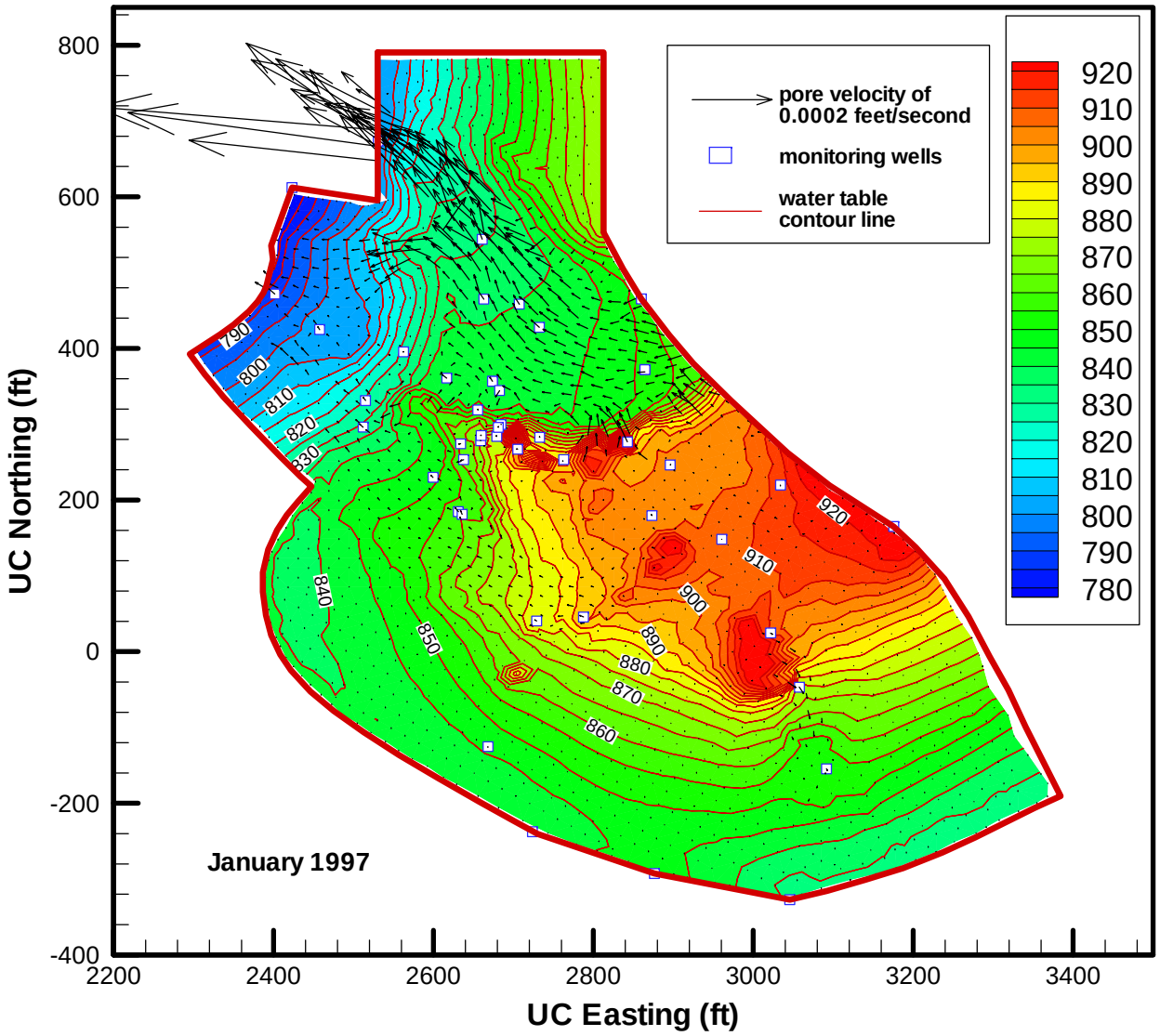

Figure 27. Contour of the simulated water table and vector field of simulated velocity on the water table at January 1997. The blue-white symbols indicate the location of monitoring wells.

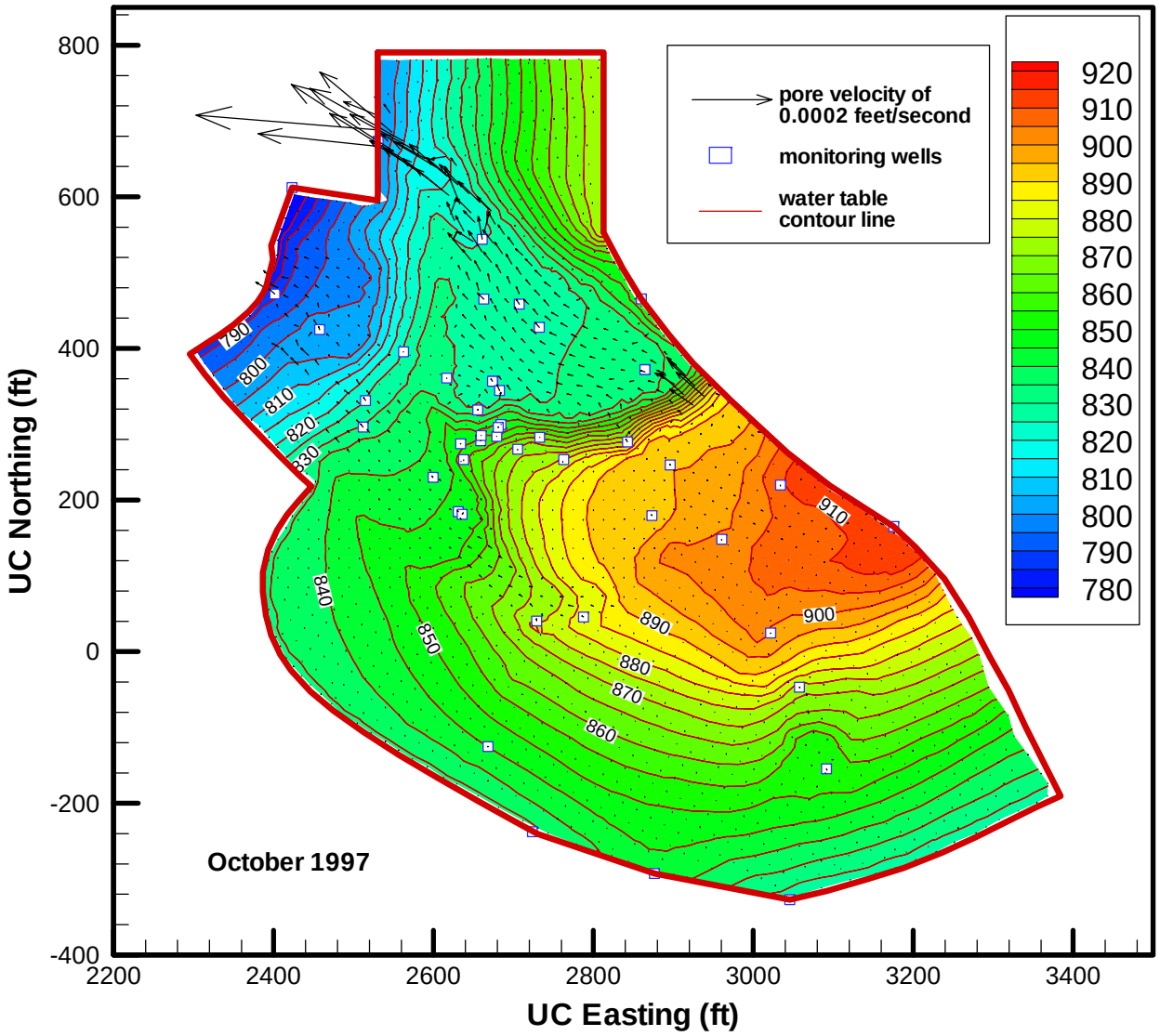

Figure 28. Contour of the simulated water table and vector field of simulated velocity on the water table at October 1997. The blue-white symbols indicate the location of monitoring wells.

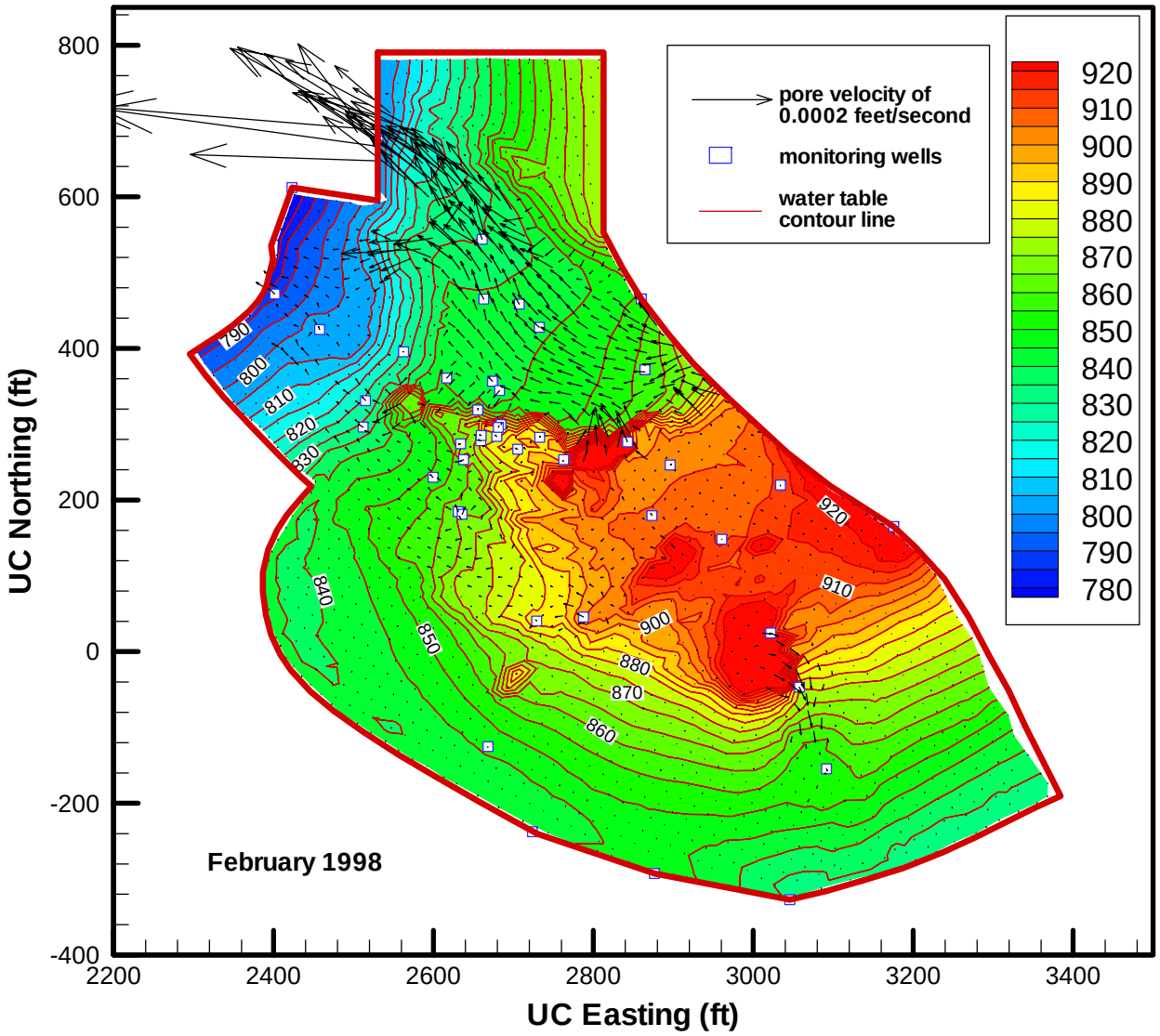

Figure 29. Contour of the simulated water table and vector field of simulated velocity on the water table at February 1998. The blue-white symbols indicate the location of monitoring wells.

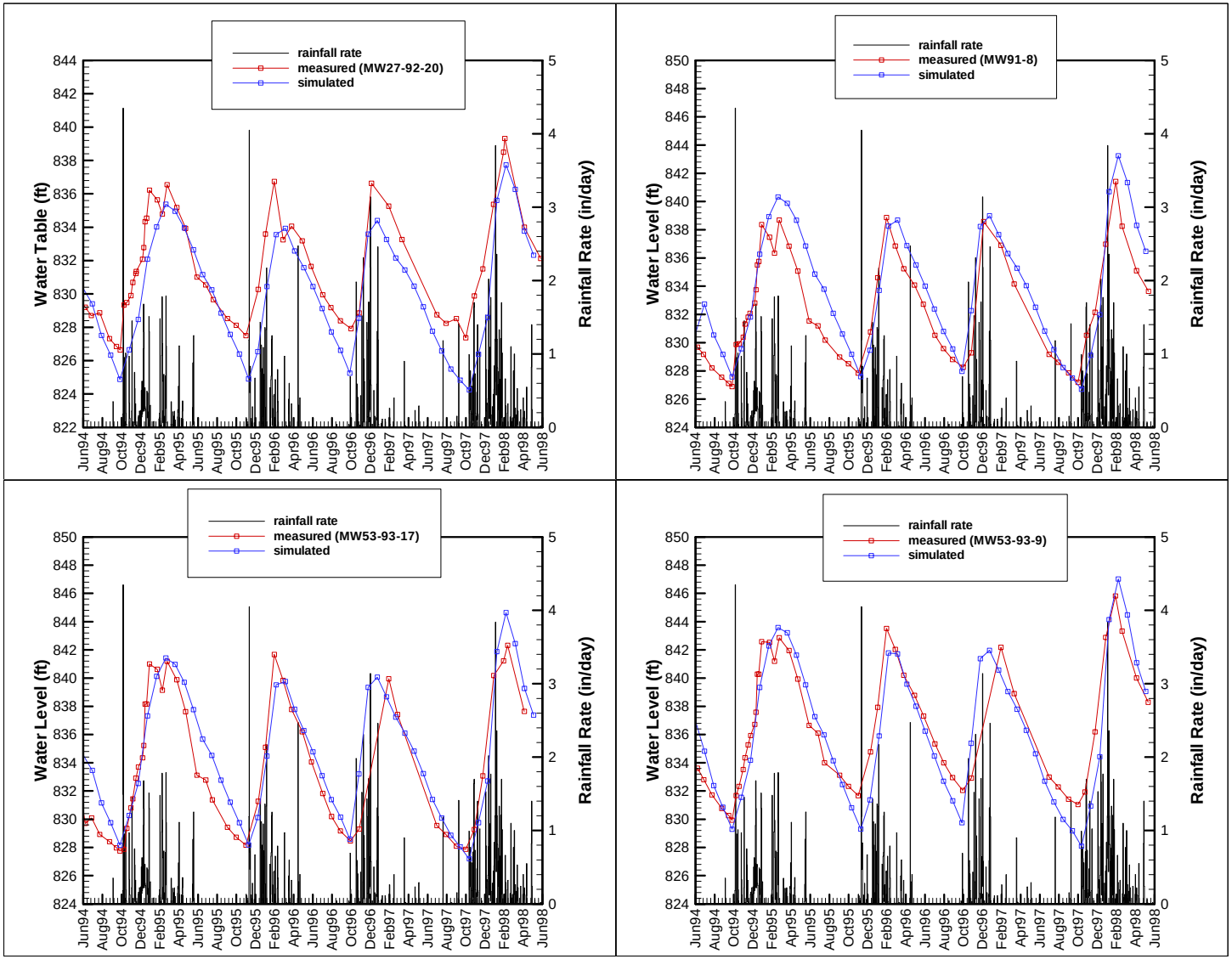

Figure 30. Match between the measured and simulated water levels at four monitoring wells in the Large-Moraga-Bowl subsystem.

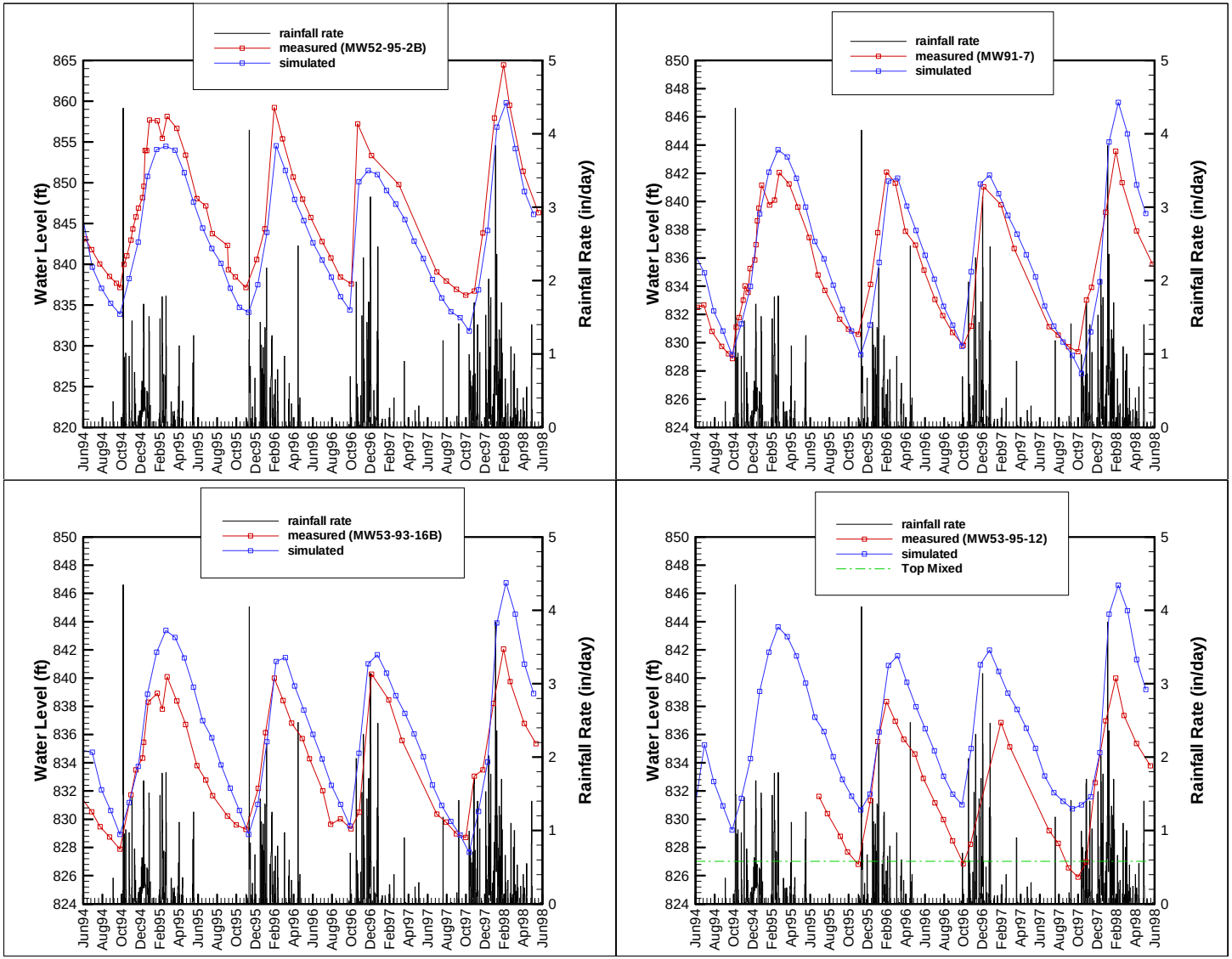

Figure 31. Match between the measured and simulated water levels at four monitoring wells in the Large-Moraga-Bowl subsystem (cont.).

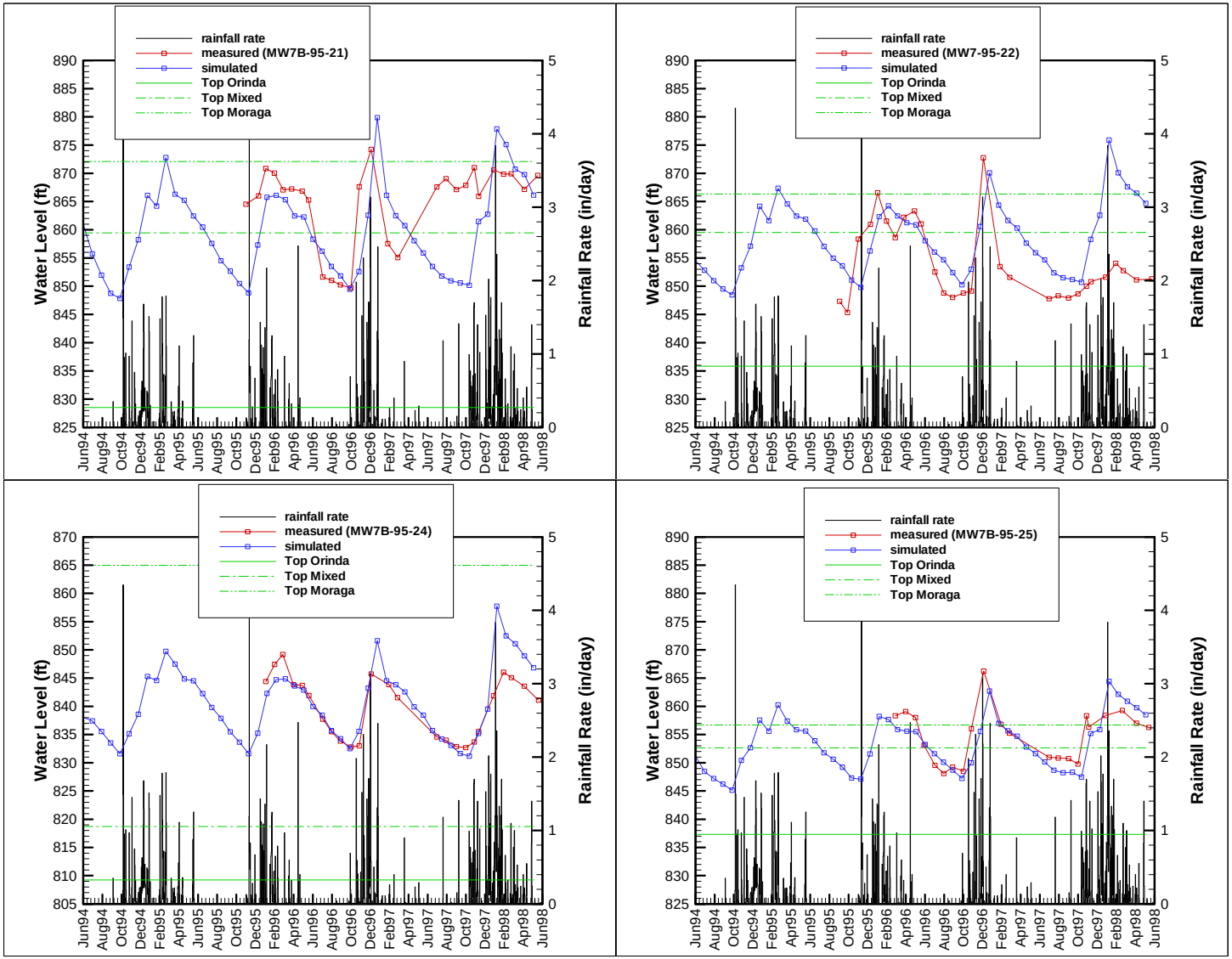

Figure 32. Match between the simulated and measured water levels at four monitoring wells in the Building 7 subsystem.

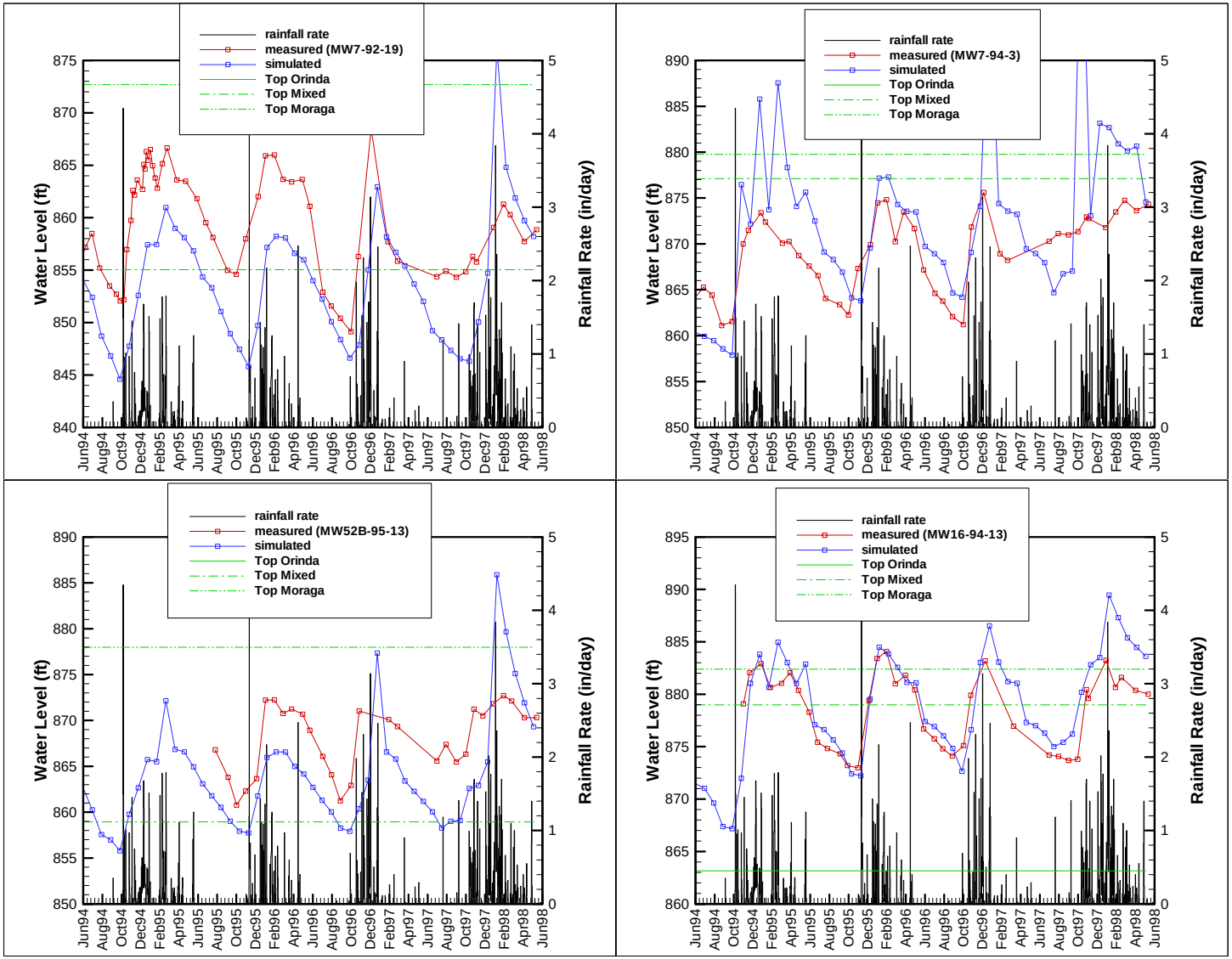

Figure 33. Match between simulated and measured water levels at four monitoring wells in the Building 7 subsystem (cont.).

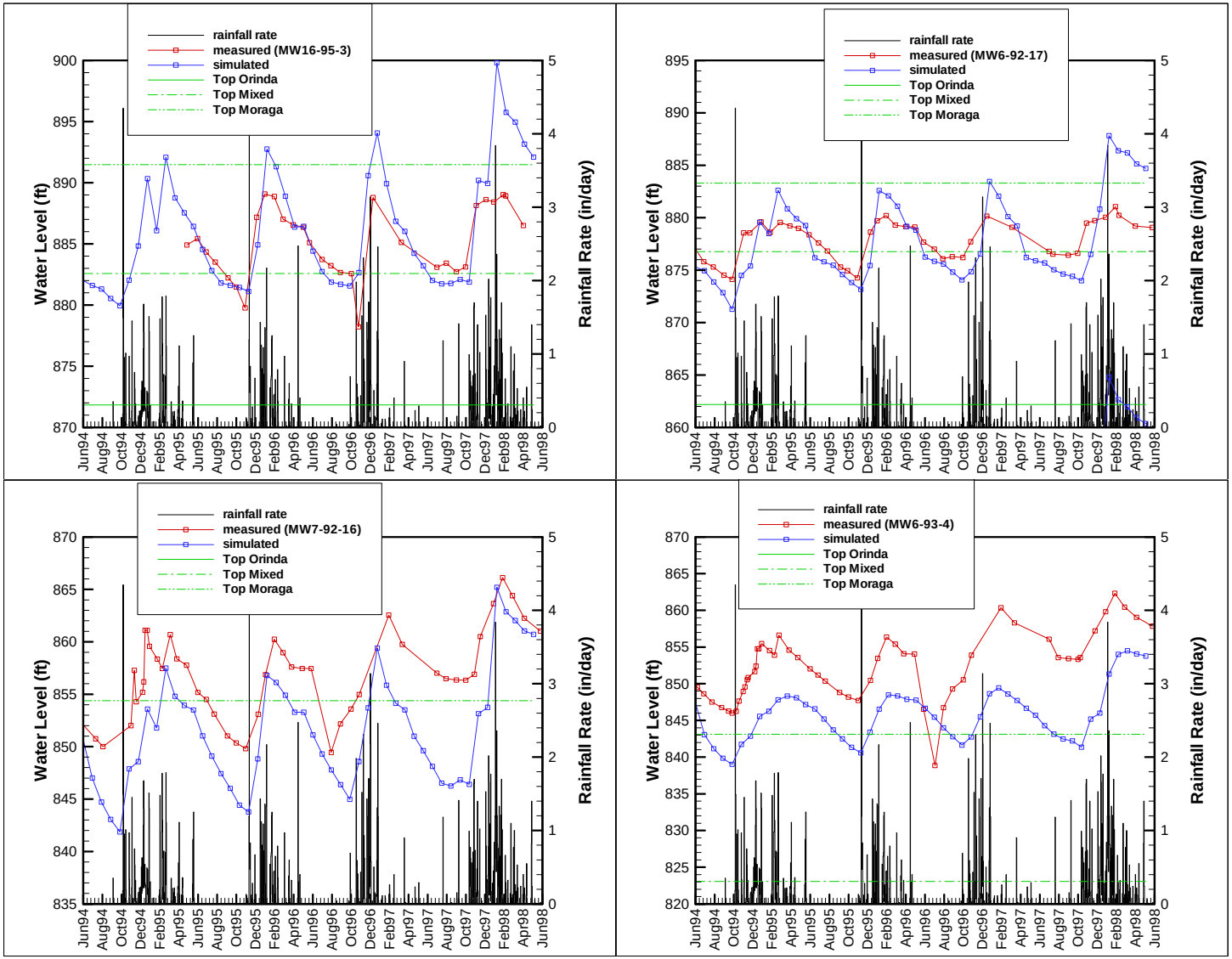

Figure 34. Match between the simulated and measured water levels at four monitoring wells in the Small-Moraga-Bowl subsystem.

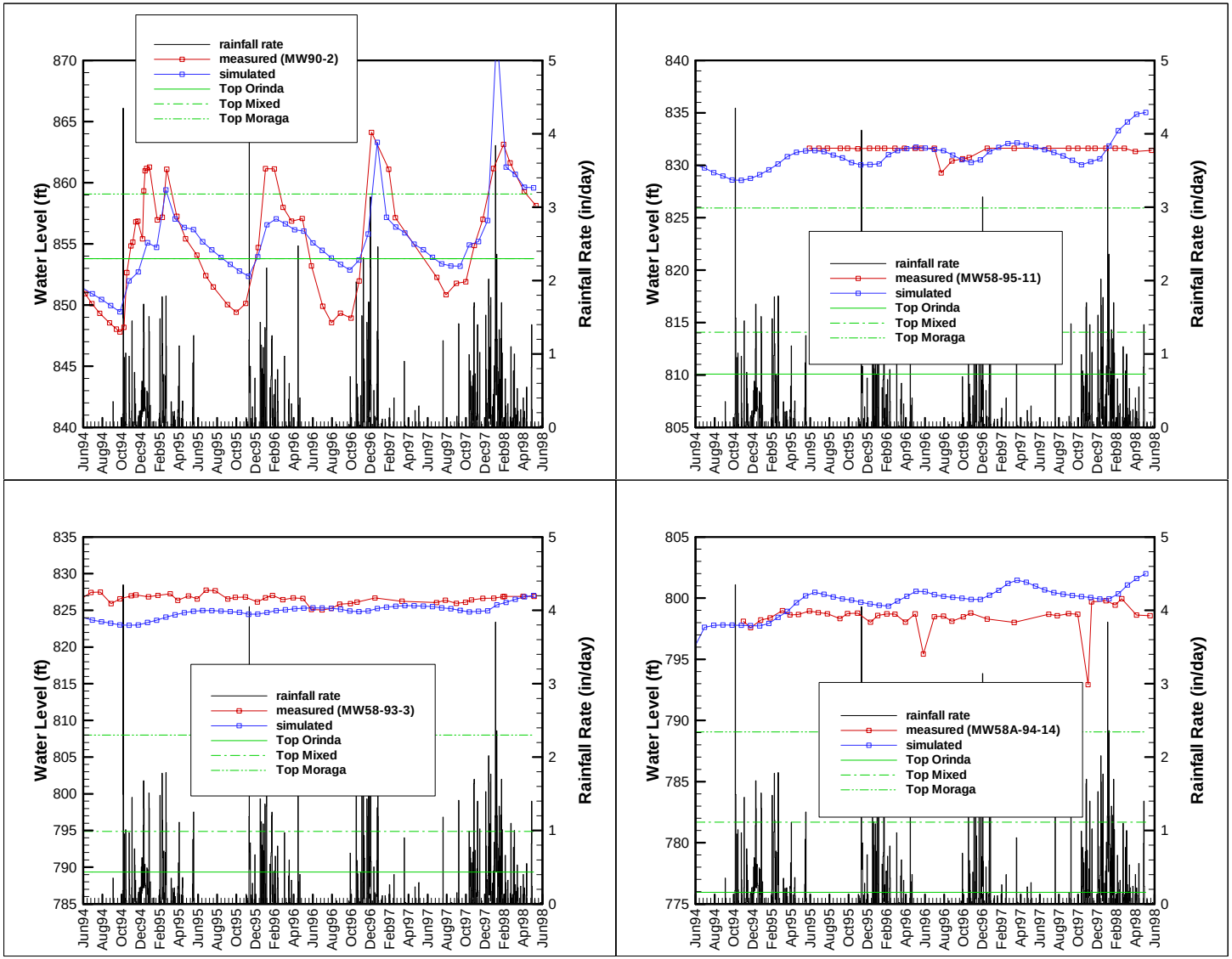

Figure 35. Match between the simulated and measured water levels at four monitoring wells in the Small-Moraga-Bowl subsystem (cont.).

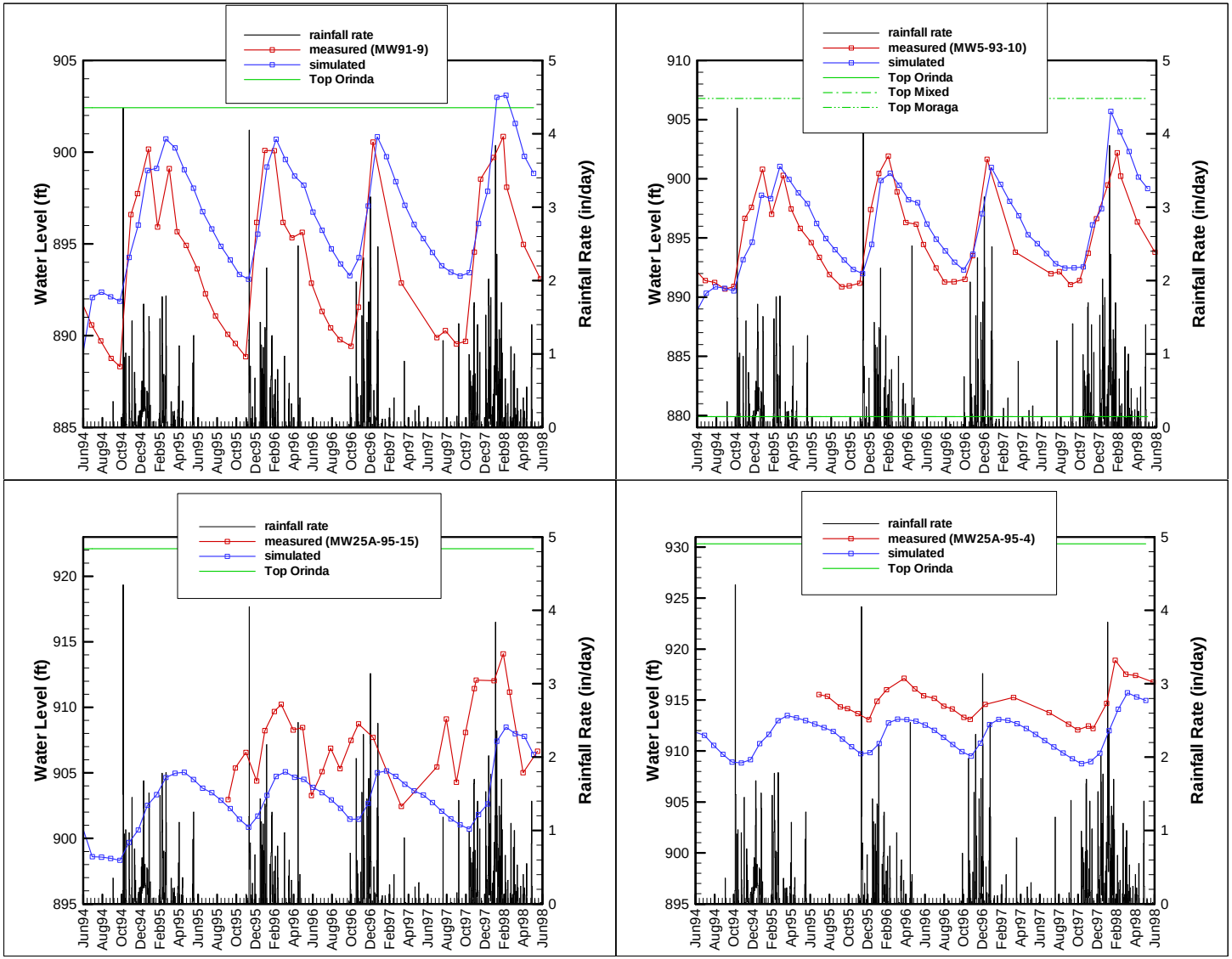

Figure 36. Match between the simulated and measured water levels at four monitoring wells in the South-Orinda subsystem.

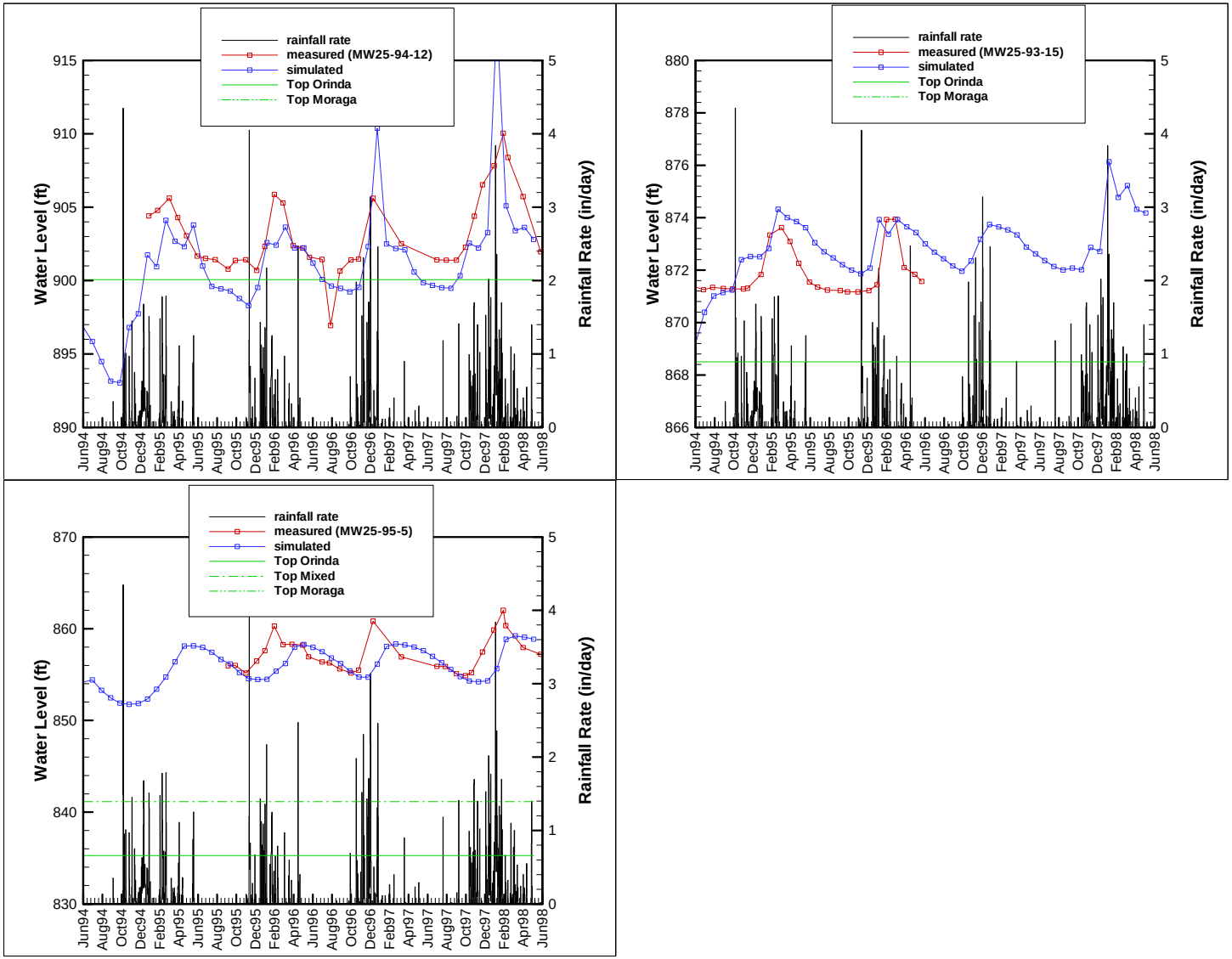

Figure 37. Match between the simulated and measured water levels at four monitoring wells in the South-Orinda subsystem (cont.).

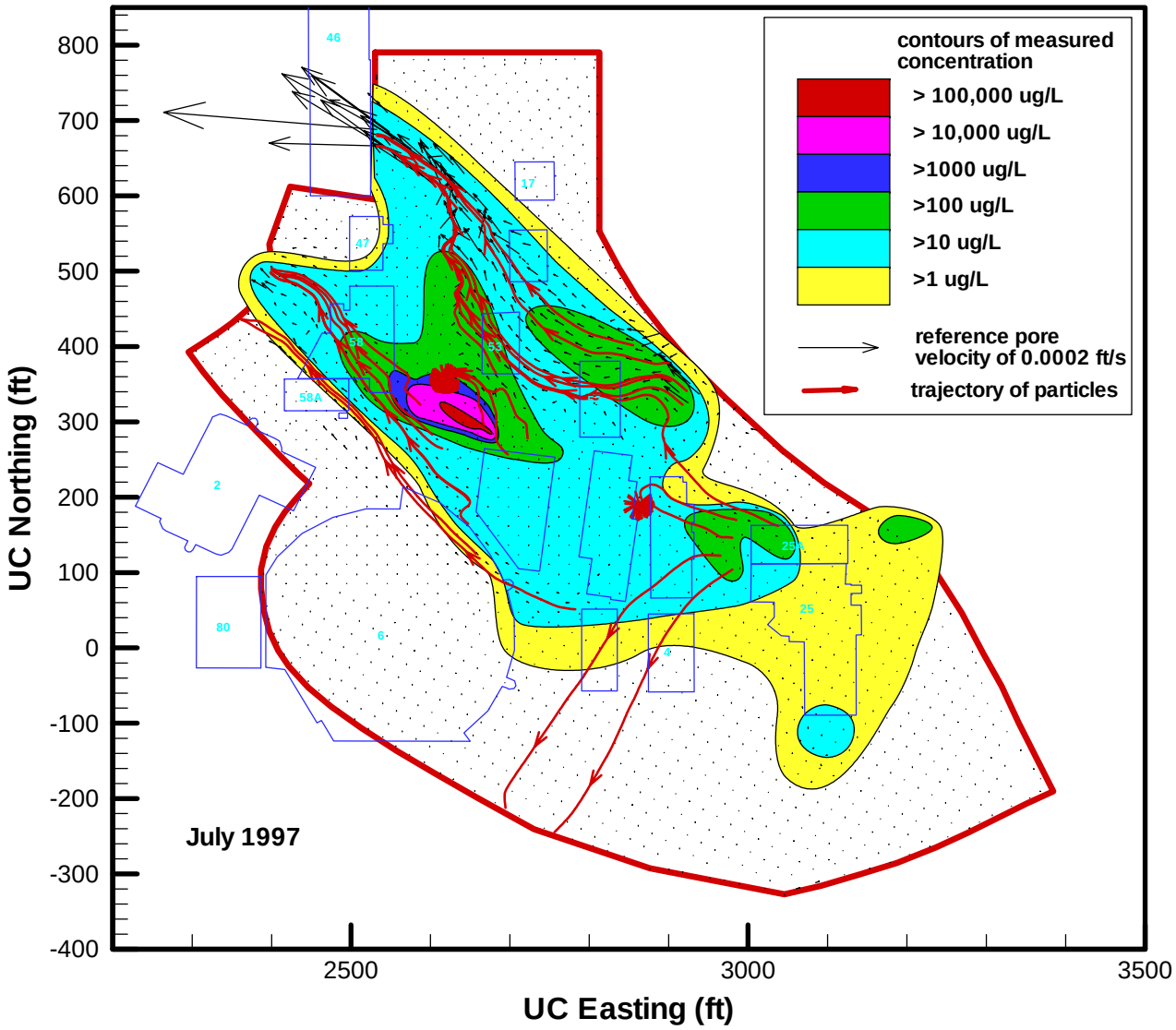

Figure 38. Trajectories of particles originating from the contaminant source areas at B7 lobe, B52 lobe, and B25A lobe. These trajectories are obtained using the steady-state flow in the dry season with pore velocity at July 1997.

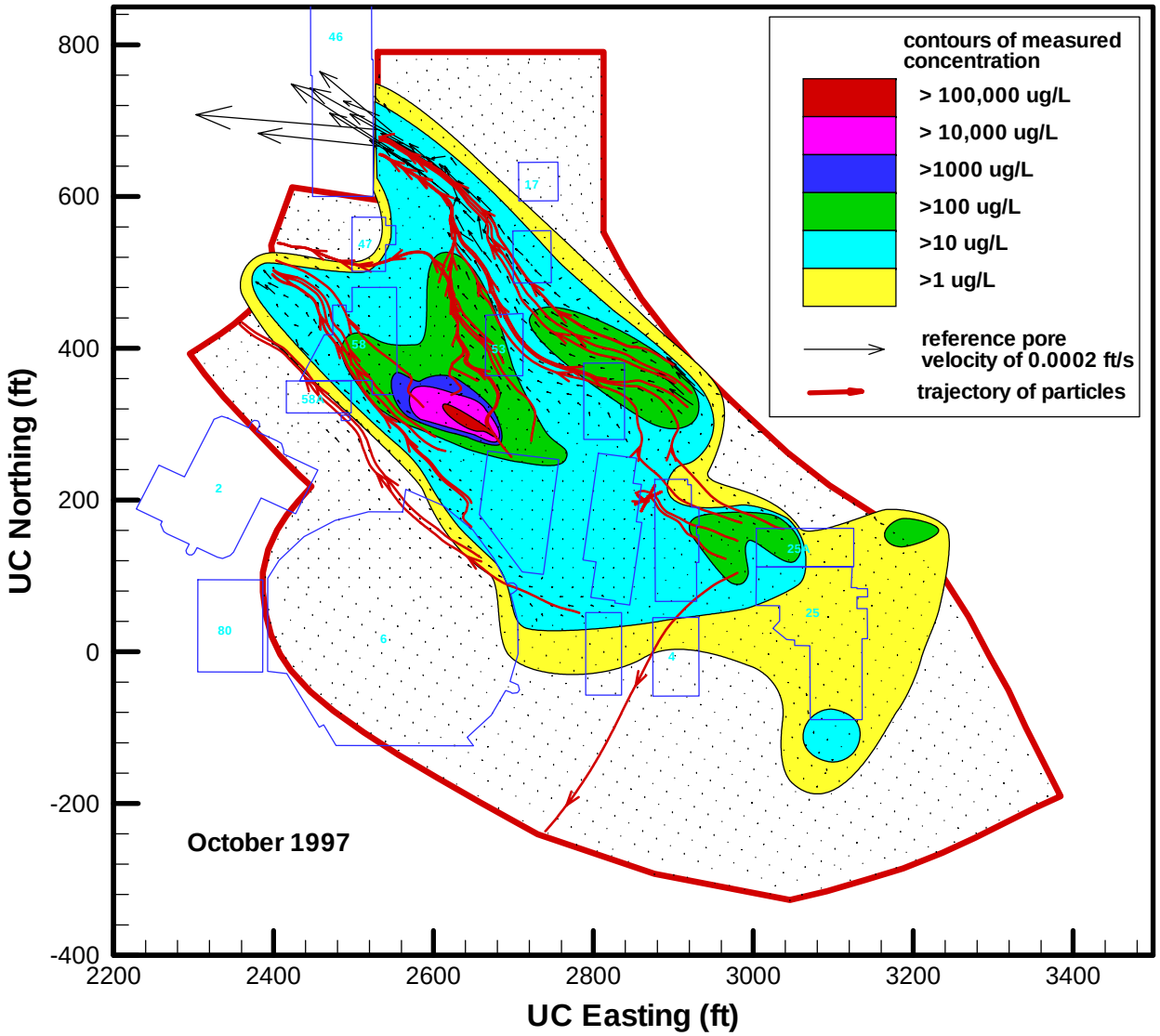

Figure 39. Trajectories of particles originating from the contaminant source areas at B7 lobe, B52 lobe, and B25A lobe. These trajectories are obtained using the steady-state flow in the wet season with pore velocity at October 1997.

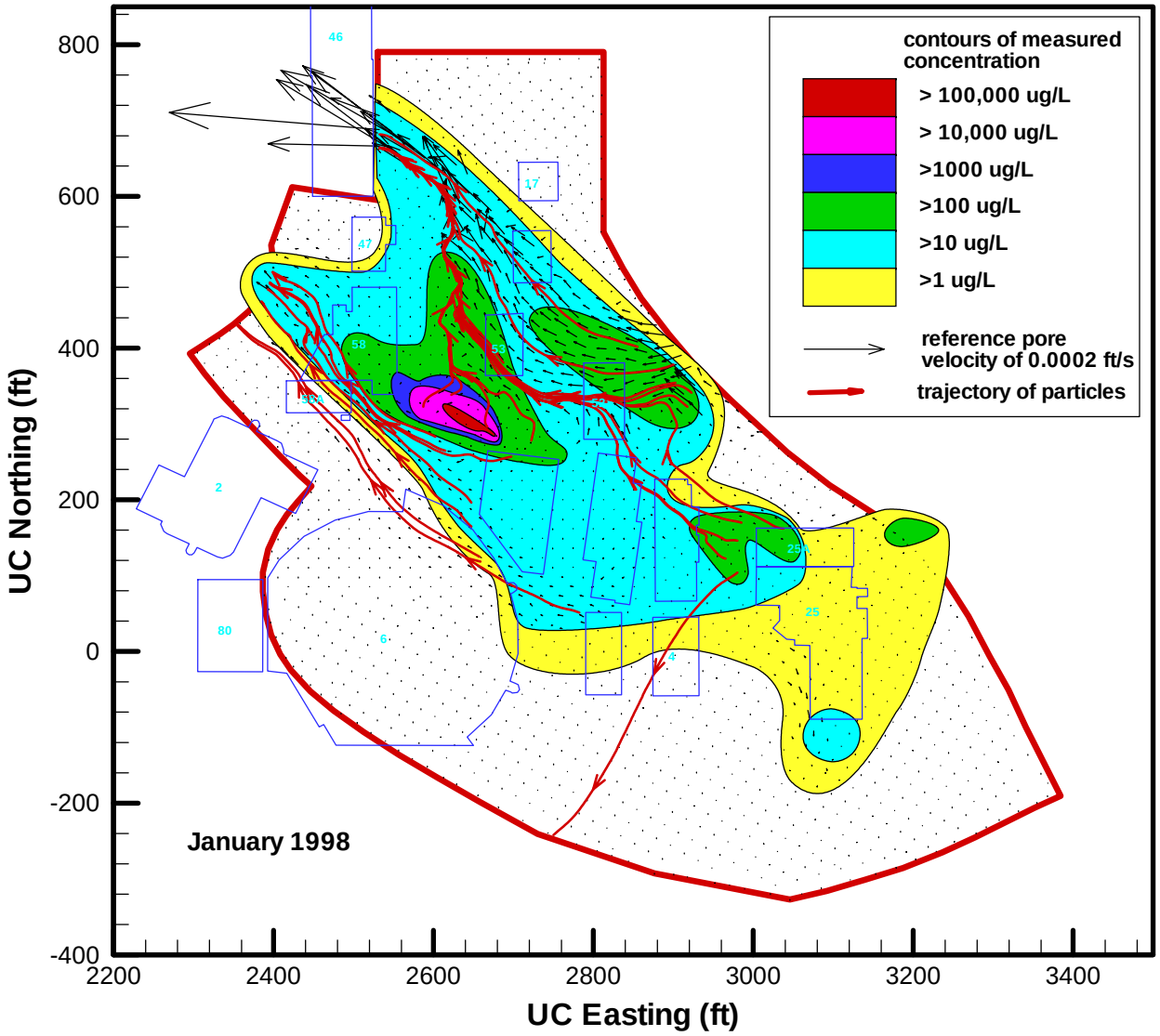

Figure 40. Trajectories of particles originating from the contaminant source areas at B7 lobe, B52 lobe, and B25A lobe. These trajectories are obtained using the steady-state flow in the wet season with pore velocity at January 1998.

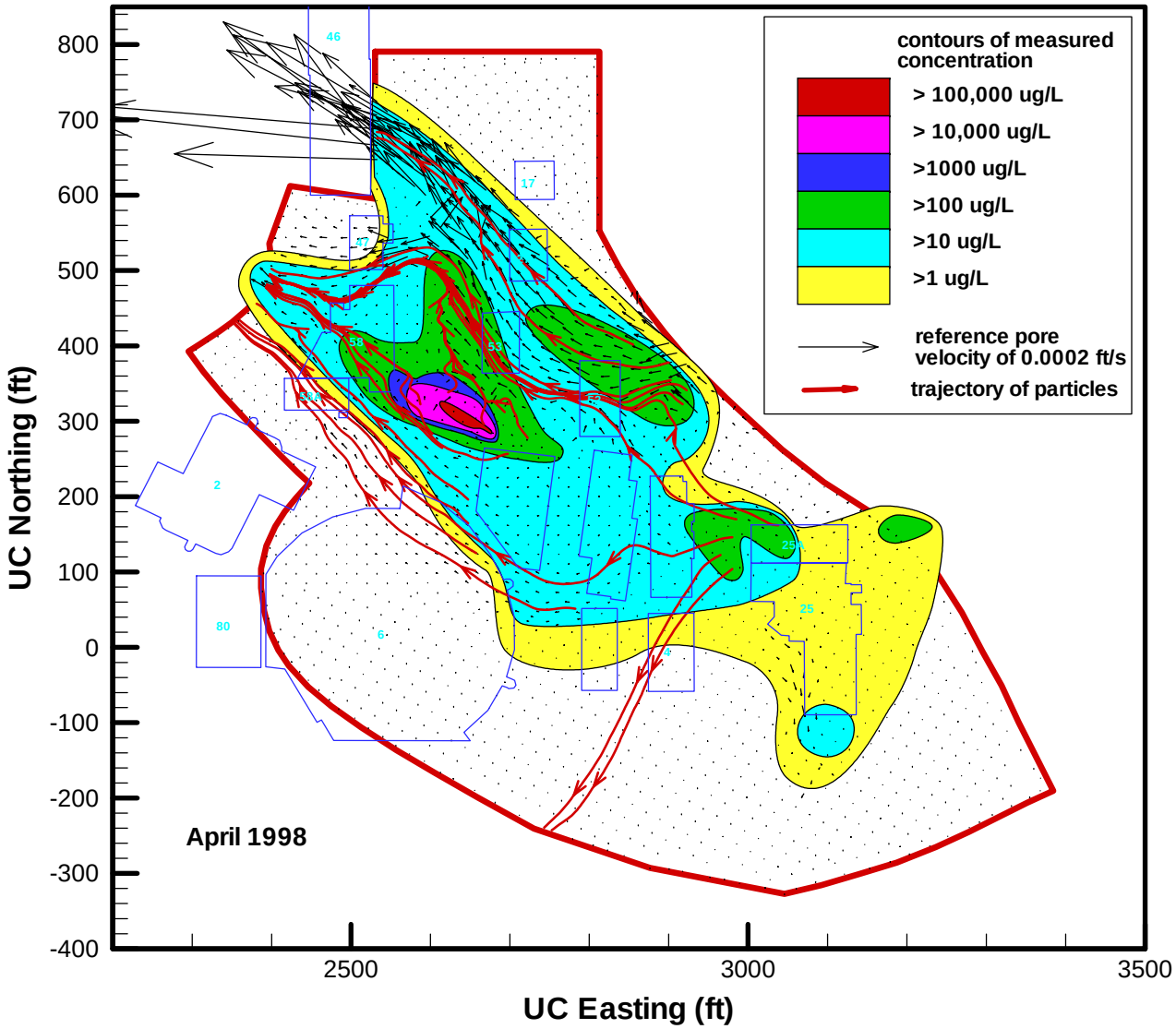

Figure 41. Trajectories of particles originating from the contaminant source areas at B7 lobe, B52 lobe, and B25A lobe. These trajectories are obtained using the steady-state flow in the wet season with pore velocity at April 1998.

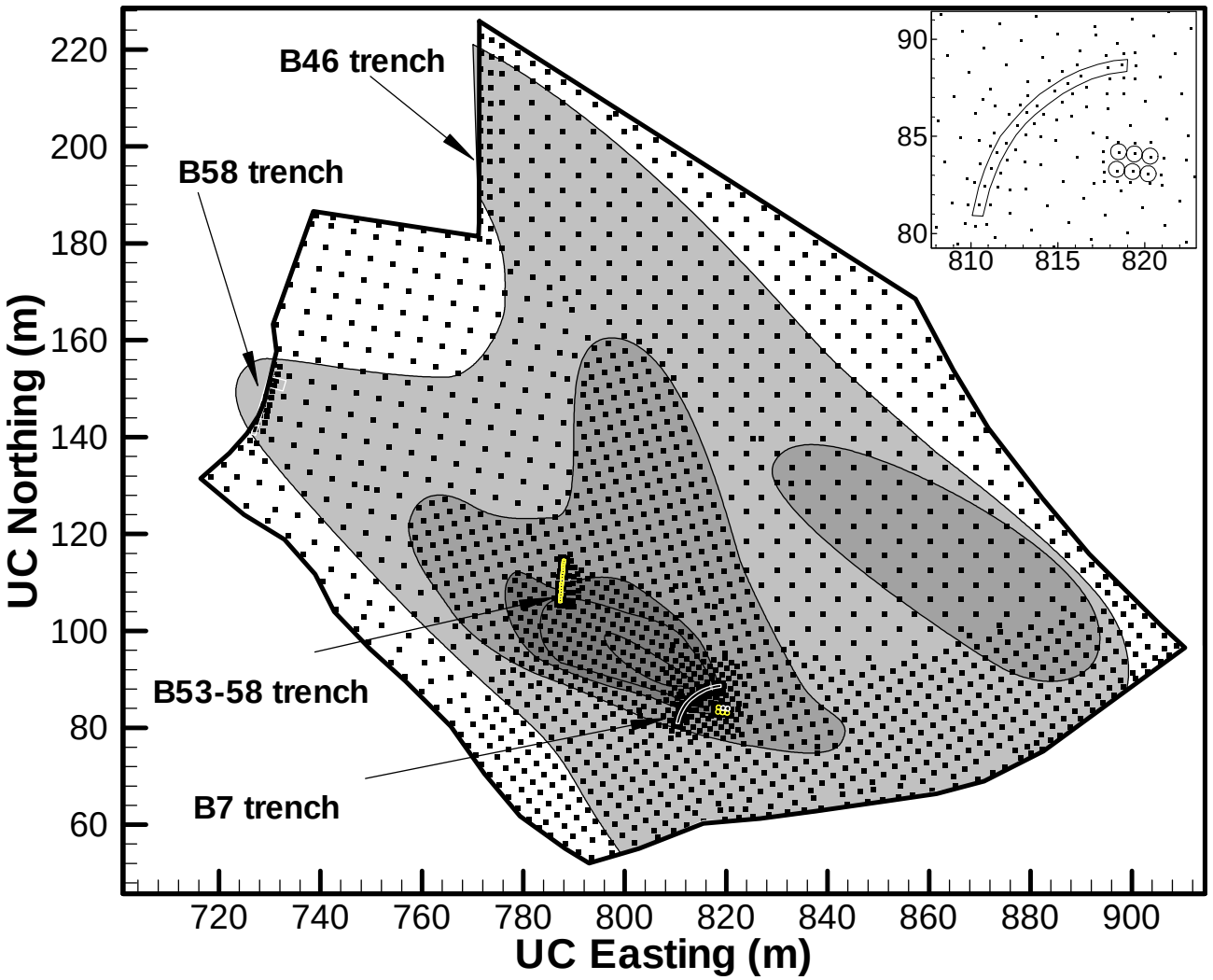

Figure 42. Boundary and plan view of the three-dimensional mesh for the refined model, showing the four trenches implemented for restoration. The background is the measured concentration contour with the contour legend shown in Figure 41. The right upper-corner plot shows a close-up view of the sump and the B7 trench system for controlling the contaminant source.

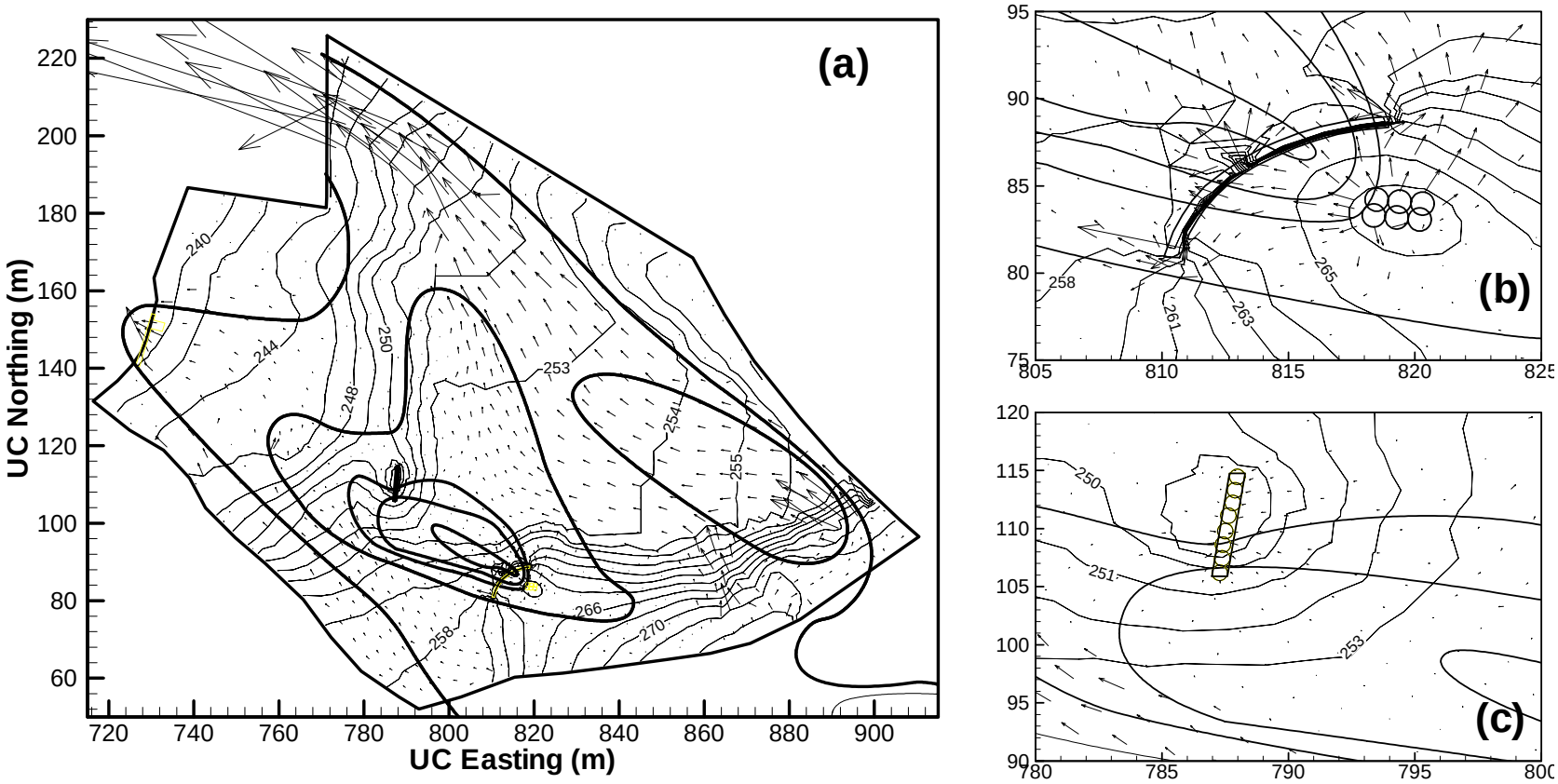

Figure 43. Contour of the predicted groundwater level (light lines) and flow velocity vector fields on the water table in October 1999 for the refined model in (a) the entire model domain, (b) in the vicinity of the B7 trench, and (c) in the vicinity of the B53-B58 trench. Note that the contaminant plume contour lines are indicated by thick lines (for scales, see Figure 41).